DISSERTATION

Gasification and Co-gasification of Coal, Biomass and Plastics in a Dual Fluidized Bed System

ausgeführt zum Zwecke der Erlangung des
akademischen Grades eines Doktors der technischen Wissenschaften
unter Leitung von

Univ. Prof. Dipl.-Ing. Dr. Hermann Hofbauer

Univ. Prof. Dipl.-Ing. Dr. Christoph Pfeifer

am
Institut für Verfahrenstechnik, Umwelttechnik und Technische Biowissenschaften der Technischen Universität Wien

eingereicht an der Technischen Universität Wien
Fakultät für Maschinenwesen und Betriebswissenschaften

von
Dipl.-Ing. Stefan Johannes Kern
Dr. Ernst Franz Straße 15
7071 Rust

Wien, 23. Mai 2013

……..
Stefan Kern

Abstract

Gasification of solid fuels attracts increasing interest within the power industry as well as for synthesis processes for liquid and gaseous fuel production. Conventional gasification systems that can be operated autothermally require an oxidizing gasification agent like O_2 or air. The drawback of using air as a gasification agent is that a lot of nitrogen is present in the product gas which consequently lowers the heating value. By using O_2 as a gasification agent, the heating value of the product gas is high, but the production of pure O_2 makes the system ecologically questionable. By using cheap pure steam as a gasification agent, the heating value of the product gas is high while costs can be kept low. In this case the gasification process becomes allothermal which means that the heat for the process has to be provided externally. This issue is solved with the dual fluidized bed system by using a solid heat carrier that transports the desired heat for gasification from a separate combustion reactor to the gasification reactor. The dual fluidized bed gasification technology has been developed at the Vienna University of Technology and has already been demonstrated at industrial scale. Originally designed for wood chips, the system can also handle a large number of alternative fuels. The advantage of fuel flexibility has turned out to be a key issue for the commercial breakthrough of this technology. Therefore, tests have been accomplished with various solid fuels beyond the standard fuel (wood), such as different chars, coals and plastics. A focus of the investigations in this work is the influence of the different fuels used pure and by blends for co-gasification on the product gas quality and conversion performance in the gasification reactor regarding organic and inorganic fuel components as well as physical properties of the fuels. As it is shown in this work, the performance of the system and especially the tar content can be influenced by the chosen feedstock and by co-gasification of two different fuels in a wide range: While for gasification of pure polyethylene a GC/MS tar content of about 20.5 g/Nm^3_{db} was detected, the GC/MS tar content for char gasification vanished completely. The comparably good conversion performance of the used lignite is explained in detail regarding the catalytic activity of the fuel ash.

To consider also the potential for process optimization by changing operating parameters, the investigations of this work also include the possibilities of changing values like gasification temperature, fuel feeding position, bed material particle size and the amount of steam used for gasification.

As a large number of different gasification tests are summarized in this thesis, the gained data is used to find a correlation between the tar content in the product gas and one of the main gas components. The idea behind this is that most of the tar determination methods are discontinuously, so an online estimation of the actual tar content can make it easier for plant operators to immediately change operating conditions towards higher gas qualities and lower tar contents.

Kurzfassung

Die Vergasung von festen Brennstoffen zur Energiebereitstellung als auch zur Synthese von flüssigen und gasförmigen Brennstoffen erfährt seit Jahren steigendes Interesse einerseits mit dem Hintergrund der Nutzung erneuerbarer Energieträger wie Biomasse und andererseits, um unabhängiger von Öl zu werden. Konventionelle, autotherme Vergasungstechnologien benötigen ein oxidierendes Vergasungsmittel, wie Luft oder Sauerstoff (O_2), um einen Teil des Brennstoffes und des entstehenden Produktgases zu oxidieren und die Vergasungsenergie bereitzustellen. Der Nachteil durch die Verwendung von Luft besteht allerdings darin, dass durch die große Mengen an Stickstoff in der Luft das Produktgas stark verdünnt wird und der Stickstoff für anschließende Syntheseprozesse hinderlich ist. Die Verwendung von Sauerstoff ist hingegen teuer (Sauerstoffproduktion) und deshalb oft ökonomisch unattraktiv. Wird hingegen reiner Dampf verwendet ist das Produktgas auch frei von Stickstoff und Dampf als Vergasungsmittel ist außerdem äußerst kostengünstig. Der Nachteil hierbei besteht darin, dass der Vergasungsprozess dadurch allotherm wird, was bedeutet dass die Energie für den Vergasungsprozess extern bereitgestellt werden muss. Diese Aufgabe wird durch die Zweibettwirbelschicht-Vergasungstechnologie, entwickelt an der Technischen Universität Wien, gelöst.

Diese Vergasungstechnologie war ursprünglich vorgesehen, um holzartige Biomasse zu vergasen. Es hat sich aber herausgestellt, dass diese Technologie eine große Brennstoffflexibilität aufweist, was sich in der industriellen Anwendung als großer Wettbewerbsvorteil zeigen wird. Um die Forschung in Richtung der Erweiterung der Brennstoffpalette über den Standardbrennstoff zu erweitern, befasst sich diese Arbeit mit den Auswirkungen von verschiedensten fossilen und erneuerbaren festen Brennstoffen, sowie Kunststoff als Rohstoff, auf die Leistung des Zweibettwirbelschicht-Vergasungssystems und die Produktgasqualität. Ein Kernaspekt hier ist der Einfluss der organischen als auch anorganischen Brennstoffzusammensetzung auf die Gasqualität und wie die positiven Eigenschaften von Brennstoffen in Brennstoffmischungen zur Steigerung der Qualität genutzt werden können, da besonders die Teerwerte in einem großen Bereich variieren können: Wurden bei der Vergasung von reinem Polyethylen (PE) 20,5 g/Nm^3_{tr} an Teer im Produktgas gefunden, was der höchste Wert war, wurden bei der Vergasung von Koks kein Teer (GC/MS detektierbarer Teer) gefunden. Als besonderes Highlight in der Brennstoffpalette stellte sich die verwendete Braunkohle heraus, die sowohl eine hohe Gasproduktion erzielte als auch niedrige Teerwerte erreichte. Hier ist auch der katalytische Effekt der anorganischen Bestandteile (Asche) gut zu beobachten.

Die Verbesserung des Prozesses wurde zusätzlich durch die Brennstoffeigenschaften auch durch die Anpassung von Prozessparametern vorangetrieben. So werden in dieser Arbeit auch Kenngrößen wie Vergasungstemperatur, Partikelgröße des verwendeten Bettmaterials und der Dampfmenge für den Prozess, als auch der Ort der Brennstoffeinbringung, untersucht.

Da im Zuge dieser Arbeit eine große Anzahl an Vergasungsversuchen an einer 100 kW Zweibettwirbelschicht Versuchsanlage durchgeführt wurden und so eine Vielzahl von Messwerten lukriert wurden, können mit diesen Werten Abhängigkeiten des Teergehaltes von Gaskomponenten abgeleitet werden. Die Idee dahinter ist, dass die gängigen Messmethoden zur Teerermittlung im Gas nicht online durchgeführt werden können und somit eine Anpassung der Betriebsparameter im

laufenden Betrieb einer Anlage für den Betreiber sehr schwierig ist. Für die Hauptgaskomponenten ist das jedoch Stand der Technik. In dieser Arbeit wird deshalb abschließend auch beleuchtet, welche Hauptgaskomponenten sich am besten zur indirekten Abschätzung des Teerwertes eignen.

Publications

This PhD thesis is based on the following related publications.

I. S. Kern, C. Pfeifer, H. Hofbauer. Gasification of wood in a dual fluidized bed gasifier: Influence of fuel feeding on process performance. *Chemical Engineering Science*, 90, 284-298, **2013**.

II. S. Kern, C. Pfeifer, H. Hofbauer. Gasification of lignite in a dual fluidized bed gasifier - Influence of bed material particle size and the amount of steam. *Fuel Processing Technology*, 111, 1-13, **2013**.

III. S. Kern, C. Pfeifer, H. Hofbauer. Co-Gasification of Wood and Lignite in a Dual Fluidized Bed Gasifier. *Energy & Fuels*, 27(2), 919-931, **2013**.

IV. S. Kern, C. Pfeifer, H. Hofbauer. Cogasification of polyethylene and lignite in a dual fluidized bed gasifier. *Industrial and Engineering Chemistry Research*, 52(11), 4360-4371, **2013**.

V. S. Kern, C. Pfeifer, H. Hofbauer. Gasification of low grade coal in a dual fluidized bed steam gasifier. *Energy Technology*, 1(4), 253-264, **2013**.

VI. S. Kern, C. Pfeifer, H. Hofbauer. Dual fluidized bed steam gasification of coal and pyrolyzed coal. In: *Proceedings of the Fluidization XIV Conference*, May 26-30, Noordwijkerhout, The Netherlands, **2013**.

VII. S. Kern, C. Pfeifer, H. Hofbauer. Dual fluidized bed steam gasification of coal and biomass: Influence of the state of pyrolysis on the process performance. In: *Proceedings of the Clearwater Clean Coal Conference*, June 2-6, Clearwater, Florida, USA, **2013**.

VIII. S. Kern, C. Pfeifer, H. Hofbauer. Co-gasification of wood and hard coal in a dual fluidized bed steam gasifier: process efficiency vs. gasification temperature. In: *Proceedings of the 21st International Conference on Fluidized Bed Combustion*, June 3-6, Naples, Italy, **2012**.

Contribution by the Author

I., II., III., IV., V., VI., VII.	Responsible for experimental work, data evaluation and writing
VIII.	Responsible for data evaluation and writing

Related publications not included in this work

The following publications are related to this work and have been published during the formulation of this Thesis. However, they are not included as their topics partially overlap with the publications in this work or are out of the scope of this thesis. The publications are listed in in chronological order.

- S. Kern, C. Pfeifer, H. Hofbauer. Product gas formation in a gasification reactor by gasification of lignite and wood in a dual fluidized bed steam gasifier. *submitted to Fuel*, **2013**.

- S. Kern, C. Pfeifer, H. Hofbauer. Reactivity tests of the water gas shift reaction on fresh and used fluidized bed materials from industrial DFB biomass gasifiers. *Biomass & Bioenergy*, **2013**, doi: 10.1016/j.biombioe.2013.02.001.

- S. Kern, M. Halwachs, G. Kampichler, C. Pfeifer, T. Pröll, H. Hofbauer. Rotary kiln pyrolysis of straw and fermentation residues in a 3 MW pilot plant – Influence of pyrolysis temperature on pyrolysis product performance. *Journal of Analytical and Applied Pyrolysis*, 97, 1-10, **2012**.

- S. Kern, C. Pfeifer, H. Hofbauer. Synergetic Utilization of Biomass and Fossil Fuels: Influence of Temperature in Dual Fluidized Bed Steam Co-gasification of Coal and Wood. *International Journal of Environmental Science and Development*, 3(3), 294-299, **2012**.

- F. Kirnbauer, V. Wilk, H. Kitzler, S. Kern, H. Hofbauer. The positive effects of bed material coating on tar reduction in a dual fluidized bed gasifier. *Fuel*, 95, 553-562, **2012**.

- S. Kern, C. Pfeifer, H. Hofbauer. Synergetic Utilization of Renewable and Fossil Fuels: Dual Fluidized Bed Steam Co-gasification of Coal and Wood. *APCBEE Procedia*, 1, 140-144, **2012**.

- S. Kern, C. Pfeifer, H. Hofbauer. Dual fluidized-bed steam gasification of solid feedstock: Matching syngas requirements with fuel mixtures. In*: Luckos, T. and P. den Hoed (Eds.), Proceedings of Industrial Fluidization South Africa (IFSA 2011)*, November 16-17, Johannesburg, South Africa: 67-78, **2011**.

- V. Wilk, S. Kern, H. Kitzler, S. Koppatz, J.C. Schmid, H. Hofbauer. Gasification of plastic residues in a dual fluidized bed gasifier - Characteristics and performance compared to biomass. In: *Proceedings of the International Conference on Polygeneration Strategies (ICPS11*), August 30 – September 1, Wien, Austria, **2011**.

- S. Kern, M. Halwachs, T. Pröll, G. Kampichler, H. Hofbauer. Rotary kiln pyrolysis - first results of a 3 MW pilot plant. In: *Proceedings of the 18th European Biomass Conference and Exhibition*, 3 - 7 May, Lyon, France, **2010**.

- M. Halwachs, G. Kampichler, S. Kern, H. Hofbauer, H. Valorisation of low grade biomass by using low temperature pyrolysis. In: *Proceedings of the 18th European Biomass Conference and Exhibition*, 3 - 7 May, Lyon, France, **2010**.

- M. Halwachs, G. Kampichler, S. Kern, H. Hofbauer. Low temperature pyrolysis of agricultural residues - first results of a pilot plant. In: *Proceedings of 1st International Conference on Polygeneration Strategies*, September 1-4, Vienna, Austria, **2009**.

Contents

1. Introduction

1.1 Energy and environment

The world's energy demand is growing constantly, and the greater part of the total amount is currently covered by oil and gas [1]. Energy is the most important fundamental base of growth for economics and prosperity of a population. Thus, the word population is growing in relative numbers approximately 1.2 % every year, the world primary energy demand is growing consequently as the energy demand is still linked to the three main reasons: growth of economics, population, and grade of urbanization of a society. For the period of the next 22 years (until 2035) an annual average growth of the world population of 0.9 % is predicted while the rate of urbanization all over the world will rise to 61 % from a today's value of 51 % [2]. As a consequence the total energy demand will continue to grow. The world primary energy demand increased about 2.5 % in 2011 which more or less goes along with the average value of the last ten years. There has to mentioned that the growth of Non-OECD countries' energy demand was even higher with an increase of 5.3 % while a decrease of the energy demand of 0.8 % was recorded for the OECD countries in 2011. This impressively shows the potential of growth of the emerging countries that are not included in the OECD counties.

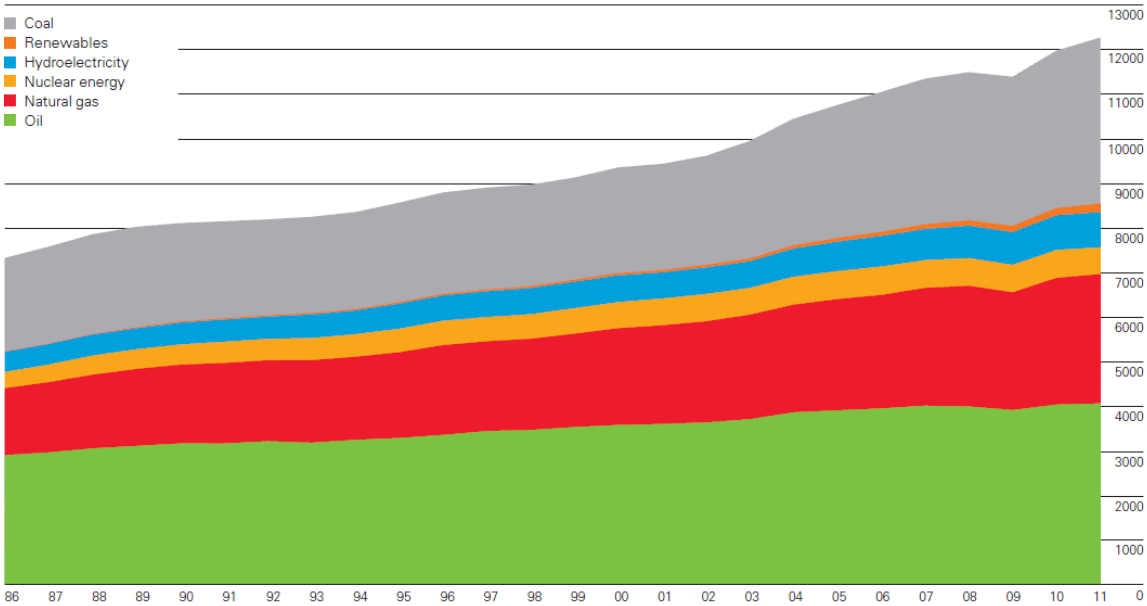

Figure 1: Trend of the world primary energy demand showing shares of each primary energy source [2].

The increase of the world primary energy demand including the shares of each energy main source is shown in Figure 1. There can be seen that the most significant contribution for the increase during a period of the last 25 years was provided by natural gas and coal. Currently the shares of the world primary energy demand of the three main fossil fuels oil, natural gas and coal are 33.1 %, 23.7 % and 30.3 %, respectively [1].

As the total amount of required energy is caused by economics and population growth as well as the grade of urbanization, the formation of the shares of the main fossil energy sources (oil, natural gas, coal) is defined by the factors that are availability as well as the price of the fuel. For a long-term energy strategy also a low fluctuation of its price combined with a steady availability is necessary. As fossil fuels are limited when used in a comparably short period as it is the case for the use by mankind, the amount of their reserves is essential for the market. Dated by the end of 2011 the reserves of oil were calculated to last for 54 years and 63 years were predicted for the range of natural gas for conventional oil and gas recovery based on the assumption that the consumption does not change from nowadays value. These numbers are comparably low compared to the worldwide resources of coal. Huge amounts of coal are currently available, with the reserves that can be mined at lowest mining costs calculated in 2011 to last for at least another 112 years [1]. These "ranges" of the fossil fuels have also an impact on the volatility of the price structure as the price of oil on the world market is the most volatile. From 2010 to 2012 the price for one barrel of crude oil (Brent) increased about 40 %, which was the highest climb of the three fossil fuels in this time period, while the average market price for coal (northwest European price and US central Appalachian coal) increased only about 26.6 %, marking the lowest price climb for fossil fuels [1]. The low price in combination with the highest resources for coal is the reason why coal will also play the role of the backbone of the energy system in the next years [2].

An issue for countries that have no access to fossil fuels in their own country is their dependency on countries that are rich in fossil fuels. Nearly 50 % of the world reserves of crude oil are located in countries of the Middle East while only 8.5 % of the reserves are located in the huge area of Europe and Eurasia and only 2.5 % in the Asian-Pacific region. The solid fuel coal is able to counterbalance this overweight as large reserves are located in countries which are poor in oil (35.4 % in Europe and Eurasia and 30.9 % in Asia-Pacific) [1]. This is an additional fact that explains the popularity of coal in the emerging countries.

For a long-term perspective of the energy system it is essential so save the limited resources of fossil fuels by using high efficiency conversion methods for fossil fuels and the change to a mix of renewable resources. As biomass represents the only renewable source of carbonaceous resources, the focus here in terms of renewable fuels is on biomass. The advantage of biomass as a fuel is that this resource is distributed more equally all over the world compared to fossil fuels and can help to strengthen the autonomy of local communities and countries that cannot benefit from own fossil fuels.

Another resource which attracts increasing interest especially in the European Union is waste material like plastics. Plastics occur in large amounts mostly in consumer goods, packaging materials and many other single-use applications. Therefore, huge quantities of plastic wastes are produced. In the countries of the European Union, more than 250 x 10^6 tons of municipal solid wastes are produced annually [3]. In 2007 in the United States, 12.1% of the waste produced contained plastics, giving an indication of the large proportion of plastics occurring as wastes [4]. The European Directive 94/62/EC promotes recycling, re-use and other forms of plastic waste recovery. One of the targets is that between 55 and 80% by weight of packaging waste has to be recycled. Recycling involves either conversion back into the monomer or into another product. Plastic waste recycling and treatment processes can be divided into four major categories: re-extrusion (primary), mechanical (secondary), chemical (tertiary) and energy recovery

(quaternary) [5]. Since plastics have a very high lower heating value (LHV) of up to 43 MJ/kg, they can be burned immediately, for example, in municipal waste incinerators to recover heat and produce electricity, or they can be used as an additional fuel for blast furnaces or cement kilns.

From the fuels discussed up to now, coal, biomass and wastes will continue to increase their share in the world primary energy demand. Therefore, effective conversion methods for the utilization of these solid fuels have to be provided.

Combustion of the solid fuels for heat or power (electricity) generation is popular and state-of-the-art. However, it has a drawback that the chemical structure of the fuels is lost. Conversion of a solid feedstock by gasification to a high quality product gas expands the possibility of the utilization of solid fuels beyond heat and power production as this gas can be used as a source for many synthesis processes that are based on oil or natural gas today.

Although coal based gasification processes of power generation have not proven themselves to have an economic advantage compared to combustion power plants using coal or other fossil fuels, as the investment costs for IGGC (Integrated Gasification and Combined Cycle) power plants are much higher, power generation via coal gasification retains certain advantages. For instance, its electrical efficiency is greater [6], and if the process is combined with carbon capture and storage (CCS) the costs are lower in terms of both initial investment and operation [7]. In the case of heat and electricity production for biomass there can also been found advantages regarding the conversion efficiency for gasification compared to combustion [7].

Gasification can also convert biomass or plastic waste into electric power with high efficiency or allow co-firing of the product gas in combustion processes that cannot deal with the physical properties (like bad grindability) of these fuels, such as pulverized coal firing [8]. Another advantage of gasification over the incineration is that the process gas volume is lower, which reduces the costs for gas cleaning [9] as the gas cleaning step turned out to be the most cost intensive part of the whole processes [10]. Furthermore, the production of undesired components like dioxins is decreased by the operating conditions in a gasifier which is especially a point of interest for waste plastics [11].

Since these three oil alternatives attract increasing interest in the energy sector, gasification of mixtures of biomass or plastic wastes with coal can be the basis for an efficient utilization of biomass or plastics. The breakthrough for this intention can only be reached by a system whose fuel flexibility allows the use of these very different types of solid fuels.

1.2 Thermochemical conversion of solid feedstock

Thermochemical conversion of solid feedstock is the main common route for the conversion of solid carbonaceous fuels (coal, biomass, wastes) to valuable products like heat and power in form of electricity. In general three main types of thermochemical conversion are highlighted, which are pyrolysis, gasification and combustion. These three main processes are in general only determined by the amount of oxidizing agent that is provided to the system and the reaction temperature, as shown in Figure 2.

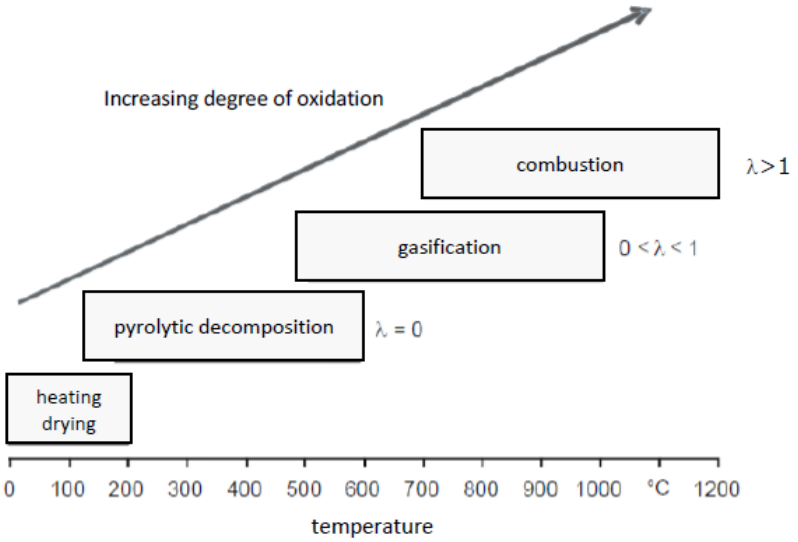

Figure 2: Sub-processes of thermochemical conversion, adapted from [12].

While for a complete combustion of the solid fuel an excessive oxygen supply has to be provided, the sub processes of combustion (gasificantion, pyrolysis) can be characterized by the air ratio λ that is defined as the amount of air used in the process in relation to the amount of air needed for a complete stoichiometric reaction [12].

$$\lambda = \frac{\dot{m}_{air}}{\dot{m}_{air,stoich..}} \tag{1}$$

Due to the O_2 rich atmosphere for the combustion process, all of the carbon and hydrogen present in the fuel is oxidized to CO_2 and H_2O. Compared to the combustion process, for an authothermal gasification process (no external heat supply) the oxygen supply can be reduced to values where the required reaction temperature can be maintained. As a result the complete oxidation of the gasification products, which are theoretically mainly H_2 and CO, is interrupted and the formed gaseous products can be utilized separately from the combustion step. The pyrolysis process is operated at the absence of oxygen in the reactor to avoid any oxidation of the char that is left after devolatilization/pyrolysis of the solid fuel. Therefore pyrolysis yields also a solid product, pyrolysis char. The gaseous pyrolysis products are often divided in non-condensable gas components (permanent gases) and condensable gas components (tar) as due to the gas formation out of the volatile matter of the fuel the gaseous array of products is very wide ranged. As shown in Figure 2,

the pyrolysis step is a sub-process of gasification and pyrolysis and gasification provide the gaseous fuel for the combustion step. More or less these steps occur simultaneously in a reactor. While for complete combustion all condensable and non-condensable gaseous products of pyrolysis and gasification are oxidized, the final products of the gasification process are usually a mix of gas made by devolatilization (pyrolysis) and gasification of solid carbon. This illustrates the complexity of the gasification process.

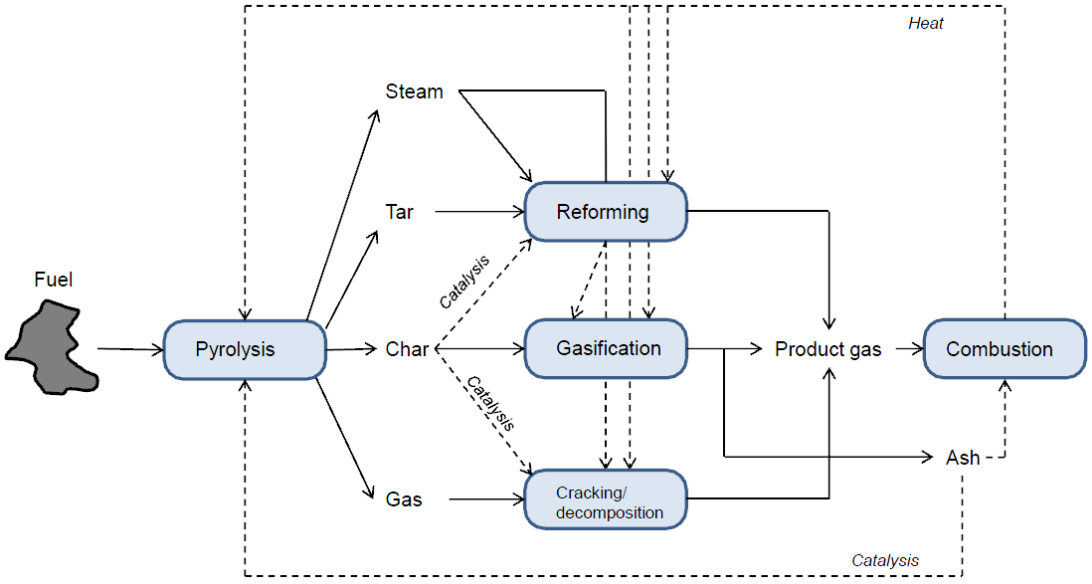

Figure 3: Illustration of the reaction network and dependencies during gasification of solid feedstock [13].

During those three steps of thermochemical conversion, explained before, several secondary reactions occur simultaneously with some of them able to improve the performance for the desired process aim. Such reactions include reforming and cracking of tars and hydrocarbons as well as homogeneous gas reactions that adjust the gas composition towards equilibrium. The most representative reaction is the water-gas-shift reaction (WGS). Figure 3 provides an overview of the reaction network for the thermochemical conversion of solid carbonaceous fuel with the solid lines showing material flows and broken lines giving information of possible interactions.

The first step for a solid fuel particle is the pyrolysis step where already included the drying step occurs and water is released of the particle. Further heating leads to devolatilization of the fuel, so pyrolysis gas is released (including tar) and char which is the fuel for the gasification step. The most common reactions that can be ascribed to the pyrolysis step are decomposition, polymerization and hydrogenation [14,15]. The solid char is gasified by a gasification agent such as O_2, H_2O or CO_2. As H_2O is released during the drying step and CO_2 can be formed by pyrolysis even in the case of autothermal gasification with an oxidizing gasification agent (O_2), a mix of those gasification agents is usually present for gasification. A very important part of desired in-situ reactions affects the reduction of condensable gaseous products (tar) in the reactor which mainly can occur by reforming (mostly by H_2O and little with CO_2) [16-18]. The char in the system can act as a catalyst for many reactions concerning tar reduction by the high surface [19] while some inorganic elements in the system (ash or bed material in fluidized bed reactors) also positively affect these reactions [20].

As the overall energy enthalpy of reaction for drying, pyrolysis and gasification is positive (endothermic processes), the required energy is provided by a partial oxidation of the gaseous products which means that an oxidizing gasification agent (air, O_2, H_2O+O_2, etc.) has to be used to drive the process autothermally. If no free oxygen is present in the gasification agent, the process becomes allothermal and the heat to drive the process has to be provided externally.

This rough explanation above shows the intricacy of the steps of thermochemical solid feedstock conversion that is the focus of this work.

1.3 Types of gasification reactors

As explained in section 1.2 there has to be distinguished between autothermal and allothermal gasification, which is basically specified by the heat supply for the endothermal gasification process. As for autothermal gasification processes the heat for gasification has to be provided simultaneously in the reactor where the gasification process occurs, an oxidizing gasification agent like air, O_2, or a mixture of air and H_2O or O_2 and H_2O that provides enough O_2 for maintaining the chosen gasification temperature. A big benefit of the autothermal gasification reactor design is its simplicity that results in lower investment costs. If the heat for the process has to be provided externally, the system is called allothermal. In the case of gasification, the system becomes allothermal if the content of free oxygen in the system is insufficient to provide the heat for gasification by partial oxidation of the product gas. Usually systems using pure H_2O or CO_2 as gasification agent are allothermal systems.

An overview of the most common basic reactor designs for gasification is shown in Figure 4. The basic groups of gasification reactors are fixed bed reactors, fluidized bed reactors and entrained flow reactors.

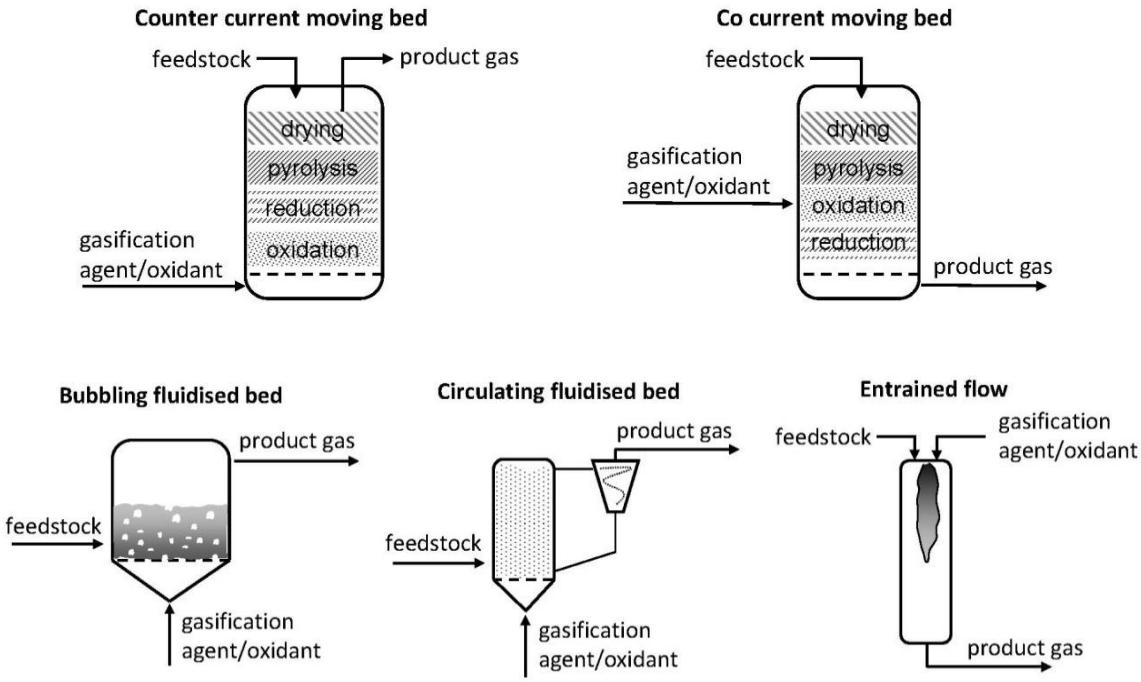

Figure 4: Basic reactor designs for authothermal gasification [21].

In general two types of fixed bed reactors are in use, which differ only in the direction of the gas flow, downdraft-fixed bed reactors and updraft-fixed bed reactors. In updraft-fixed bed gasifiers the gas flow inside of the reactor is upwards which means that the gasifying agent is fed from the bottom and the solid fuel is fed from the top. This counter-current flow system is characterized by a high thermal efficiency as the hot gas from the bottom is used to heat up the fresh solid fuel and therefore the gas leaving the reactor has a comparably low temperature. However the gas quality

suffers by this counter-current flow as the gas has a high load of tar due to the missing residence time of pyrolysis gas in the hot zone [22]. In the case of a downdraft design of the reactor the gas and fuel flow directions are co-current. Therefore, the gas-exit temperature is high, which results in a penalty of the thermodynamic efficiency but this design the gas made in the pyrolysis zone has to pass the hot zone at the end of the reactor, so tar levels are low using this system. The general benefit of the fixed bed system is simplicity. However the scale up of the reactor design is limited and the product gas quality limits the downstream utilization of the gas to heat and power production [23].

In a fluidized bed reactor, the reaction zones are not distinguished like in a fixed bed (Figure 4), the reactor can be described as nearly ideally stirred vessel as the hot bed material in the reactor leads to a more uniform temperature distribution [24]. Fluidized bed technology for gasification offers several advantages, listing some of them below [25]:

- Excellent temperature control
- High heating rates (>1000 K/sec)
- Moderate tar levels in the product gas
- Good scale up potential
- Wide fuel particle size range applicable
- Excellent gas-solid contact
- Possibility to use catalytic active bed material to enhance reactions

To types of fluidized bed reactors are used for gasification which are bubbling fluidized beds and circulating fluidized beds. The fluidized bed gasification technology was first commercialized in 1926 with the Winkler gasifier, a bubbling fluidized bed [26]. This was the first industrial application of a fluidized bed reactor. For large scale applications, circulating fluidized beds are used that are operated with higher superficial velocities.

For large scale gasification (>100 MW_{th}) of coal, entrained flow reactors are the most used reactors. This reactor benefits from a very simple and robust design. A fuel slurry of fine grinded fuel particles are introduced into the reactor with the gasification agent (in most of the cases a mixture of O_2 and H_2O) and converted at very high temperatures (>1200 °C) to gas. Due to the small particles and the high temperatures, the residence time of the particles is very short; the whole gasification process takes place in the entrained flow phase. A big benefit is the low amount of tar in the product gas due to the high reaction temperatures. However the system is economically feasible only at large scale and the fuel has to be suitable to be grinded to fine particles.

1.4 Dual fluidized bed gasification for allothermal gasification

Fluidized bed gasification turned out to be the most suitable reactor design for biomass gasification, especially regarding fuel particle size [27]. For coal gasification, the most common technology is entrained flow gasification with oxygen and steam as the gasification agent. The disadvantage is the huge amount of pure oxygen that is required to drive the process autothermally; this is an expensive medium and, moreover, its use is ecologically questionable. The drawback of using air instead of oxygen is that a lot of nitrogen is introduced, which dilutes the product gas and lowers the heating value of the product gas down to about 3-6 MJ/Nm³ [23,28]. The utilization of oxygen produces a higher quality gas, but increases operating costs as the production of oxygen requires 0.25-0.30 kWh/kg_{O2}[29] for an O_2 purity of 99.5%. When steam or CO_2 are used as the gasification agent, the product gas is free of nitrogen and the calorific value of the gas is quite high; for steam gasification, values between 10 and 18 MJ/Nm^3_{db} can be reached [30,31].

The advantage using steam instead of CO_2 is that the reactivity of steam is, on average, about four times higher than that of CO_2[32], so residence times of the char in the gasification section would have to be longer, and gasification efficiency would suffer. With H_2O or CO_2 as the gasification agent, the process becomes allothermal, so the heat for the endothermic gasification reactions has to be provided externally. A solution for the external introduction of the heat for gasification at an industrial scale can be provided by dual fluidized bed gasification (DFB). This technology separates the combustion reactor, which provides the energy for gasification, from the gasification reactor and pure steam is used as the gasification agent. Circulating bed material between these two reactors carries the heat from the combustion reactor to the gasification reactor.

The dual fluidized bed technology makes a separation of process steps possible by coupling two reactors. While in the main reactor the desired reaction takes place in the second reactor decoupled reactions can occur [33]. The first and most known application of such a system is the fluid catalytic cracking (FCC) process in refinery technology. In the main reactor of a FCC unit the cracking reactions take place which leads to char deposition on the catalyst. This makes regeneration by burning the char in the coupled reactor necessary. Therefore, this second reactor is often called regenerator. The released heat from catalyst regeneration is transported with the solid catalyst particles to the main reactor where heat for feed evaporation and cracking reactions is needed.

Figure 5 shows the basic principle of the dual fluidized bed technology with its application for steam gasification. Further applications where dual fluidized bed technology plays a key role are, in addition to the fluid catalytic cracking process [34] and dual fluidized bed steam gasification, the use for gasification with simultaneous removal of CO_2 by sorbents as bed material (sorption enhanced reforming) [35], chemical looping combustion [36] or chemical looping reforming [37].

This dual fluidized bed (DFB) gasification technology has been successfully demonstrated, in Güssing and Oberwart, Austria, on the 8 and 10 MW_{th} scale, since 2001 and 2008, respectively [38-40]. Further plants in Villach, Austria [41], Gothenburg, Sweden [42] and Senden, Germany, are currently under construction or in the startup period, and will gain a fuel power of 15 MW (Villach, Senden) and 32 MW (Gothenburg).

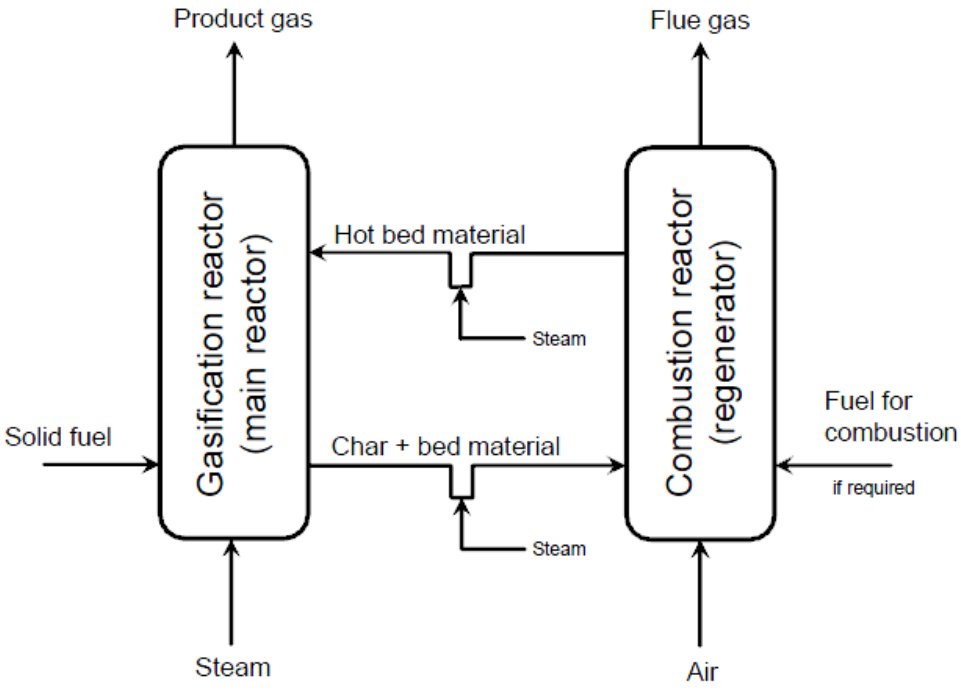

Figure 5: Basic principle of the dual fluidized bed process

1.5 Review of autothermal gasification plants at industrial scale

This section provides an overview of the status of coal gasification facilities worldwide. Based on the basic types of reactors for autothermal gasification (section 1.3.1), different modifications of the already explained basic types are in operation. Thus, the most common types are explained briefly below.

Lurgi gasifier

The Lurgi gasifier, also known as the Lugri dry-ash gasifier, was first developed in the 1930s. It is a pressurized, updraft-fixed bed gasifier using an oxygen/steam mix as gasification agent. A high ratio of steam to oxygen is used to keep the temperature at a moderate level. Therefore the ash does not melt and can be removed in a dry state. Since the reaction takes place at relatively low temperature, highly reactive feedstock is preferred. The system was acquired in the early 1950s by Sasol for commercial use of coal gasification and is therefore also known as Sasol-Lurgi gasifier. Working as a counter-current flow gasifier the product gas contains a relatively high amount of tar [43].

Winkler gasifier

The Winkler gasifier was developed in 1926 in Germany, thus making it the oldest gasification technology. It was firstly designed as a gasification process for using lignite coal. The Winkler gasifier was the first industrial application of a bubbling fluidized bed reactor, commercialized in 1926 [44]. The gasification agent is a mixture of steam with air or O_2. The process was further developed to the High Temperature Winkler gasifier (HTW). This fluidized bed reactor works as a dry-feed, pressurized, dry ash system. The pressurized operation (1 MPa) should increase carbon conversion. Therefore a sophis-ticated coal lock system is required [7].

GE gasifier

The GE gasifier is an entrained flow gasification reactor with fuel feeding from reactor top. It was developed by the company Texaco and acquired by General Electrics Energy in 2004 [45]. Originally designed for gasification of oil, the system was adapted for coal slurry gasification and started its first operation for solid feedstock in 1983. The feedstock reacts authothermally with oxygen at temperatures between 1250 and 1550 °C [46]. There are two different possibilities for product gas cooling downstream of the reactor. The radiant cooling design uses a radiant product gas cooler generating high-pressure steam. A different approach is the usage of an exit water quench where the hot syngas after the gasifier is directly cooled passing a water quench. The latter method is less effective but also less expensive and thus also commonly applied.

Shell gasifier

The Shell gasifier is also an entrained flow reactor design with the fuel feeding at the bottom of the gasifier. The feedstock is introduced at two places, located opposite from each other at the reactor. Pure O_2 is used to gasify the solid feedstock at temperatures around 1600 °C (up to 2000 °C) and a pressure of between 3.0 and 4.2 MPa [7,46]. The ash-slag is removed in liquid state from the reactor bottom. As downstream gas cooler could suffer from the high gas temperatures, the gas is cooled at

the end of the gasification reactor by a cool recycled stream of product gas. Due to this, the gas is cooled down to 900 °C and can be processed in the gas cooler for further cooling. The shell gasifier was developed jointly with Krupp-Koppers with the system known as Prenflo [47].

ConcoPhillips E-Gas gasifier

The CocoPhillips E-Gas gasifier is an entrained flow reactor originally developed by DOW Chemicals and demonstrated at the Louisiana Gasification Technology Inc. (LGTI) from 1987 through 1995 [48]. The feedstock used is a coal/water slurry and O_2 is the gasification agent. The basic idea of the reactor design is to use more effectively the heat generated of the gasification with pure O_2 for the process, so a two-stage reactor has been developed. This means that about 80-85 % of the fuel is introduced together with the gasifying agent (O_2) in the first stage which is located in the lower area of the reactor while the rest of the feedstock is then added without oxygen in the hot atmosphere which is made in the first stage. By increasing ratios of feedstock used in stage two, the cold gas efficiency increases, but the load of unconverted char in the product gas simultaneously increases. Therefore unconverted char is recycled back to stage one.

Siemens gasifier

The Siemens gasifier was developed in the 1970s and firstly commercialized in 1984 at the Schwarze Pumpe power station in Germany. The gasifier is an entrained flow reactor that can basically be compared with the GE gasifier with the water quench arrangement for gas cooling. The main difference to the GE gasifier is that the used arrangement of the water quench at the Siemens gasifier is a water spray while for the GE system a water bath is used. Furthermore for the Siemens gasifier there is the option to use dry feed which requires a lock system for the fuel feeding system as the system is pressurized up to 2.8 MPa [7]. In the reactor temperatures between 1300 and 1800 °C are reached that form a tar free product gas [49].

KBR transport gasifier

The KBR transport gasifier is a circulating fluidized bed gasifier developed by Kellog, Brown and Root (KBR) in 1999. The special part of this system is the riser that is designed in the lower part with a wider diameter which lowers gas velocities and therefore enhances the reactions in this mixing zone. The coal is fed at the top of this mixing zone and the gasification agent is injected at the reactor bottom and below the fuel feeding point to balance the temperature differences. For the purpose of heat and power production, air and steam are used to be the gasification agent while for providing feed for synthesis processes O_2 and steam are used [7]. The process takes place at pressures between 1.1 and 1.8 MPa and a temperature of approximately 1000°C [50].

Beside the above explained gasification technologies used at large scale size there are of course further technologies available but there has to be kept in mind that most of them are modifications and developments of the explained types based on the three main reactor types which are fixed-bed, fluidized bed and entrained flow reactors. For example the Foster-Wheeler-partial gasifier is basically a circulating fluidized bed reactor that can be compared with the KBR transport gasifier without the mixing zone (enlargement of the riser diameter in the lower area). The Mitsubishi Heavy Industries (MHI) gasifier is an entrained flow gasifier that can be compared with the GE gasifier employing two stages (combustor and redactor). Table 1 provides a summary of actual

operated industrial gasification units and their general specifications. The list is ordered regarding the technology used. There can be seen that most of the gasification plants are operated with a GE gasifier, followed by systems delivered by Shell. However there has to be kept in mind that these two types provide only 32 % of the total product gas power of installed gasification plants while plants that are operated with the Lurgi-Sasol system achieve a product gas output of enormous 17 GW. This is more than half of the worldwide production by gasification which is about 32 GW. The huge production of this fixed-bed system can be explained with the two large plants in South Africa from Sasol that are producing liquid fuels and the gasification plant from the Dakota gasification Company (Great Plains Synfuels Plant) in North Dakota, USA. In total, the number of single gasification units is also the most for the Lurgi-Sasol system with 131 reactors.

In 2010, 53 gasification reactors for solid fuels were under planning, construction or in the start-up period which shows that newer technologies like ConocoPhillips, Prenflo or the KBR Transport Reactor are pushing into the market.

Table 1: Review of operated autothermal gasification plants worldwide in 2010 [51].

Plant Name	Country	Technology	Startup	Total gasifiers	Product gas capacity (Nm^3/day)	Product gas capacity (MW_{th})	Feedstock
Skive CHP	Denmark	Carbona/GTI	2008	1	232 000	32	Biomass/Waste
Jiangsu Sopo Group	China	ECUST/YKG	2009	1	5 184 000	708	Coal
Yankuang Cathay Coal Chemicals Co., Ltd.	China	ECUST/YKG	2005	1	3 792 000	518	Coal
Jiangsu Linggu Chemicals Co.,Ltd.	China	ECUST/YKG	2009	1	2 832 000	387	Coal
Yankuang Lunan Fertilizer Plant	China	ECUST/YKG	2007	1	1 896 000	259	Coal
Hualu Hengsheng Chemicals Co., Ltd.	China	ECUST/YKG	2005	1	1 152 000	157	Coal
Wabash River Gasification	United States	E-GAS (ConocoPhillips)	1995	2	4 320 000	591	Petcoke
Kymijärvi ACFBG Plant	Finland	Foster Wheeler ACFBG	1998	1	351 118	48	Biomass/Waste
Varkaus ACFBG Plant	Finland	Foster Wheeler ACFBG	2001	1	234 133	32	Biomass/Waste
Pietarsaari ACFBG Unit	Finland	Foster Wheeler ACFBG	1983	1	204 819	28	Biomass/Waste
Rodao ACFBG Unit	Portugal	Foster Wheeler ACFBG	1985	1	87 800	15	Biomass/Waste
Norrsundet ACFBG Unit	Sweden	Foster Wheeler ACFBG	1984	1	146 299	20	Biomass/Waste
Värnamo IGCC Demonstration Plant	Sweden	Foster Wheeler PCFBG	1993	1	105 000	14	Biomass/Waste
Haolianghe Ammonia Plant	China	GE	2004	1	2 200 000	300	Coal
Sinopec Jinling	China	GE	2005	1	2 100 000	287	Coal
GE China 4	China	GE	2005	1	2 100 000	287	Coal
GE China 3	China	GE	2005	3	2 100 000	287	Coal
GE China 5	China	GE	2006	3	2 080 000	284	Coal
GE Haolianghe, Heilongjiang	China	GE	2005	1	2 045 000	280	Coal
Shaanxi Ammonia Plant	China	GE	1996	3	2 040 000	279	Coal
Shaanxi Shenmu Chemical Plant	China	GE	2005	2	1 925 000	263	Coal
Shanghai Coking & Chemical	China	GE	1995	3	1 530 000	209	Coal
Hefei City Ammonia Plant	China	GE	2000	3	1 400 000	191	Coal
GE Jinling, Nanjing	China	GE	2005	1	1 275 000	174	Coal
Gas Plant No. 2	China	GE	1997	1	765 000	105	Coal
Lu Nan Ammonia Plant	China	GE	1993	2	525 000	72	Coal
Methanol Plant	Former Yugoslavia	GE	1987	1	1 540 000	211	Gas
Lavéra Syngas Plant	France	GE	1977	1	590 976	81	Gas
Pont-de-Claix Syngas Plant	France	GE	1989	1	278 000	38	Gas

Ube City Ammonia Plant	Japan	GE	1984	4	2 150 000	294	Coal
Ube City CO Plant	Japan	GE	1982	1	200 000	27	Petcoke
Polk County IGCC Project	United States	GE	1996	1	3 300 000	451	Coal
Coffeyville Syngas Plant	United States	GE	2000	2	2 141 200	293	Petcoke
Kingsport Integrated Coal Gasification Facility	United States	GE	1983	2	1 600 000	219	Coal
Zhao Zhuang	China	GTI U-GAS	2007	2	400 000	55	Coal
Gorazde Ammonia Plant	Former Yugoslavia	LP Winkler	1952	1	120 000	16	Coal
Nakoso IGCC	Japan	MHI	2007	1	6 880 800	449	Coal
Fuel Gas Plant	Germany	Sasol Lurgi CFB	1996	1	732 000	100	Biomass/Waste
Americentrale Fuel Gas Plant	Netherlands	Sasol Lurgi CFB	2000	1	614 300	84	Biomass/Waste
Puyang Ammonia Plant	China	Sasol Lurgi Dry Ash	2000	4	2 282 492	312	Coal
Shaanxi Ammonia Plant	China	Sasol Lurgi Dry Ash	1987	4	2 282 492	312	Coal
Zhong Yuan Dahua Group Ltd.	China	Sasol Lurgi Dry Ash	2000	3	2 282 492	312	Coal
Vresova IGCC Plant	Czech Republic	Sasol Lurgi Dry Ash	1996	26	4 700 000	636	Coal
Sasol Synfuels	South Africa	Sasol Lurgi Dry Ash	1977	40	39 600 000	7 048	Coal
Gasification East Plant	South Africa	Sasol Lurgi Dry Ash	1982	40	39 600 000	7 048	Coal
Great Plains Synfuels Plant	United States	Sasol Lurgi Dry Ash	1984	14	13 900 000	1 900	Coal
Shenhua, Majiata	China	Shell	2008	2	6 300 000	861	Coal
Sinopec, Anqing	China	Shell	2006	2	3 410 000	509	Coal
Dong Ting Ammonia Plant	China	Shell	2006	1	3 410 000	466	Coal
Hubei Ammonia Plant	China	Shell	2006	1	3 500 000	466	Coal
Yuntianhua Chemicals, Anning	China	Shell	2007	1	3 400 000	465	Coal
Yunzhanhua Chemicals, Huashan	China	Shell	2007	1	3 400 000	465	Coal
Puyang Plant	China	Shell	2008	1	3 410 000	463	Coal
Yongcheng Shell Plant	China	Shell	2007	1	3 100 000	424	Coal
Sinopec, Zhijiang	China	Shell	2005	1	n.i.	273	Coal
Kaixiang Chemical Plant	China	Shell	2008	1	1 720 000	257	Coal
Liuzhou, Guanxi, PRC	China	Shell	2005	1	1 720 000	256	Coal
Dahua Chemicals, Dalian	China	Shell	2007	1	1 700 000	232	Coal
Yinchenge Chemical	China	Shell	2006	1	1 320 000	197	Coal
Buggenum IGCC Plant	Netherlands	Shell	1994	1	3 408 000	466	Coal
Puertollano IGCC Plant	Spain	PRENFLO	1998	1	4 300 000	588	Coal

2. Scope of the work

The dual fluidized bed gasification system was originally designed for using woody biomass as a feedstock, but during operation of the industrial sized DFB biomass gasifiers, it turned out that fuel flexibility is a key issue for economic breakthrough. Beside the positive effects of using biomass as a feedstock for heat and power production as well as for the synthesis of liquid and gaseous fuels, there are currently some issues for operators that are faced with regional available biomass. The most important are mentioned below:

- The rate of the price growth for wood chips in the mid Europe region was excessively higher compared to the price increase for the products, which are currently made out of product gas, heat and electric power, which was negligible. This limits the profit margin of biomass based plants seriously.
- In some regions the danger of supply bottlenecks is sometimes present.
- The feedstock quality is fluctuating in a certain range as bioorganic feedstock is somehow a seasonal product. Here especially the water content of the fuel is varying.
- The plant size is in many cases limited to the supply chain. Thus, plant efficiencies often cannot reach its highest values.

As fluidized bed systems are well suited to fuel flexibility, a focus of this work is to expand the fuel portfolio of the biomass based DFB gasification system beyond biomass to the fossil fuel coal and plastic wastes. The variety of types of coals is huge as explained in section 3.1, ranging from lignite to anthracite. To represent three typical cases of coals used for heat and power generation, in this study two types of hard coal (Polish hard coal and Spanish hard coal) and lignite (Germany) are used (Table 4). The reasons for the choice of these coals are briefly explained below.

- Polish hard coal is characterized by a comparably high heating value while the ash content and the concentration of undesired species (S, N) is within the limits for conventional systems. Classified by ASTM D 388-05 [52], the coal is a High Volatile A bituminous coal. This coal is commonly used in Austria as a fuel for electricity production in pulverized fired power stations [53] and therefore easily available.
- The Spanish hard coal is mined in Puertollano, in the province of Ciudad Real, Castile-La Mancha, in the south of Madrid. According to ASTM D 388-05 [52], this coal is classified as medium volatile bituminous coal. In this study this coal has been chosen to represent a more or less cheap low grade coal as it is characterized by a huge content of inorganic matter (ash), which lowers the heating value, and a wide particle size distribution with a high fraction of fines.
- The German lignite is mined out for fluidized bed combustion systems and is characterized by a relatively low content of sulfur, nitrogen and ash, compared to other types of lignite. This fuel (Lignite A, according to ASTM D 388-05 [52]) was chosen as its properties seemed to be perfectly suited for fluidized bed gasification - the high content of volatile

matter improves reactivity in the system which can be beneficial in terms of efficiency considerations.

As an example for plastic wastes, polyethylene (PE) has been chosen to be used for this study with the reason that PE is the most used plastic resin and therefore the quantities of this polymer in the waste plastic fraction is the highest [54].

Biomass is still a matter of interest, especially wood pellets in this study. Gasification of wood pellets marks the benchmark for the DFB gasification system.

In addition to gasification of the pure fuels, two co-gasification campaigns of wood pellets and PE with lignite should give information about gas quality, process performance as well as any beneficial effects of the addition of coal to biomass or plastic in this process.

A second focus is to use state methods for improving gas quality with an emphasis of the reduction of condensable gaseous products (tars) in the product gas. This is important as it has turned out that the gas cleaning step is still the most cost intensive process step for removal of tars. While tar removal by scrubbers is economic unattractive [55], the use of ceramic filters comes with the drawback of a high pressure drop [56]. The strategies for reduction of the tar content will be

- Fuel oriented, and
- Process oriented

The fuel oriented strategy will include the influence of the fuel properties on the process, mainly the fuel composition with a focus in the ratio between volatile matter and fixed carbon, but also the fuel particle size and any catalytic potential of the fuel ash (if crucial).

The process oriented strategy of product gas quality improvement will include the dependency of the product gas composition by varying parameters like **gasification temperature**, **fluidization conditions** or the **fuel feeding position**.

As the tar content in the product gas is one of the main issues for fluidized bed gasification processes, a reliable indication of tar in the gas is necessary. Most of the methods available for tar sampling are discontinuous and cost intensive. One scope of this work will also be to find out if there is a reliable correlation between main gas components, whose measurement is state of the art, and the tar content.

3. Fundamentals

3.1 Solid fuels

3.1.1 Biomass

To build up biomass, green plants convert CO_2 into organic matter with the use of sunlight and water. Biomass represents stored solar energy that can be used at the time the energy is required. A part of the built biomass is used for the maintenance of the metabolism operation, as the built CO_2 has lower energy content than the organic molecules. This procedure is called CO_2 exhalation. During vegetation, only a small part of the primary irradiated energy is chemically bound. An illustration of this process is shown in Figure 6.

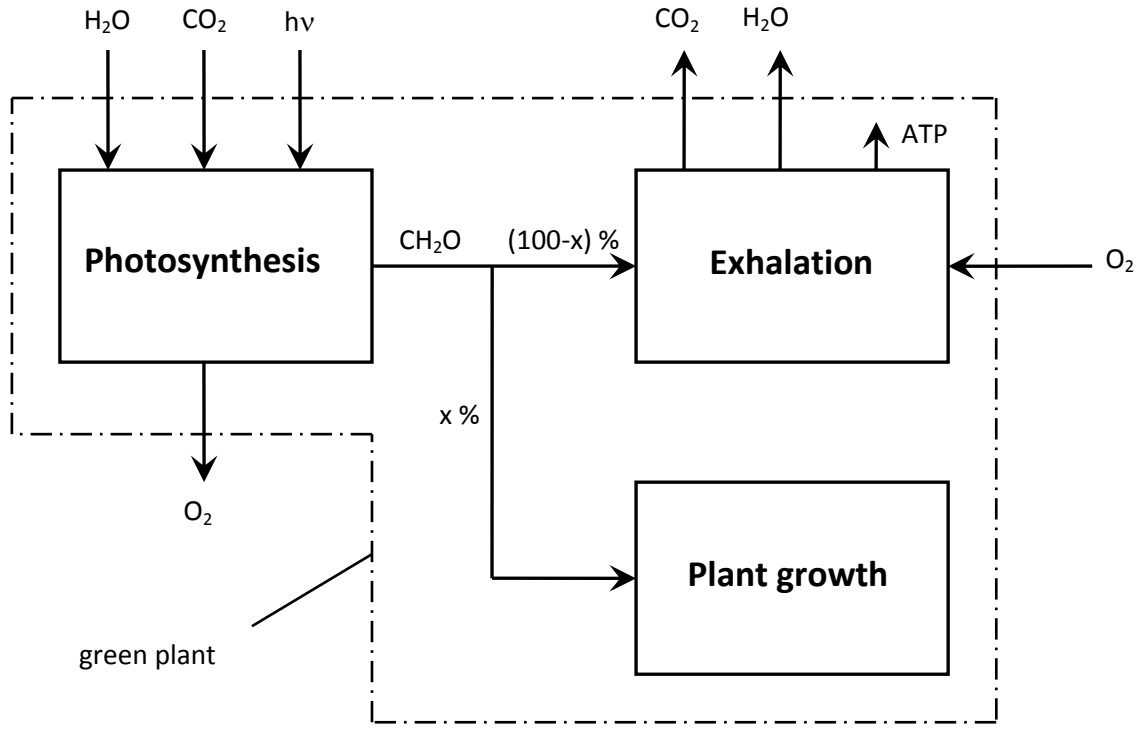

Figure 6: Photosynthesis and exhalation in a green plant [57].

The plant is able to use the radiation wavelength range from 400 to 700 nm. For the formation of glucose a theoretical efficiency of 33.2 % can be achieved. Considering the CO_2 exhalation and energy losses, the efficiency of the biomass formation is much lower than the theoretical efficiency. The average utilization of the radiation ranges between 0.04 % in the dessert and almost 2 % in the rain forest [58]. The highest conversion efficiencies are also dependent on the type of plant. There has to be distinguished between C3 and C4 crops. While C3 crops use the common way of photosynthesis, for photosynthesis of C4 crops an intermediate step is introduced which fixes the CO_2 before it can be used for photosynthesis. Therefore the energy demand for carbohydrate synthesis is higher but the loss due to photorespiration of C4 crops can be neglected. Thus, the efficiency of photosynthesis for C4 crops is higher as shown in Figure 7. However, more than 95 %

of the crops are C3 plants like woody biomass. In the larger part of Europe the net efficiency is between 0.8 and 1.2 %. For example in a central European hornbeam forest, there is an annual growth of 5.7 t above ground and 2.4 t in the form of roots, if an efficiency of 1 % is assumed [58].

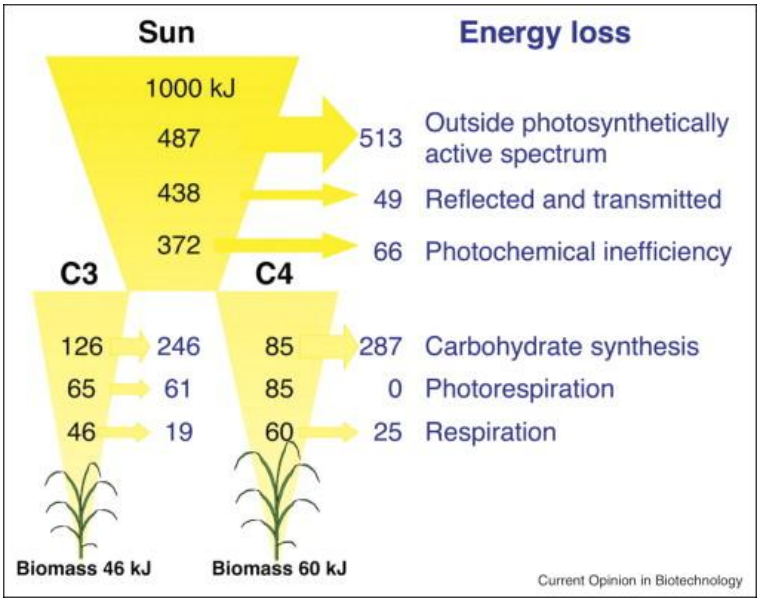

Figure 7: Effieiency of photosynthesis for C3 and C4 crops [59].

Every type of lingo-cellulosic biomass has a different composition with regard to its three major components: cellulose, hemicellulose and lignin. These three components also have different behavior during thermal decomposition. Kumar and Pratt [60] investigated the temperature range for the initiation of pyrolysis for cellulose between 275°C and 350°C, for hemicellulose between 150°C and 350 °C and for lignin from 250°C to 500°C. The main sources for gaseous products during the pyrolysis process of biomass are cellulose and hemicellulose, whereas hemicellulose causes more non-condensable gases and less tar than cellulose. Lignin behaves differently as it degrades slowly and the majority of its products are condensable, such as tar, and solid, such as char. Only about 10% of the initial mass of lignin is converted to gas [18].

Table 2: Structural analysis data of biomass samples (wt.% of dry and extractive free basis) [61].

Sample	Hemicelluloses	Cellulose	Lignin
Oriental beech	31.8	45.8	21.9
Oriental spruce	21.2	50.8	27.5
Wheat straw	39.1	28.8	18.6
Corncob	32.0	52.0	15.0
Tobacco stalk	28.2	42.4	27.0
Tobacco leaf	34.4	36.3	12.1

With this knowledge, a first estimation of the product yield of the pyrolysis process can be made depending on the type of biomass and the distribution of the main components. Examples for this distribution for beech and spruce wood, wheat straw and other biomass types are shown in Table 2.

3.1.2 Coal

Coal is usually found in deposits all over the world. The process of coal formation is called coalification. Basically, coal is fossilized peat as it is the final result of decaying vegetation, deposition and burying by sediments and movements in the earth crust. The conversion from peat to coal takes place when high pressure and temperature are applied to the peat which is responsible for the physical and chemical change of the coal. As this process takes a time of millions of years, today the whole range of coal products can be found on the world. In this coalification process the so called coal rank changes from lignite over sub-bituminous coal and bituminous coal to anthracite (Figure 8). The highest rank of coal is graphite which is not used commonly as a fuel and therefore not considered here.

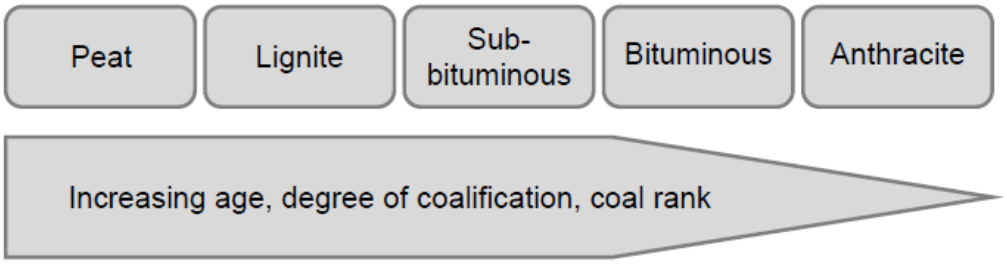

Figure 8: Coal rank

The formation of the coal ranks can be explained by the following reactions. Decaying plant matter is accumulated and forms peat by bacterial and fungal organisms (aerobic bacteria). By air oxidation, followed by decarboxylation and dehydration, lignite is produced from peat. The next steps for the formation of sub-bituminous coal are further decarboxylation and hydrogen disproportioning. Then, condensation to small aromatic ring systems is responsible for the elevation to bituminous coal. Anthracite is then also formed by condensation in addition with dehydrogenation [62].

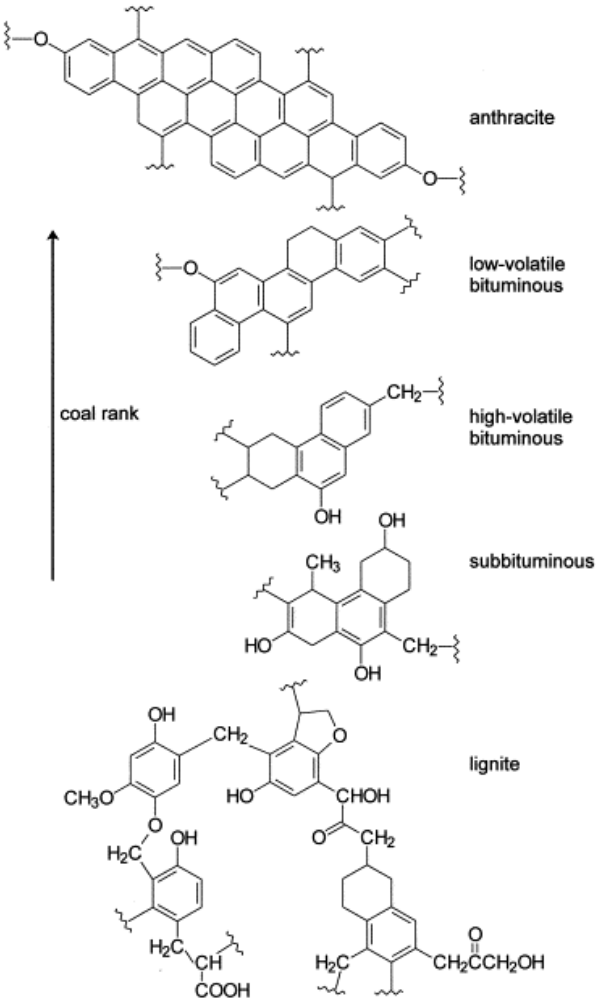

Figure 9: Examples of coal structures according to coal rank [63].

With increasing rank, less functional groups are present and the oxygen as well as the hydrogen content are reduced. Thus, the ring system becomes more polycondensed. An illustration of this process is shown in Figure 9. By analyses of typical representatives of each main coal type, given in Table 3, there can be seen that the carbon content increases while the oxygen content decreases with increasing coal rank.

Table 3: Analytical data for typical coals of different degrees of coalification [64]

Component	Unit	Peat	Lignite	Sub-bituminous	Bituminous	Anthracite
H_2O	wt.%	>75	56.7	31.2	3.7	1.0
Carbon	$wt.\%_{db}$	58.20	71.40	73.40	82.60	92.20
Hydrogen	$wt.\%_{db}$	5.63	4.79	4.86	4.97	3.30
Nitrogen	$wt.\%_{db}$	1.94	1.34	1.16	1.55	0.15
Sulfur	$wt.\%_{db}$	0.21	0.60	0.31	1.50	0.98
Oxygen	$wt.\%_{db}$	34.02	21.87	20.27	9.38	3.37

3.1.3 Plastics

Plastics display a huge variety in their types. There are currently more than 20 types of plastics available and each exhibits different potentials for recycling and thermal treatment. The main types of plastics used in the European Union (EU) are shown in Figure 10, where the most frequently used is polyethylene (PE), a thermoplastic resin that is mostly used for packaging.

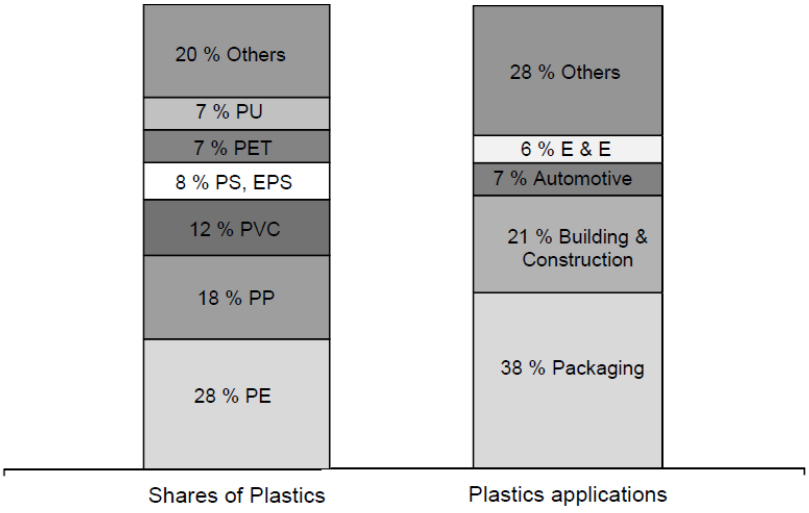

Figure 10: Shares of plastic types used and applications for plastics in the European Union [54].

Figure 10 also gives information about the use of plastics in the EU and confirms the fact that most of the plastics are PE used for packaging purposes. This is the reason why pure PE was used as the representative fuel for plastics in this study. Polyethylene $(C_2H_4)_n$, is a thermoplastic resin with a melting point between 120 and 130 °C.

3.1.4 General behavior of solid fuels in thermochemical conversion

As pyrolysis is a sub-process of gasification, a first estimation of the thermochemical behavior of the three main fuels investigated in this work, biomass (wood), coal and polyethylene, can be made by their pyrolysis behavior. A drawing of thermo gravimetric analysis of wood, PE and a typical bituminous coal is shown in Figure 11. There is illustrated that, as mentioned before, wood decomposes over a wider range compared to PE. This wide range of the weight loss can be ascribed to the presence of the three main components, cellulose, hemicellulose and lignin which decompose in different temperature ranges. However, the trend is still distinctive and shows clear borders when the reaction starts and ends. Also for PE pyrolysis the curve is very sharp and the temperature range is very small, between 450 and 490 °C. In the case of bituminous coal, the situation is different as the complex chemical structure leads to different steps in pyrolysis. Nevertheless, the trend is that pyrolysis of coal is much slower. By a more closer look on the final mass fraction at higher temperatures, there can be seen that only PE is decomposed completely while for wood a weight fraction of around 15 wt.% is left and for coal a much higher content is present as a residual char. This can be explained by the different volatile matter of the fuels. A high content of volatile components and a low content of fixed char results in a high gas production during pyrolysis. This knowledge will be essential for the gasification tests discussed in this work.

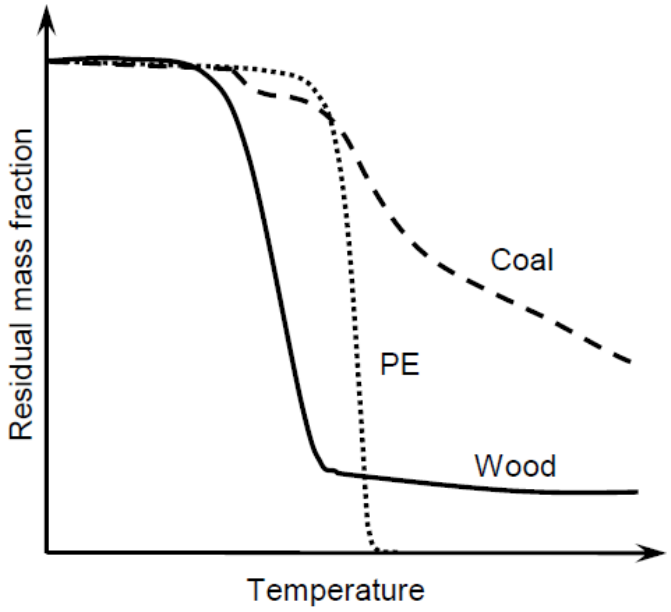

Figure 11: Illustration of thermo gravimetric anylysis of wood, coal and PE [12,65,66].

3.2 Solid fuels used for gasification in this work

To expand the range of fuels used in a dual fluidised bed steam gasifier, seven different fuels, whose origins are biomass, coal and plastics, are used for the tests in this work, so with the expanded fuel line-up more information of the influence of very different fuels can be gained. The fuels tested are:

- Biomass
  - Wood pellets
- Coal
  - German lignite
  - Spanish hard coal
  - Polish hard coal
- Waste plastics
  - Polyethylene (PE)
- Char
  - Char from polish hard coal
  - Char from wood pellets

The results of the proximate and ultimate analyses for the seven fuels are can be found in Table 4.

Table 4: Proximate and ultimate analyses of the used solid fuels.

		Biomass	Coal			Plastics	Char	
	Unit	Wood pellets	Lignite	Spanish coal	Polish coal	PE	Wood char	Coal char
Water content	wt.%	6.11	18.63	3.6	9.86	0	10.18	1.09
Ash content	$wt.\%_{db}$	0.29	4.23	31.09	7.41	0.00	3.07	3.98
C	$wt.\%_{db}$	50.23	65.53	55.13	76.49	85.90	92.70	87.07
H	$wt.\%_{db}$	6.04	3.75	3.39	3.87	14.08	<0.10	1.76
O	$wt.\%_{db}$	43.38	25.22	8.18	10.29	0.00	4.02	5.45
N	$wt.\%_{db}$	0.05	0.84	1.39	1.34	0.02	0.18	1.40
S	$wt.\%_{db}$	0.005	0.38	0.78	0.46	n.d.	0.02	0.25
Cl	$wt.\%_{db}$	0.003	0.05	0.04	0.15	n.d.	0.01	0.09
Volatile components	$wt.\%_{db}$	86.45	51.8	27.16	34.66	>99	4.82	7.48
Fixed carbon	$wt.\%_{db}$	13.55	48.2	72.84	65.34	<1	92.18	92.52
Lower heating value	MJ/kg	17.458	19.326	20.154	26.03	43.379	28.635	32.349
O/C	mol/mol	0.65	0.29	0.12	0.10	0.00	0.03	0.05
H/C	mol/mol	1.43	0.68	0.73	0.60	1.94	0.01	0.24

Wood pellets produced according to the Austrian standard ÖNORM M 7135 are usually used as a standard fuel for the gasification tests to represent wood in the gasifier. For the processing of

biomass in a power plant, wood chips are mostly the designated fuel, but for the pilot plant, the pieces have to be smaller, and the quality of the fuel has to be held constant for the entire test campaign. Therefore, instead of wood chips, wood pellets are normally used for the tests.

The German lignite is mined out for fluidised bed combustion systems and is characterized by a relatively low content of sulphur, nitrogen and ash, compared to other types of lignite. During the steam gasification tests it turned out that the lignite showed a surprisingly good performance. The Spanish hard coal is mined in Puertollano, in the province of Ciudad Real, Castile-La Mancha, in the south of Madrid. This coal is characterized by its high content of ash by that also the calorific value suffers markable. The Polish hard coal was chosen as this type is widely used in Austria for coal fired power plants [53].

For characterization of the performance of plastics gasification one very common component, polyethylene (PE), is considered here. Polyethylene is used in a lot of consumer products like packings or insulations. Some types of PE are often used in the food industry.

For a further scientific point of view, chars originating from Polish coal and wood pellets, were gasified. This allows splitting the devolatilization step from char gasification in the gasification reactor and provides further information regarding tar forming and gas formation during pyrolysis in the dual fluidised bed system. The chars were produced in rotary kiln pyrolysis reactors. The Polish hard coal was pyrolyzed at a temperature of 600 °C and the wood pellets were processed at 850 °C. The temperature for wood pellets was chosen at 850 °C as this temperature is similar to the standard operating temperature in the fluidised bed gasification reactor for wood pellets gasification, so at this temperature the particles are normally devolatilized in the gasification reactor. In this way a similar char quality was produced to the char that is present usually in the gasification reactor during wood pellets gasification.

The char from wood pellets was made by the German company Pyreg (http://www.pyreg.de). A rotary kiln reactor was used. The relatively high water content, as measured to be 10 wt.%, found in the char from wood pellets was due to moistening after pyrolysis to avoid spontaneous combustion during transport. The Polish coal was pyrolyzed in a 3 MW pyrolysis pilot plant, described in [8]. The maximum operable pyrolysis temperature was 600°C. As a result of this the content of volatile components is slightly higher for the coal char.

The fuel analysis in Table 4 shows the huge variety in the fuel properties of the used fuels is documented. The range of the lower heating value (LHV) of the fuels is ranging from 17 MJ/kg for wood pellets up to 43 MJ/kg for PE, which is more than twice of the value of wood pellets. The coal rank can be estimated by the carbon and oxygen content showing that the Spanish coal has a slightly higher rank but is affected with extremely high ash content. Therefore this coal is classified in this study as low grade bituminous coal or as low grade hard coal. A further aspect that will play a major role in the gasification process is the ratio of volatile matter to fixed carbon. There can be seen that pyrolysis of char and wood pellets (char production) effectively removed a large part of the volatile components of the fuel (Figure 12).

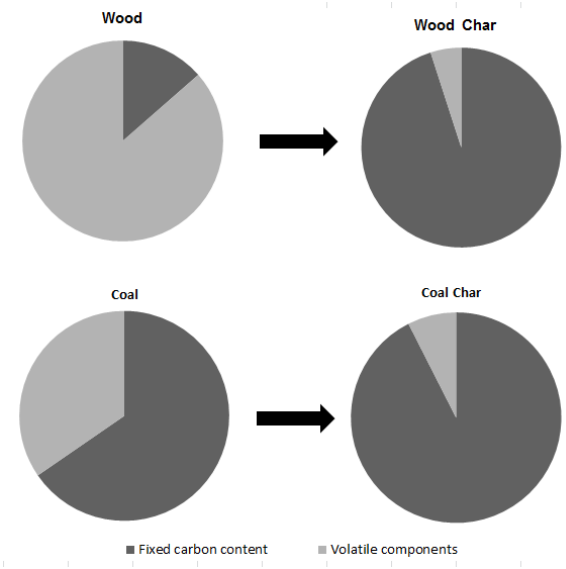

Figure 12: Influence of the pyrolysis step on the distribution of volatile matter and fixed carbon of in the fuels.

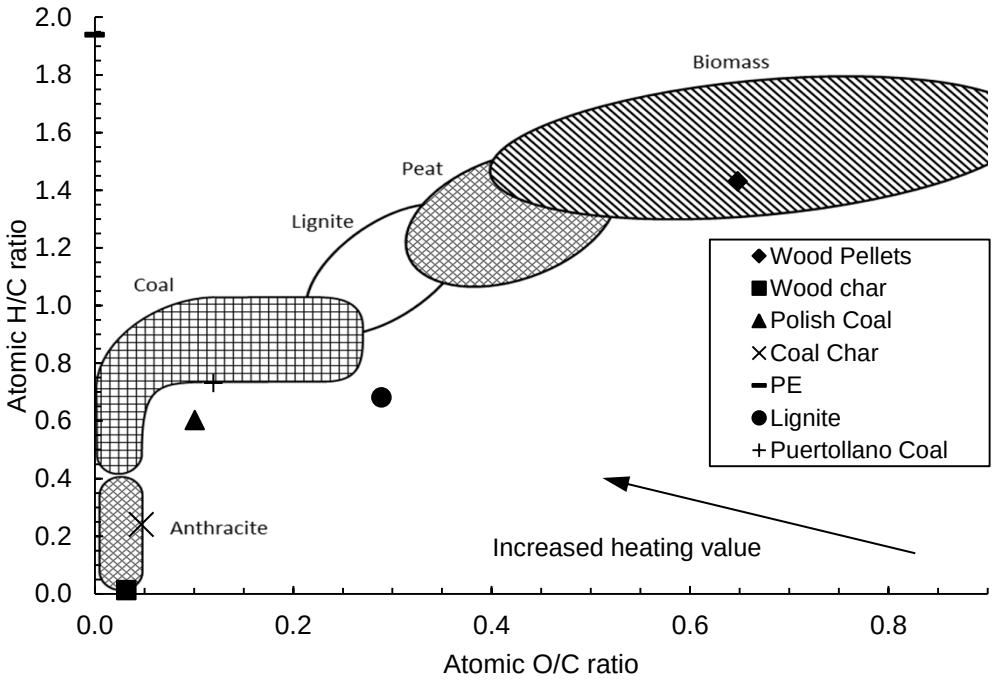

Figure 13: Typical ranges for H/C and O/C ratios of solid fuels [62].

Other characteristic fuel properties are the atomic ratios of oxygen to carbon (O/C) and hydrogen to carbon (H/C). Those ratios are important for the gasification process as they influence the amount of gasification agent that has to be used for a stoichiometric conversion of the feedstock (will be calculated in section 3.2). Van Krevelen [62] used these ratios to illustrate the fuel properties in a chart that shows the typical ranges for the most common coal ranks and biomass types (Figure 13). With the fuels selected in this work (Table 4), the whole range of the diagram is covered. A special case are PE as, on the one hand, it does not contain any oxygen and therefore marks a O/C ratio of 0.0 and, on the other hand, it shows the highest H/C ratio, and wood char which has the highest carbon content and is nearly free of hydrogen and poor in oxygen.

3.3 Gasification of solid feedstock with steam

3.2.1 Heterogeneous and homogeneous reactions

The conversion of solid fuels into gaseous products by gasification occurs in several steps. As described in section 1.2, the first step is drying of the fuel, followed by the release of volatile components respectively pyrolysis. The residual char can be converted into product gas by the gasifying agent. In fluidized beds, gasification takes place at temperatures typically between 800 and 900 °C. For DFB gasification, pure steam will be used as a gasification agent, so this is the type that will be considered here.

For the gasification step there has to be distinguished between heterogeneous reactions, which are the reactions of a gasifying agent with the solid carbon and homogeneous reactions that occur in the gas phase and influence the product gas composition. The main heterogeneous gasification reactions are shown in Table 5.

Table 5: Heterogeneous equilibrium reactions in carbonaceous feedstock gasification.

Name of reaction	Chemical equation	$\Delta H_{R,850}$, kJ mol^{-1}	Equation
Oxidation	$C + O_2 \leftrightarrow CO_2$	-394.9	(2)
Partial oxidation	$C + 0.5\ O_2 \leftrightarrow CO$	-112.7	(3)
H_2O gasification	$C + H_2O \leftrightarrow CO + H_2$	+135.7	(4)
Boudouard	$C + CO_2 \leftrightarrow 2\ CO$	+169.4	(5)
Methanation	$C + 2\ H_2 \leftrightarrow CH_4$	-89.8	(6)

These reactions are considered as equilibrium reactions with changing equilibrium conditions depending on temperature and pressure. For the applied temperature range of fluidized bed gasification, equilibrium will normally not be reached. The behavior can be shown by the equilibrium constant (K_p). All of the considered reactions with solid carbon (Table 5) are reactions of second order, whose general formulation is shown in Equation 7 with ν_i as the stoichiometric coefficients.

$$|\nu_A| \cdot A + |\nu_B| \cdot B \leftrightarrow |\nu_C| \cdot C + |\nu_D| \cdot D \tag{7}$$

Such a chemical reaction can proceed forward and reverse. The state of equilibrium is reached when the forward reaction is at the same rate as the reverse reaction. In practical terms there can be said that the reaction does not proceed anymore and the reagents and products remain at the same amount. With the equilibrium constant (Equation 8) there can be found whether the equilibrium is on the side of the reagents ($K_p < 1$) or the products ($K_p > 1$).

$$K_P = \frac{(p_C)^{\nu_C} \cdot (p_D)^{\nu_D}}{(p_A)^{\nu_A} \cdot (p_B)^{\nu_B}} \tag{8}$$

In Equation 8, p_i, as the partial pressure of each component, represents the concentration of each component and the stoichiometric coefficients (ν_i) of the products are signed positive while those for the reagents are used negative in this equation. A plot of K_p for the heterogeneous reactions

mentioned in Table 5, with variable temperature and constant pressure (1 bar), is provided in Figure 14.

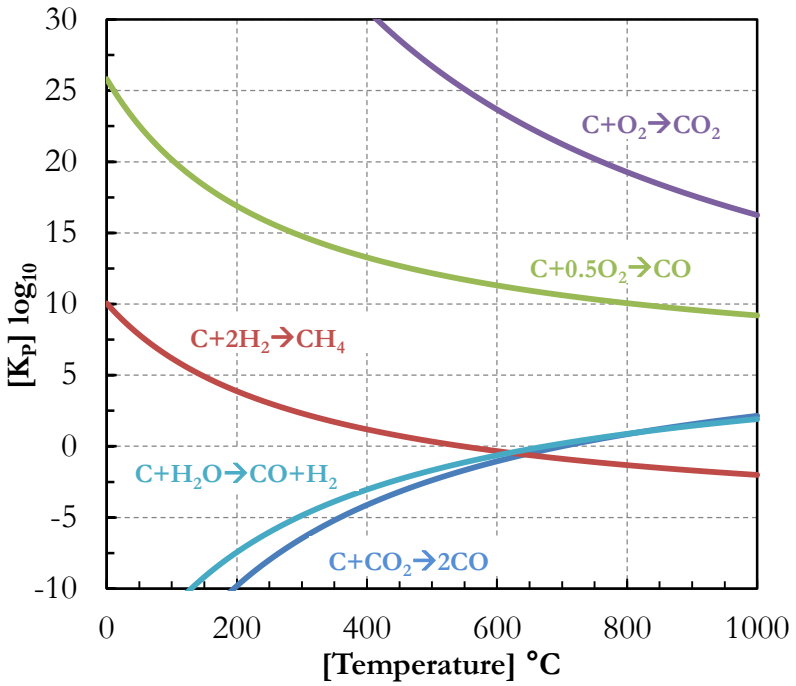

Figure 14: Temperature dependency of the equilibrium constant K_p for the heterogeneous reactions (1 bar) [67].

In this graph there can be seen that at around the gasification temperature that will be used in this study (850 – 870 °C) the equilibrium for carbon oxidation is very far on the side of the products as in a conventional combustion process. However, as free oxygen is not provided by the gasification agent these reactions (Equations 2-3) do not occur in a large extent in the reactor. What is more important here are the reaction for carbon gasification with H_2O and the Boudouard reaction that produce H_2 and CO at the applied gasification conditions. With this graph there can also be estimated the character of the reactions in terms of their reaction enthalpy (ΔH_R). While exothermic reactions proceed to lower values of K_p for higher temperatures, endothermic reactions move towards higher values of K_p. The methanation reaction does not has to be considered in the following sections as its equilibrium is on the side of its reactants at the applied gasification conditions and furthermore its reaction kinetics is very slow compared to steam gasification [68]. In general the state of equilibrium shows that a chemical reaction can take place but the speed of a reaction can only be described by reaction kinetics. The speed ω of a reaction of second order (Equation 9) is depending on the concentration of their reactants:

$$\omega = -\frac{dv_A}{dt} = -\frac{dv_B}{dt} = k \cdot v_A \cdot v_B \qquad (9)$$

As the temperature is an essential factor for the speed of a reaction, the Arrhenius equation includes the dependency of the rate constant k of a chemical reaction, where T is the temperature in K, A is the pre-exponential factor, E_A is the activation energy and R the universal gas constant.

$$k = A \cdot e^{-\frac{E_A}{R \cdot T}} \qquad (10)$$

$$\omega = A \cdot e^{-\frac{E_A}{R \cdot T}} \cdot \nu_A \cdot \nu_B \quad (11)$$

In the DFB gasification reactor the essential steps are pyrolysis/devolatilization and char gasification with steam. To give an insight of the kinetics of these two main heterogeneous reactions, the reaction rates are given for pyrolysis of biomass in Table 6 while the reaction rates for char gasification of beech wood with H_2O and CO_2 as gasifying agent are shown in Table 7. As pyrolysis is forming gas, tar (liquid) and char, separate reaction rates are calculated (k_G, k_L, k_C) whose sum is the reaction rate for the pyrolysis step [69].

Table 6: Biomass pyrolysis kinetic rates (k calculated at 850 °C) [70].

Process step	A, s^{-1}	E, kJ mol^{-1}	k, s^{-1}
k_G	$4.38 \cdot 10^9$	152	$3.46 \cdot 10^2$
k_L	$1.08 \cdot 10^{10}$	148	$1.41 \cdot 10^3$
k_C	$3.27 \cdot 10^6$	111	$2.10 \cdot 10^1$
Pyrolysis			$\mathbf{1.78 \cdot 10^3}$

Table 7: Biomass char gasification kinetic rates (k calculated at 850 °C) [71].

Gasifying agent	A, s^{-1}	E, kJ mol^{-1}	k, s^{-1}
CO_2	$1.8 \cdot 10^6$	200	$8.98 \cdot 10^{-4}$
H_2O	$1.4 \cdot 10^7$	200	$6.98 \cdot 10^{-3}$

From the reaction rates in Table 6 and Table 7 it can be seen that the pyrolysis step is much faster than char gasification. Based on this fact it is assumed that in the bubbling bed section of the gasification reactor the majority of fuel particles is already converted to char. Therefore it is assumed that only char is present in the bubbling bed. The influence of the gasifying agent in the char gasification reaction rates is shown in Table 7. There can be seen that the reaction rate for gasification with H_2O proceeds faster compared using CO_2 as gasifying agent. This fact, and the reason that steam is easy to provide and cheap, is responsible for choosing H_2O for gasification in this work. In addition to the heterogeneous reactions, the homogeneous reactions in the gas-phase are very important for the process as they influence the product gas composition essentially. The most important reactions are listed in Table 8 and the temperature dependency of their state of equilibrium is plotted in Figure 15.

Table 8: Homogeneous equilibrium reactions in the gasification reactor.

Name of reaction	Chemical equation	$\Delta H_{R,850}$, kJ mol^{-1}	Equation
CO combustion	$CO + 0.5\ O_2 \leftrightarrow CO_2$	-282.1	(12)
H_2 combustion	$H_2 + 0.5\ O_2 \leftrightarrow H_2O$	-248.5	(13)
Water-gas shift	$CO + H_2O \leftrightarrow CO_2 + H_2$	-33.6	(14)
Methane steam reforming	$CH_4 + H_2O \leftrightarrow CO + 3\ H_2$	+225.5	(15)
Methane dry reforming	$CH_4 + CO_2 \leftrightarrow 2\ CO + 2\ H_2$	+259.1	(16)

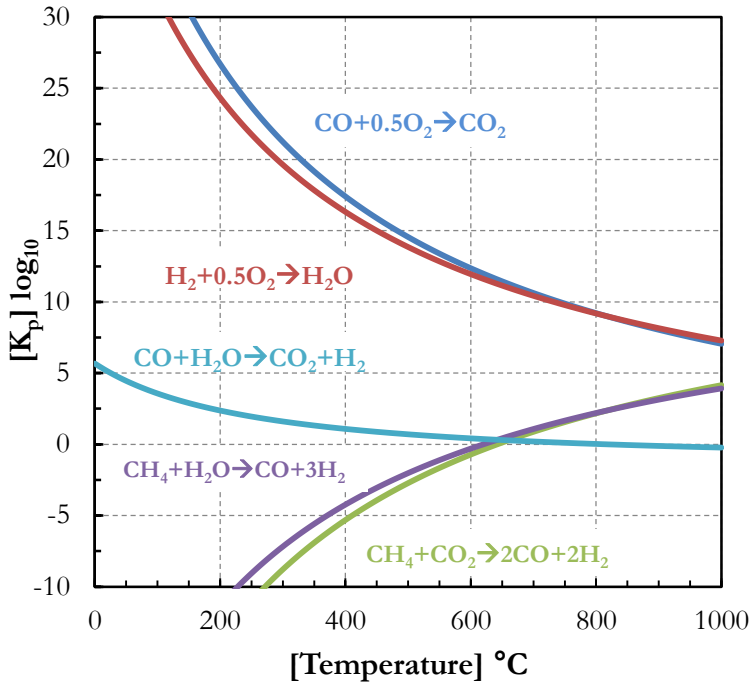

Figure 15: Temperature dependency of the equilibrium constant K_p for the homogeneous reactions (1 bar) [67].

The water-gas shift reaction is always on side of the products, but the potential for a reaction decreases with higher temperatures. However a higher temperature increases the speed of the reaction and can lead to higher quantities of its products [72]. The methane reforming reaction of interest here is the steam reforming reaction as it was found that the presence of CO, H_2 and especially H_2O inhibit the dry reforming reaction [73]. So, for steam gasification that forms a product gas with a high content of H_2 and CO and high values of unconverted water present in the product gas is formed.

In the gasification reactor these reactions can take place at the same time and place and some reactions can be forced by operating parameters and by the utilization of catalytically active bed material. When applying steam for gasification, the water–gas shift reaction is forced, so carbon (C) is converted into H_2 and CO (Equation (4)), and carbon which is also present in the gas in the form of CO can be converted to H_2 and CO_2 (Equation (14)) already in the gasification reactor. This leads to a product gas with a high content of hydrogen.

From the facts mentioned above it can be assumed that the water-gas shift reaction takes place in the reactor. In general, this reaction is desired, as a high hydrogen content is welcome in many applications of the product gas. Moreover, materials that promote this reaction also force the decomposition of tar compounds [74] and reduce the energy required for the process due to its exothermic character (Equation 14). To quantify the distance to equilibrium of this reaction, a model parameter is introduced which is defined as the logarithm of the ratio of the actual partial pressure product to the equilibrium constant (Equation 17).

$$p\delta_{eq,CO-shift}(p_i,T) = log_{10}\left[\frac{\prod_i p_i^{\nu_i}}{K_{p,CO-shift}(T)}\right] \quad (17)$$

If $p\delta_{eq,CO-shift} < 0$, the actual state is still on the side of the reactants, so further reaction is thermodynamically possible. If $p\delta_{eq,CO-shift} = 0$, the water-gas shift equilibrium is fulfilled by the product gas composition, and if $p\delta_{eq,CO-shift} > 0$, the actual state is on the side of the products. The latter case cannot be reached thermodynamically by the water-gas shift reaction, but can be a result of the products of pyrolysis/devolatilization, the other gasification reactions and the water content in the product gas. If, for example, the gasifier is operated with a low amount of steam for gasification, the water content will be lower in the product gas. This moves the distance to water–gas shift equilibrium beyond 0 ($p\delta_{eq,CO-shift} > 0$). The water-gas shift reaction will then move towards its reactants and consume energy. $K_{P,CO\text{-}shift}$ is the equilibrium constant of the water–gas shift reaction and can be determined via several sources (Figure 15) [67].

3.2.2 Steam demand for gasification

Based on the gasification reactions in Table 5, the overall reaction for gasification of solid fuels can be expressed as Equation (18):

$$C_xH_y + x \cdot H_2O \rightarrow x \cdot CO + \left(x + \frac{y}{2}\right) \cdot H_2 \qquad \Delta H_{R,850} > 0 \qquad (18)$$

Equation (18) states that for each mole of carbon in the feedstock one mole of water is required for a stoichiometric conversion of the fuel. But in reality, the main elements of a feedstock are not only carbon and hydrogen: oxygen can also make up a large part; for example the oxygen content of wood pellets is about 44 $wt.\%_{daf}$. Including this aspect in the overall steam gasification reaction results in Equation (19):

$$C_xH_yO_z + (x - z) \cdot H_2O \rightarrow x \cdot CO + \left(x + \frac{y}{2} - z\right) \cdot H_2$$

$$\text{for} \quad (x > z) \qquad \Delta H_{R,850} > 0 \qquad (19)$$

From Equation (19) the minimum amount of steam that must be present during the process for a known composition of the fuel can be defined. The stoichiometric steam demand can be calculated using Equation (20):

$$\phi_{H_2O} = (x - z). \qquad (20)$$

For the tests in this work the feedstock can be expressed as the system $C_xH_yO_z$ free of sulfur and free of nitrogen. From the fuel analysis (see Table 4), the molarities of C, H, and O are found and with the knowledge of the fuel composition, the stoichiometric steam demand can be calculated as listed in Table 9 for the fuels used. With these values a first estimation of their behavior in the gasification reactor can be made. The lowest steam demand requires the used biomass. This can be explained with the high amount of hydrogen and oxygen in this feedstock.

Table 9: Molarities and theoretical stoichiometric steam demand for the used fuels.

		Biomass	Coal			Plastics	Char	
Unit		Wood pellets	Lignite	Spanish coal	Polish coal	PE	Wood char	Coal char
x		1	1	1	1	1	1	1
y		1.44	0.69	0.73	0.61	1.95	0.01	0.25
z		0.66	0.29	0.12	0.10	0.00	0.00	0.05
ϕ_{H2O}	$mol_{H2O}/kg_{daf,N,S,Cl\ free}$	14.76	41.06	60.04	63.17	71.59	77.27	73.28
ϕ_{H2O}	$kg_{H2O}/kg_{daf,N,S,Cl\ free}$	0.26	0.74	1.08	1.13	1.29	1.39	1.32

In most of the cases of gasifier operation, the real amount of H_2O in the system would differ from the amount needed stoichiometrically. To quantify the ratio of H_2O actually present to that needed theoretically, an equivalent ratio for H_2O can be defined, similar to that which is used for combustion systems to determine the amount of air.

$$\lambda_{H_2O} = \frac{\dot{m}_{H_2O,actual}}{\dot{m}_{H_2O,stoich.}} \tag{21}$$

In real gasifiers the water introduced for conversion of the feedstock will not be converted, as a result of several facts. On the one hand, to maintain a good fluidization, a steam flow higher than that required stoichiometrically is typically chosen. On the other hand the aspects discussed before only consider the conversion of the feedstock to H_2 and CO. In a real case many simultaneous reactions take place, such as pyrolysis, gasification, reforming, and cracking as well as recombination reactions for tar compounds that lead to the actual product gas composition.

For practical operation of gasifiers another expression for the amount of steam is used. The steam-to-fuel ratio expresses the sum of water present in the system in relation to the total mass of dry and ash free fuel introduced (Equation 22). As the steam is initially required for gasification of carbon particles (Equation 4) the formulation of the so-called steam-to-carbon ratio will also be used here (Equations 23 and 24). This formulation makes it easier to compare the gasification of fuels from with different origins, like coal and biomass, because due to the high heating value of coal compared to wood, the amount of coal required to reach the same fuel power is smaller than the amount of wood. This would result in very different steam-to-fuel ratios, but a constant steam-to-carbon ratio is essential for maintaining comparable gasification conditions, especially with regard to fluidization conditions.

$$\varphi_{SF,wt} = \frac{\dot{m}_{steam} + w_{H_2O} \cdot \dot{m}_{fuel}}{(1 - w_{H_2O} - w_{ash}) \cdot \dot{m}_{fuel}} \tag{22}$$

$$\varphi_{SC,wt} = \frac{\dot{m}_{steam} + w_{H_2O} \cdot \dot{m}_{fuel}}{w_C \cdot \dot{m}_{fuel}} \tag{23}$$

$$\varphi_{SC,mol} = \frac{\dot{m}_{steam} + w_{H_2O} \cdot \dot{m}_{fuel}}{w_C \cdot \dot{m}_{fuel}} \cdot \frac{12}{18} \tag{24}$$

3.2.3 Conversion performance

In steam gasification, the amount of water introduced related to that which is consumed for the gasification and steam reforming reactions is an indicator for the whole process, called water conversion. The specific water conversion is defined as the amount of water consumed per mass unit of converted fuel (Equation 25).

$$X_{H_2O,rel} = \frac{\dot{m}_{H_2O,con.}}{(1-w_{H_2O}-w_{ash})\cdot\dot{m}_{fuel}} \quad (25)$$

Compared to the specific water consumption, the water conversion simply expresses the relation between the amount of water consumed and the amount of water introduced (Equation 26).

$$X_{H_2O} = \frac{\dot{m}_{H_2O,con.}}{w_{H_2O}\cdot\dot{m}_{fuel}+\dot{m}_{H_2O,steam}} \cdot 100 \quad (26)$$

The conversion of carbon in the gasifier to gaseous products can also be used as a key figure for the performance of the gasification process. For a dual fluidized bed gasifier, one has to distinguish between the conversion of carbon to product gas in the gasification reactor itself and the conversion of carbon in the whole system to product gas and flue gas. In the first case, the carbon conversion is the ratio of carbon leaving the gasification reactor in the form of gaseous products in the product gas stream to the amount of carbon introduced by the feedstock (Equation 27).

$$X_{C,G} = \frac{\dot{m}_{C_{PG}}}{w_C\cdot\dot{m}_{fuel}} \cdot 100 \quad (27)$$

(1 - $X_{C,G}$) can be used as a kind of parameter for determination of the amount of char that leaves the gasification reactor and enters the combustion reactor, neglecting char present in the product gas stream. The overall carbon conversion of the DFB system , $X_{C,DFB}$, gives information of the carbon conversion in the gasification reactor and in the combustion reactor of the carbon introduced by the solid feedstock (Equation 28).

$$X_{C,DFB} = \frac{\dot{m}_{C_{PG}}+\dot{m}_{C_{FG}}}{w_C\cdot\dot{m}_{fuel}} \cdot 100 \quad (28)$$

To provide a value for the efficiency of the gasification system, the cold gas efficiency is used here. For calculation of this value in the case of tests on the pilot plant it has to be kept in mind that a pilot plant usually does not reach a low value of heat losses like an industrial large scale plant does. In the case of the DFB pilot plant the heat losses are nearly 20% of the fuel power. Stidl [75] calculated the heat losses by radiation for the main parts of the 10 MW_{th} DFB gasification plant in Oberwart, Austria [76]. Based on the reported heat losses, the heat loss by radiation for an industrial plant can be assumed to be 2 % of the input fuel power. To compare the cold gas efficiency to other plants, it is calculated for an industrial plant size according to Equation 29. The cold gas efficiency for the pilot plant, neglecting the high heat loss is shown in Equation 30.

$$\eta_{C,IP} = \frac{\dot{V}_{PG}\cdot LHV_{PG}}{(P_{fuel,G}+P_{fuel,C}-\dot{Q}_{PP}+\dot{Q}_{IP})\cdot 3600} \quad (29)$$

$$\eta_{C,PP} = \frac{\dot{V}_{PG}\cdot LHV_{PG}}{(P_{fuel,G}+P_{fuel,C})\cdot 3600} \quad (30)$$

3.4 Fluidization fundamentals

In this section a brief overview about fluidization including the most relevant equations for the calculation of the minimum fluidization velocity (U_{mf}) and the terminal velocity (U_t) of a particle will be explained. The topic of fluidization is explained in detail in literature [77-80].

In general, fluidization occurs when a bulk of solid particles is transferred from a static solid-like state to a dynamic fluid-like state. This is reached by an upward gas flow through the bulk solid particles. By different gas velocities, a wide range of different fluidization states can be reached, as shown in Figure 16a.

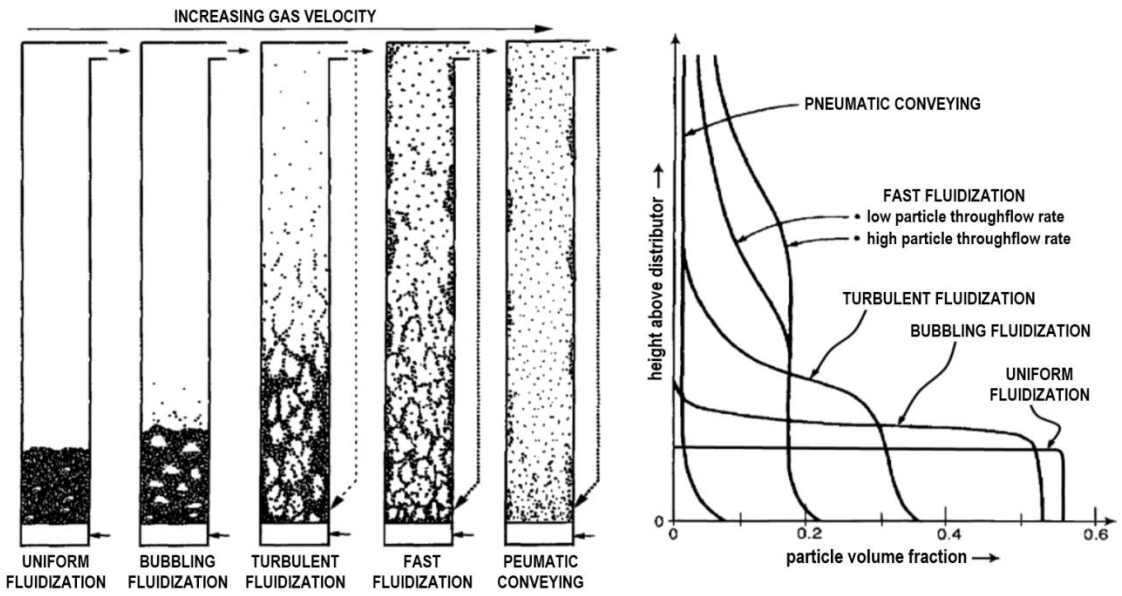

Figure 16: Fluidization regimes due to different gas velocities illustrated in a column (a) and by the particle volume fraction (b) [80].

When the gas velocity is below a value where the uplift force by the gas counterbalances the weight of the particles (U_{mf}), the solid particles, called bed material, remain static solid-like on the bottom. When the gas velocity reaches U_{mf} some particles are moved slightly and the bed starts forming bubbles, so a bubbling fluidization regime is made. By a further increase of the gas velocity the fluidization regime becomes turbulent and as a result the bed expands further, so the holdup of the particles in the column is significantly higher compared to the case before. In the case of the turbulent regime the gas velocity can be increased until its value reaches the second characteristic velocity, the terminal velocity (U_t). U_t is the velocity where the gas velocity causes an uplift force on the particle which is exactly the value of the weight, reduced by the buoyancy of the particle. Theoretically, the particles are in the state of flotation. In this case the bed fluidization is turbulent and the bed is expanded extensive. By a slight increase of the gas velocity the particles start to move upwards and are carried with the gas flow out of the column. The gas velocity where this starts is U_{SE}, the velocity where significant entrainment of particles start. Starting with U_{SE}, this fluidization regime is called fast fluidization. The removal of particles with the gas stream makes a particle separation and recycle stream of particles, depending on the application, necessary. At the regime of pneumatic conveying, the gas velocity is that high that all of the particles are entrained immediately.

An illustration of the fluidization regimes can be made by the distribution of the particles in the column. The particle volume fraction (ε_S) is the difference of the total volume of the column and the void fraction (ε_f):

$$\varepsilon_S = 1 - \varepsilon_f \tag{31}$$

In Figure 16b, the particle volume fraction over the height of the column for different fluidization regimes is shown. There can be seen that the bed expands with increasing fluidization gas velocities, from uniform fluidization (bubbling bed) to pneumatic conveying. In the case of pneumatic conveying the distribution of particles over the height is uniform except at the bottom of the column where acceleration of the particles takes place.

What also should be mentioned here are the particle characteristics which influence the fluidization behavior. Those are:

- the particle density ρ_p
- the particle diameter d_p,
- particle shape, and
- particle size distribution.

The particle size is essential, as in addition to the drag coefficient that is dependent on the size, also other effects can occur which influence the fluidization behavior. Therefore Geldart [81,82] introduced a classification scheme based on the size of the particles to be fluidized. In this scheme (Figure 17), the particles are classified into four categories which are listed here with increasing particle diameters.

- Group C
- Group A
- Group B
- Group D

As the classification into these four groups according to Geldart is also dependent to the density of the particles, the particle size ranges for the four groups vary with their density. Therefore Figure 17 provides a proper overview for the classification.

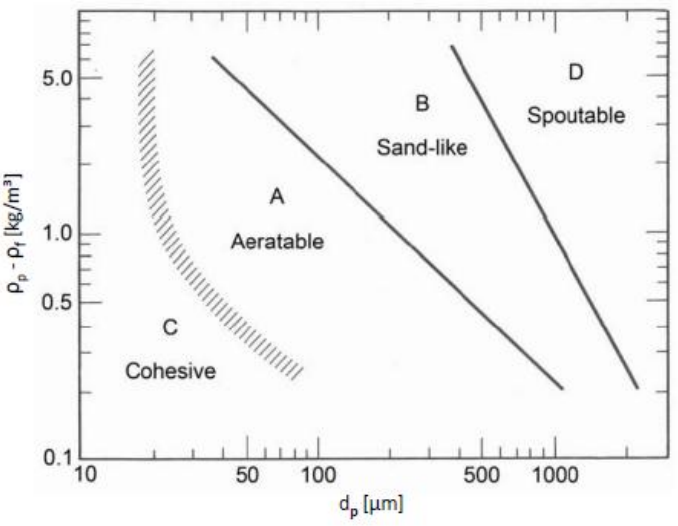

Figure 17: Geldart particle classification [81].

A further important value for the fluidization behavior is the shape of the particle. For calculation of the values for fluidized bed it is assumed that the particles are spherical, but real bed materials are not. Therefore, the sauter diameter d_{SV} of the particles is used for all of the calculations introducing the sphericity ϕ of a particle (Equation 32).

$$d_{SV} = d_P \cdot \phi \tag{32}$$

ϕ gives the deviation from a spherical particle and is defined as the ratio between the surface of a sphere with the same volume as the particle (d_V) to the surface of the real particle (d_S).

$$\phi = \left(\frac{d_V}{d_S}\right)^2 \tag{33}$$

For characterization of the fluidized bed regime, the most important values are the two gas velocities U_{mf} and U_t whose calculation will be briefly explained in the following lines.

For the calculation of the minimum fluidization velocity the equations for the pressure drop according to Ergun and the fundamental equation for fluidization are combined and form Equation 34, where the Archimedes number is expressed by the Reynolds number and two constants K1 and K2.

$$Ar = K1 \cdot Re_{mf} + K2 \cdot {Re_{mf}}^2 \tag{34}$$

$$Re_{mf} = \frac{\rho_g \cdot d_{sv} \cdot U_{mf}}{\mu} \tag{35}$$

$$Ar = \frac{\rho_g \cdot d_{sv}^3 \cdot (\rho_p - \rho_g) \cdot g}{\mu^2} \tag{36}$$

As the velocity is in the Reynolds number, a quadratic equation has to be solved, using Equations 35 and 36, which leads to Equation 37:

$$U_{mf} = \frac{\mu}{\rho_g \cdot d_{sv}} \cdot \left(\sqrt{K2^2 + K1 \cdot Ar} - K2\right) \quad (37)$$

It has been found that K1 and K2 are nearly constant for this purpose for Reynolds numbers between 0.001 and 4000 [83]. These values have been found empirically by several researchers up to now and diversify in a comparably close range. To give an overview of this, the numbers for K1 and K2 are listed in Table 10. In this study the values of Grace [87] have been used.

Table 10: Values of the two constants (K1 and K2) for calculation of U_{mf}.

Researchers	K1	K2
Wen and Yu, 1966 [83]	0.0408	33.7
Richardson, 1971 [84]	0.0365	25.7
Saxena and Vogel, 1977 [85]	0.0571	25.3
Babu et al., 1978 [86]	0.0651	25.3
Grace, 1982 [87]	0.0408	27.2
Chitester et al., 1984 [88]	0.0494	28.7

The terminal velocity U_t can be calculated by balancing particle weight, uplift force and friction force, which leads to Equation 38.

$$U_t = \sqrt{\frac{4}{3} \cdot \frac{\rho_p - \rho_g}{\rho_g} \cdot \frac{d_{sv} \cdot g}{C_D}} \quad (38)$$

In this expression of the terminal velocity a coefficient C_D can be found, the drag coefficient. The calculation of C_D is dependent on the Reynolds number and there has to be distinguished for the three cases of laminar flow region, turbulent flow region and transition region:

- Laminar flow region (Stokes region), Re < 0.2

$$C_D = \frac{24}{Re} \quad (39)$$

- Turbulent flow region (Newton region), Re > 1000

$$C_D = 0.43 \quad (40)$$

- Transition region, 0.2 < Re < 1000

$$C_D = \frac{24}{Re} + \frac{4}{\sqrt{Re}} + 0.4 \quad (41)$$

4. Experimental

4.1 The 100 kW dual fluidized bed gasification pilot plant at Vienna University of Technology

For pilot scale experiments, Vienna University of Technology operates a 100 kW_{th} dual fluidized bed (DFB) gasification reactor. The overall gasification reactions which take place in the gasification reactor for steam gasification results in an endothermic effect (Equation (18)), so energy is required to keep the gasification process running. The DFB gasification system provides heat for the gasification reactor by a separate combustion reactor while circulating bed material carries the heat from the combustion reactor to the gasification reactor. The basic principle of the DFB gasification process was already shown in Figure 5 and a schematic drawing of the pilot plant is shown in Figure 18

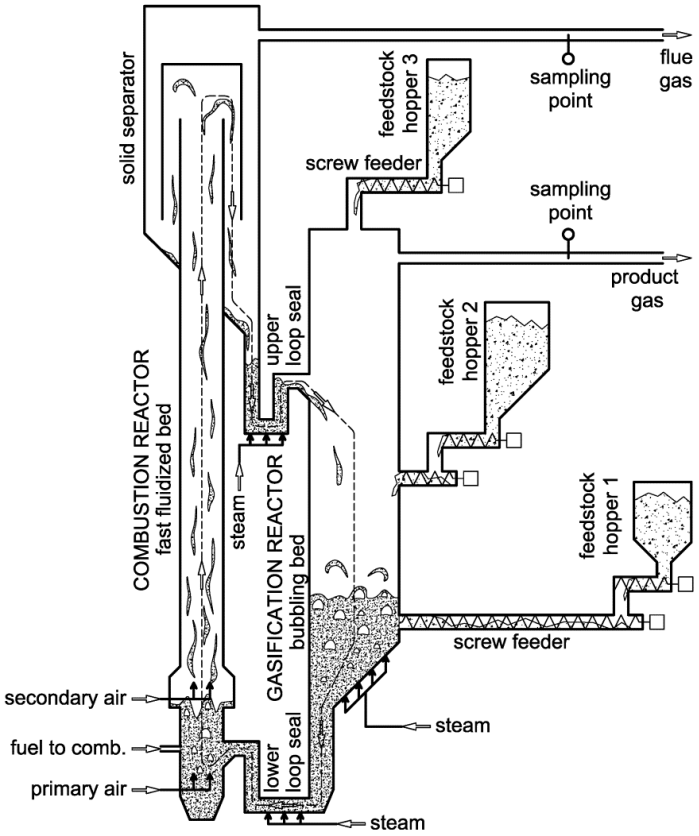

Figure 18: Schematic of the dual fluidized bed gasification pilot plant used for the gasification tests at Vienna University of Technology.

This system separates gasification and combustion in terms of gas flows as two fluidized bed reactors, connected together by loop seals, are used. The solid fuel enters the gasification reactor, a bubbling bed fluidized with steam, where drying, pyrolysis, and heterogeneous char gasification, as well as homogenous gas reactions, take place. The remaining residual char leaves the gasification reactor at the bottom together with bed material, which circulates between the two reactors, through the lower loop seal to the combustion reactor. This reactor is designed as a fast fluidized

bed that is fluidized with air to maintain combustion of the residual char and additional fuel for combustion, if required. By burning char and additional fuel in the combustion reactor, the bed material is heated up, and after particle separation from the flue gas at the exit of the combustion reactor, the bed material flows back to the gasification reactor via the upper loop seal. Both the lower and upper loop seals are fluidized with steam to ensure a high throughput of bed material and to avoid any leakage of gases between the reactors. In practical operations, the gasification temperature is normally controlled by the addition of fuel (e.g. recycled producer gas, part of the feedstock, etc.) into the combustion reactor. In case of the 100 kW_{th} pilot plant, light heating oil is used as fuel in the combustion reactor as it is easy to handle in pilot scale processes. The pressure in both gasification and combustion reactors is close to atmospheric conditions. The main basic geometry data of the DFB reactor system are summarized in Table 11.

Table 11: Basic geometry data and main operating conditions of the dual fluidized bed system.

	Unit	Gasification reactor	Combustion reactor
Geometry	-	Conical bottom section with square-shaped upper freeboard section	Cylindrical
Reactor inner dimensions[1]	mm or mmxmm	270 x 270	ø 98
Reactor free height	m	2.35	3.9
Operable temperature range	°C	650-870	750-920
Fluidization agent	-	Steam	Air
Fluidization regime	-	Bubbling fluidized bed	Fast fluidized bed
Steam-to-fuel ratio	-	0.5-2.0	
Bed material particle size (applicable)	µm	200 - 800	

The process yields two separate gas streams at high temperatures: a high quality product gas and a conventional flue gas. The product gas for biomass gasification is generally characterized by a relatively low content of condensable higher hydrocarbons (2-16 g/Nm³ of so called tars, heavier than toluene) and a high H_2 content of 35-40 $vol.\%_{db}$. A N_2 content of up to 1.5 $vol.\%_{db}$ in the product gas can occur during gasification by nitrogen flushing of the hoppers for inertization.

The pilot plant is equipped with three hoppers to enable different fuels to be fed into the gasification reactor at different locations as well as to give the possibility of co-gasification of several feedstock at any mixing ratio. The three hoppers are used for the following feeding locations or fuel requirements:

- **Hopper 1:** For feeding of solid fuels into the bubbling bed of olivine particles. The screw conveyor introduces the fuel about 0.3 m below the splash zone of the bubbling bed. In most cases this hopper is used.

[1] Gasification reactor: Square shaped freeboard section;
Combustion reactor: Cylindrical fast fluidized bed section;

- **Hopper 2:** For feeding of solid fuels from the side into the freeboard of the gasifier. The screw conveyor introduces the fuel about 0.3 m above the splash zone of the bubbling bed.
- **Hopper 3:** For feeding of solid fuels from the top of the gasifier (top-down feeding). This feeding position is designed for fuels with a low melting point like plastics and ensures that the fuels do not come into contact with hot surfaces (free-falling into the reactor) before getting into contact with the hot bed material.

4.2 Analytics

4.2.1 Product gas composition

Main product gas composition

The composition of product gas is measured after the gasification reactor. The permanent gas components CH_4, H_2, CO, CO_2, and O_2 are measured with a Rosemount NGA 2000. The components N_2, C_2H_4, and C_2H_6 are measured using an online gas chromatograph (PerkinElmer Clarus 500). To avoid any contamination and damage of the gas analyzer and the column of the online gas chromatograph, the product gas has to be cleaned in terms of particulate matter and condensable components like higher hydrocarbons (tars) and water, as both gas measurement devices require dry gas. To maintain this, the gas cleaning line with its arrangement similar to the sampling line in Figure 19 is used (more detailed Figures of this gas cleaning line can be found in Paper I). Particles like dust and char are removed by a glass-wool-stuffed filter. After this particle removal the gas is led through six impinger bottles. Water and hydrocarbons that condense at temperatures higher than 4 °C are collected in the first two bottles. They are followed by three further impinger bottles. Those are filled with rapeseed oil methyl ester where tars are washed out of the gas. The last bottle ensures that no rapeseed oil methyl ester can leave the gas cleaning line accidentally and cause damage to the online gas analyzer or the online gas chromatograph.

Tar, entrained particulate matter (char, dust), and water content

Tar is sampled isokinetically using impinger bottles, with both gravimetric and GC/MS tar subsequently determined. Tar sampling was applied discontinuously by condensing and dissolving the tar components. The measurement method was based on the tar protocol according to CEN/TS 15439 [89], focusing on tars originating from biomass gasification, although the applied method differed as toluene was employed as a solvent; CEN/TS 15439 suggests the use of isopropanol (IPA). The choice of toluene allowed the simultaneous detection of product gas water content, since the latter could be measured as a separate phase in the impinger bottles. Although this meant that certain tar components such as benzene, toluene and xylene (BTX) could not be detected, when using toluene the separation performance for tar components larger than BTX is higher than for IPA. A schematic drawing of the arrangement of the tar sampling line is shown in Figure 19.

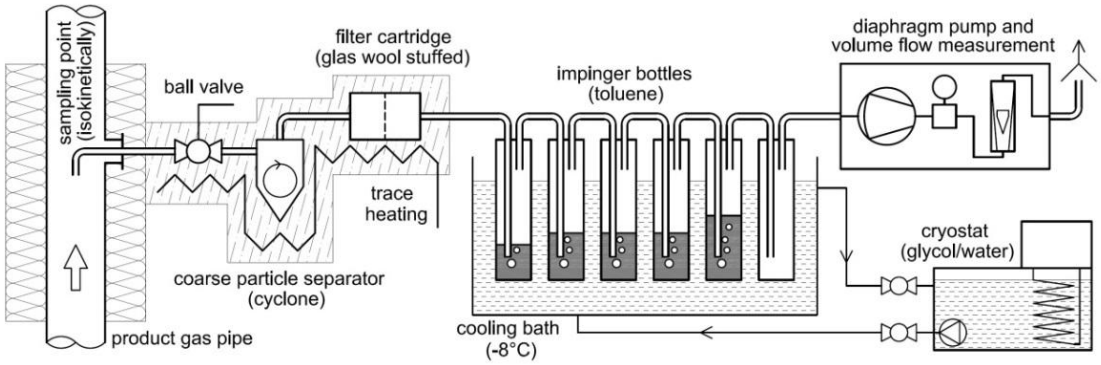

Figure 19: Sampling line for tar, water and entrained particulate matter (char and dust).

The gas enters the heated sampling line, which consists of a cyclone and a glass wool stuffed filter cartridge, where dust as well as condensed tar components are deposited. Afterwards, the gas is led through six impinger bottles, the first five of which are filled with toluene. The impinger bottles are located in a cooling bath maintained at -8 °C by a cryostat, leading to the condensation of tars and steam. The liquid phases in the impinger bottles are then unified and the aqueous phase separated from the toluene phase. The volume of water was determined in order to calculate the water content of the gas stream, while the amount of toluene was also recorded and a GC/MS sample taken, with the majority of the toluene evaporated from the sample in a petri dish. To analyze the oil deposited in the filter cartridge, a soxhlet extraction was carried out using IPA; again a GC/MS sample of the IPA phase was taken, with the latter then processed in the same manner as the toluene phase. The results of the toluene and IPA phases were summed, the result of which represents the amount of gravimetric tar in the product gas. The filter cartridge was then reduced to ash in a furnace; by weighing the cartridge before and after muffle furnace treatment, the amount of entrained char and dust could be calculated. In summary, the described measurement method produced the following data:

- Gravimetric tar content
- GC-MS tar content
- GC-MS tar composition
- Water content
- Char load (organic matter)
- Dust load (inorganic matter)

H_2S and NH_3

For ammonia measurement, the gas is sampled in a similar way to the tar measurement, i.e. using impinger bottles, although in this case the solvent employed is diluted sulfuric acid at a temperature of about -2 °C. Several impinger bottles are filled with diluted sulfuric acid, before being placed in a glycol/water mix whose temperature is cooled via a cryostatic temperature regulator. In order to avoid tar condensation in the pump, a bottle containing toluene is added after the bottle with solvent for NH_3 absorption. Following this procedure the concentration of ammonium ions in the sulfuric acid can be detected via a photometric method according to DIN 38 406 part 5 and ISO 7150.

Hydrogen sulfide is sampled again using impinger bottles filled with an aqueous potassium hydroxide solution at a temperature of about -2 °C. H_2S values are subsequently determined potentiometrically according to ISO 10530.

4.2.2 Fuel analysis

The feedstock for the gasification tests was analyzed by the "Testing Laboratory for Combustion Systems" at Vienna University of Technology. Sampling and preparation of the fuels were carried out according to DIN 51701. After determination of water content, described in DIN 51718 (drying at 30 °C to constant mass, grinding of the dried sample to a maximum particle size of 1 mm and drying of this sample at 106±2 °C in an inert atmosphere to constant mass), the ash content was determined according to DIN 51719 by burning the sample to constant mass. C, H, N and S were measured by an EA 1108 CHNS-O elementary analyzer (Carlo Erba). This procedure involved burning the sample under an oxygen atmosphere, while to ensure complete oxidation and possible CO formation was avoided, the gas was passed through a tungsten catalyst. Afterwards the gas was passed through a layer of copper at a temperature of 860 °C where free oxygen was bound and nitrogen oxides reduced to N_2. The resultant gas then consisted only of the components CO_2, H_2O, N_2 and SO_2 that could be detected. Chlorine present in the gas was absorbed by an aqueous perhydrol solution (H_2O_2) which was subsequently analyzed by capillary electrophoresis.

4.2.3 Analysis of inorganic components (XRF analysis)

Detection of bed material and fuel inorganic matter (ash) composition was carried out via X-ray fluorescence (XRF) analysis using a PANalytical Axios Advanced analyzer. This method is based on the emission of characteristic fluorescent X-rays from a material excited by bombardment with high-energy X-rays or gamma rays. Samples to be analyzed were melted at 1050 °C in a Merck Spectromelt and dumped at 400 °C on a stainless plate. Analysis was performed in a vacuum with a rhodium anode, an excitation voltage of 50 kV and a tube current of 50 mA. As a result, the components were calculated as oxides.

4.2.4 Olivine as bed material

During the last few years, olivine has become a widely known and used bed material and in-bed catalyst for fluidized bed gasification. It is a naturally occurring mineral formed of silicate tetrahedra which contain iron and magnesium $(Mg_{1-x}, Fe_x)SiO_2$. The content of iron and magnesium usually differs depending on where the olivine has been mined. The effect of catalytic tar reduction olivine as a bed material was reported by Koppatz et al. [90]. Calcination of the olivine before using it can greatly improve its catalytic activity [91]. For long-term utilization of olivine in biomass gasification systems, Kirnbauer et al. [92] investigated the interaction of the fuel ash with the olivine particles to form layers, rich in calcium, on the particles. The impact on the gasification process is that the catalytic effect is considerably improved, so the GC/MS tar values were found to be around 80% lower and the gravimetric tar produced was approximately 65% lower in the operation with coated olivine particles compared to the operation using fresh, uncoated olivine particles [74].

The bed material that is used for the tests is olivine, provided by the Austrian manufacturer Magnolithe GmbH. As discussed before it has been observed that calcination of olivine before using it in the gasifier increases its catalytic potential. This thermal preparation is done by the manufacturer in a rotary kiln reactor at a temperature of up to 1600 °C for about four hours. Due to this the material is sintered. The results of the XRF analysis as well as the mechanical properties are shown in Table 12. Due to its high hardness and heat capacity it is perfectly suitable for fluidized bed applications.

Table 12: Chemical composition and mechanical properties of olivine used as bed material.

Composition	Unit	Olivine
Na_2O	wt.%	0.43
MgO	wt.%	46.76
Al_2O_3	wt.%	0.40
SiO_2	wt.%	39.84
P_2O_5	wt.%	0.03
SO_3	wt.%	0.06
K_2O	wt.%	0.32
CaO	wt.%	0.90
Cr_2O_3	wt.%	0.28
MnO	wt.%	0.15
Fe_2O_3	wt.%	10.32
NiO	wt.%	0.31
Cl	wt.%	0.10
Others	wt.%	0.11
Hardness	Mohs scale	6-7
Particle density	kg/m^3	2850

4.3 Balance of the DFB pilot plant

In the field of energy technology, various simulation tools are available for description of combustion-based processes. The aim of combustion processes is the complete conversion of fuels into exhaust gas releasing heat. Therefore, the focus of these simulation tools is on the transformation of heat into power.

Gasification technologies generally offer possibilities for process routes with high electrical efficiencies and heat decoupling at reasonable temperature levels at the same time. Fluidized bed steam gasification of solid biomass, for instance, produces a high quality synthesis gas, which can be used for efficient CHP production using gas engines, gas turbines, or fuel cells and as an intermediate product for chemical syntheses (Fischer-Tropsch, methanol, synthetic natural gas, etc.). As the thermal decomposition of organic matter requires high temperatures, such gasification processes normally provide heat from hot gas streams as a by-product. Gasification based processes show a much more complex primary product range (i.e. product gas, tar, unconverted char). Therefore, some specific issues need to be taken into account when focusing on gasification.

For this purpose, the balance tool IPSEpro was used. IPSEpro is a stationary, equation-oriented flow sheet simulation tool that has been developed for power systems [93]. Detailed information about IPSEpro, its mode of operation, and its utilization for biomass-based energy systems can be found in a previous report [94] or in the publication from Pröll and Hofbauer [95]. The main reasons for using this software package is:

- high complexity of thermo chemical fuel conversion processes (e.g. heat integration, recycle streams, etc.) would lead to problematic iterations when using a sequentially modular solver
- high performance of the equation solver included in the package
- transparency with respect to all model equations used in the standard models and possibility to implement user defined model libraries (scientific reproducibility)
- the physical and chemical property data used are well documented and property databases can be implemented by the user

In order to introduce the description of the specific gasification process library presented in the present work, a few notes on the structure of the software may be helpful. IPSEpro consists of different modules according to Figure 20.

The package PSE (process simulation environment) has a graphical interface for displaying the simulation flow sheet. The structure of the flow diagram, the simulation parameters and the initial values of the variables are stored in project files. The model equations of the individual process components are available in a model library. Together with the structural parameters of the information and process flow diagram, an equation system can be established. The entire system is broken down into smallest groups that can be processed. For solving the subsystems there is a multidimensional Newton-Raphson method used. Good starting values are essential for the convergence of the non-linear models. External functions can be recalled from dynamic link

libraries (DLL's). The integration of such features in the model equations is already defined in the model editor (MDK). The model development kit (MDK) is a standalone program, in which the base models of the process components can be created and changed.

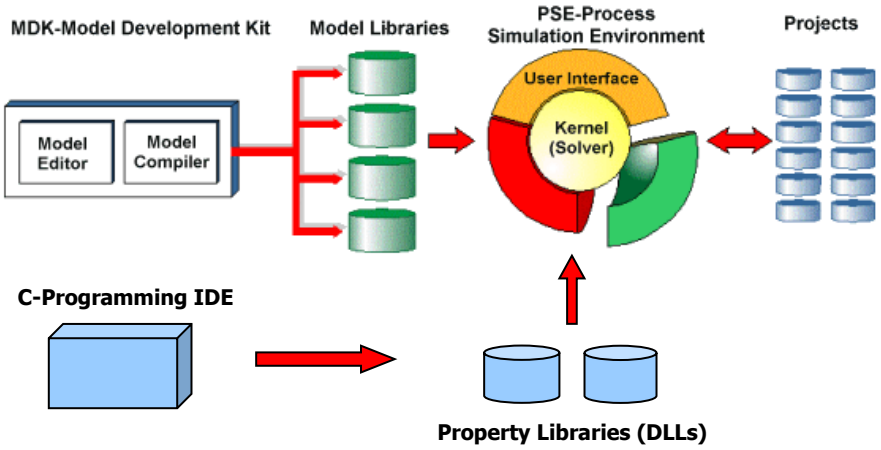

Figure 20: Structure of IPSEpro, adapted from [96].

Measured data is always afflicted with certain wobbliness. If a system that is already defined gets additional measured data, the system is over determined. In most of the cases this datasets do not coincide with each other exactly. For over determined systems a statement about the quality of the individual measurements is possible by confirmation of plausible values and disagrees of obvious erroneous values with the balance of the plant model. This system of equations is converted by use of the method of Lagrange multipliers into a form that can be solved by the simulation tool. The method for solving these systems is described in more detail in a previous work [97].

$$\sum_i \left(\frac{x_i - \bar{x}_i}{tol_{x_i}} \right)^2 \rightarrow Min \tag{42}$$

The absolute tolerances tol_x account for varying units and include information about the quality of the measured value. Comparison between calculated errors and estimated tolerances allows the localization of systematic errors in both simulation and measurements. After exclusion of systematic errors and adjustment of tolerances to reasonable values, the simulation describes the actual plant operation best within the limits of the model structure.

Besides the validation of the measured quantities, all process variables that are not directly measured are known then from simulation. This is essential for quantities, which practically cannot be measured easily (solid circulation rate, heat extraction, solid composition, gas composition, etc.).

5. Results

5.1 Overview of the publications

To give a better overview of the publications related to this work the papers are summarized in Table 13, where in addition to the used fuels a short description of the emphasis of research for each paper is provided. Moreover, to make indication easier which paper deals with fuel oriented or process oriented investigations and if co-gasification of fuels is applied, the last three columns have been included.

Table 13: Overview of the publications related to their focus of investigation.

Paper	Fuel (s)	Focus of the investigations	co-gasification	fuel oriented	process oriented
I	Wood pellets	Influence of fuel feeding position on general process performance and gas quality		✓	✓
II	Lignite	Variation of bed material particle size and fluidization conditions for maximizing performance and gas quality		✓	✓
III	Wood pellets, lignite	Co-gasification, lignite ratios 0-100 %: general process performance and gas quality for fuel mixtures	✓	✓	
IV	PE, lignite	Co-gasification, lignite ratios 0-100 %: general process performance and gas quality for fuel mixtures	✓	✓	
V	Low grade hard coal	Gasification of low grade (high ash content) coal, influence of fuel particle size distribution: general process performance and gas quality, ash balance		✓	✓
VI	Hard coal, coal char	Gasification of coal and pyrolyzed coal (char) for minimizing tar production		✓	
VII	Wood pellets, wood pellets char, hard coal, coal char	Gasification of pyrolyzed feedstock (chars) compared to the original feedstock for minimizing tar production		✓	
VIII	Hard coal, wood pellets	Co-gasification, coal ratio 20 %, temperature variation 750-870 °C: general process performance and gas quality	✓	✓	✓

5.2 Summary of the papers

5.2.1 Paper I

Gasification tests of wood pellets with the following operating conditions were performed with fresh olivine as bed material:

- Gasification temperature: 850°C
- Bed material particle size: dp_{50} = 375 μm (d_{sv} = 370 μm)
- Input fuel power: 90 kW_{th}
- Steam-to-carbon ratio φ_{SC}: 1.3 kg_{H2O}/kg_{carbon}

This paper focuses on the investigation of the influence at the location where the solid feedstock for gasification is introduced into the gasification reactor. In one case the fuel was fed directly into the bubbling fluidized bed while in the second case the fuel was fed from the top onto the bubbling bed. The results are compared in terms of gas quality and conversion performance. With in-bed feeding much lower tar contents and a higher H_2 content were observed, while for on-bed feeding the amount of product gas generated was significantly higher. The tar content was found to be lower for:

- in-bed feeding (7.2 g/Nm^3_{db} GC/MS- and 1.5 g/Nm^3_{db} grav. detectable tars), compared to
- on-bed feeding (16.8 g/Nm^3_{db} GC/MS- and 9.7 g/Nm^3_{db} grav. detectable tars).

A second focus of these test series was the gas formation in the reactor. To investigate this, gas measurements were carried out at different height levels in the gasification reactor for both fuel feeding options. It was observed that the gas composition changed drastically along the height of the gasifier. A decrease in the H_2 content of about 12 $vol.\%_{db}$ was measured from the lowest to the highest sampling point in the gasifier while the contents of higher hydrocarbons, such as CH_4, C_2H_4, and C_2H_6, increased towards the gasifier outlet.

Basically this paper is an essential requirement for Papers III and IV as for the co-gasification tests the lignite was introduced into the reactor by in-bed feeding while the second fuel (wood pellets or PE) was provided by on-bed feeding. For an accurate validation of the co-gasification tests the influence of the feeding position has to be evaluated before which has been done by the tests presented in Paper I.

5.2.2 Paper II

Three gasification tests were performed with lignite with an input fuel power of **90 kW_{th}** at a gasification temperature of **850 °C**. **Olivine** was used as bed material with two different mean particle sizes (**370 and 510 µm**). The steam-to-carbon ratio was varied between **1.3** and **2.1 kg_{H2O}/kg_{carbon}**. In addition to standard online measurements of the permanent gas components of the product gas, impurities like NH_3, H_2S and tar were also measured. It turned out that a lower amount of steam for fluidization caused a better performance of the gasification reactor in terms of product gas yield, carbon conversion and water conversion.

This paper is relevant for the further work, especially for the co-gasification tests, as the tests were performed to find operating conditions where the highest process efficiency and product gas quality was reached by choosing a smaller bed material particle size to enhance the contact with it and to reduce turbulence and gas velocities by lowering the fluidization velocity of the gasification reactor.

As a result the operating point with the highest conversion rate of solid fuel to product gas in the gasification reactor was chosen as a base-case for the tests in Paper III, IV, V and VII (for wood pellets and wood pellets char gasification only). Consequently, the tests in those publications were done at the same operating conditions, which were found to be optimal in Paper II, to provide comparable results. These operating conditions are:

- Gasification temperature: 850°C
- Bed material particle size: dp_{50} = 375 µm (d_{sv} = 370 µm)
- Input fuel power: 90 kW_{th}
- Steam-to-carbon ratio φ_{SC}: 1.3 kg_{H2O}/kg_{carbon}

A second highlight that was found during these investigations was the comparably low tar content (GC/MS tar: 3.0 – 3.3 g/Nm^3_{db}, grav. tar: 0.7 – 1.0 g/Nm^3_{db}) which was not influenced by the changed operating conditions. It was found that the high catalytic activity of the lignite ash might affect the gas quality positively.

5.2.3 Paper III

This paper focuses on the co-gasification of lignite and wood pellets in the dual fluidized bed system. As mentioned before, the operating conditions have been kept at the values defined in paper II (Gasification temperature: **850 °C**, bed material particle size (d_{sv}): **370 µm**, input fuel power: **90 kW_{th}**, steam-to-carbon ratio (φ_{sc}): **1.3 kg_{H2O}/kg_{carbon}**). Co-gasification was investigated for lignite ratios (blends with wood pellets) of 0, 33, 66 and 100 % in terms of energy. The pure fuels, lignite and wood pellets, were fed separately into the reactor by using two hoppers (simultaneously for co-gasification). While lignite was fed by hopper 1 into the bubbling bed, wood pellets were fed by hopper 2 on the bubbling bed. The influence of the feeding position was described in paper I.

It turned out that increasing lignite ratios in the fuel mix with biomass improved the quality in terms of reducing tar load and offered possibility to adjust the main components of the product gas. The beneficial effects of lignite can be reached already at low proportions of lignite (33 %) in the fuel mix with wood. The tar content dropped in this case (33 % lignite, in terms of energy) about 59 % for GC/MS tar and 51 % for gravimetric tar, compared to 100 % wood pellets gasification.

5.2.4 Paper IV

Paper IV focuses on the utilization of plastics (polyethylene), pure and by direct co-gasification with lignite. Also here the operating conditions defined in Paper II were maintained (Gasification temperature: **850 °C**, bed material particle size (d_{sv}): **370 µm**, input fuel power: **90 kW_{th}**, steam-to-carbon ratio (φ_{sc}): **1.3 kg_{H2O}/kg_{carbon}**) As it is commonly known that the product gas made by plastics is characterized by a high tar load, the beneficial effect of adding lignite, which worked already well for wood pellets in Paper III. Thus, positive effects can be expected here. The tests were carried out at four operating points employing fuel blends of PE with lignite of 0, 33, 66 and 100 % in terms of energy. The effect of adding coal in this case was even more drastically compared to the case of wood pellets co-gasification with lignite.

In the case of gravimetrically detectable tars, the tar content in the product gas decreased from 11.2 g/Nm^3_{db} for the gasification of PE to 0.8 g/Nm^3_{db} for the gasification of pure lignite, giving a reduction of 92.9 %. The situation was similar for the GC/MS detectable tars where a reduction of 85.3 % was reached, from 20.5 to 3.0 g/Nm^3_{db}. Using a lignite ratio of 66 %, 73.6 % of the GC/MS tars produced from pure PE vanished and reached values that were lower than those from pure biomass gasification at comparable process conditions.

5.2.5 Paper V

The investigations carried out in paper V concentrate on the low-grade bituminous coal from Spain that is characterized by a high (31 $wt.\%_{db}$) ash content (Gasification temperature: **850 °C**, bed material particle size (d_{sv}): **370 µm**, input fuel power: **90 kW_{th}**, steam-to-carbon ratio (φ_{sc}): **1.3 kg_{H2O}/kg_{carbon}**). Moreover, the particle size distribution of this coal is very wide which means that the coarse fuel particles are affected by a very high fraction of fine fuel and ash particles. Fine particles attract interest as fuels with a particle size below a critical diameter are entrained immediately after feeding into the freeboard of the gasification reactor and to the product gas. The basic investigations of this paper can be summarized as:

- Ash-related issues in the dual fluidized bed system
- Particle size-related issues in the dual fluidized bed system

To investigate these aspects a test series was done where the fine fraction of the coal was removed. The effect of this was that the tar content decreased without using the fines fraction and process efficiency increased as the residence time of larger fuel particles in the system is significantly higher.

The ash balance of the system showed that the fines fraction also contains fuel ash that is entrained into the gas streams and therefore removed from the system. By sieving out the fines fraction before using, the particle size of ash also increased and caused increased accumulation of inorganics in the system.

5.2.6 Paper VI

To determine the influence of volatile matter in the fuel on the gasification process, char from Polish hard coal was gasified. The results were compared to the results made by gasification of the original feedstock, Polish coal. These investigations were done to identify the effect of volatile matter on the product gas quality, so the sampling for tar as well as for the impurities NH_3 and H_2S have been accomplished. These tests also provide information about the gas formation out of the volatile matter (devolatilization) and solid carbon (char gasification with H_2O). The tests were carried out at a gasification temperature of **870 °C**, a steam-to-carbon ratio φ_{SC} between **1.9 and 2.0 kg_{H2O}/kg_{carbon}**, an input fuel power of **78 kW_{th}** and the used bed material particle size was **510 µm** (d_{sv}). These operating conditions differ from those defined in paper II. They were chosen as the reference test with Polish hard coal was done in a test campaign prior to the tests with lignite, Spanish hard coal and PE (Papers I, II, III, IV, V). This is also the reason why different process conditions were applied for the tests in paper VIII.

Surprisingly, the tests showed that the tar in the product gas vanished completely (<10 mg/Nm^3_{db}) while the gas production was respectable. However, the pyrolysis step has to be considered to produce the char. This was devolatilized in a rotary kiln pyrolysis reactor. As also tar measurement (pyrolysis oil) and a balance of the pyrolysis step was done, the energy balance can be closed and is shown in this paper.

5.2.7 Paper VII

This paper is a follow-up of paper VI. Since these results were very promising, the procedure of pre-pyrolysis for the original feedstock was done for wood pellets as well, so char from wood pellets was gasified and the results were compared with the results gained by wood pellets gasification. For this comparison of wood pellets and its char the process conditions suggested in paper II were applied Gasification temperature: **850 °C**, bed material particle size (d_{sv}): **370 µm**, input fuel power: **90 kW_{th}**, steam-to-carbon ratio (φ_{sc}): **1.3 kg_{H2O}/kg_{carbon}**).

Any tar formation could be avoided effectfully, however, with a higher penalty to pay by the pyrolysis step.

5.2.8 Paper VIII

In paper VIII the focus is laid on the influence of the gasification temperature on the process when co-gasification of biomass and hard coal is applied. The gasification temperature was therefore varied between 750 °C and 870 °C. The applied coal ratio was **20 %** in terms of energy for all operating points (**750, 800, 850, 870 °C**). The used olivine particle size was **510 µm** (d_{sv}) and here the steam-to-fuel ratio was kept constant to **0.8 $kg_{H2O}/kg_{fuel,db}$**.

At higher operating temperatures the gasification reactions were enhanced, so the H_2 content increased and the product gas quality increased as well resulting in a lower tar content due to forced tar reforming and tar cracking reactions at higher temperatures.

5.3 Results of the fuels tested

In this section the general results of the gasification tests, such as gas composition, conversion performance and balance are discussed in terms of the organic composition of the used fuels. To provide a better overview this section is divided into three subsections where the pure fuels are compared, the study of char gasification, and co-gasification of PE or wood pellets with lignite are listed separately.

5.3.1 Gasification of pure fuels

To summarize the gasification performance of the used original fuels, gasification tests with the same operating conditions, which are a gasification temperature of 850 °C (mean temperature in the bubbling bed), a input fuel power of 90 kW_{th}, a mean bed material particle size of 375 µm (dp_{50}) and a steam-to-carbon ratio (φ_{SC}) of 1.3 kg_{H2O}/kg_{carbon} (1.4 for PE gasification), are compared. For each test, a fresh batch of bed material (olivine) was used. The data basis for this comparative study can be found in Paper I, II, IV and V.

Mean values of the main permanent gas components are summarized in Figure 21, which provides a good impression of the influence of the feedstock on the product gas composition. Compared with the results of wood pellets gasification (first bar) as the base case, the other tested fuels reach in general higher concentrations of H_2 in the product gas. In general two reasons can be identified to be responsible for this in terms of the organic feedstock composition:

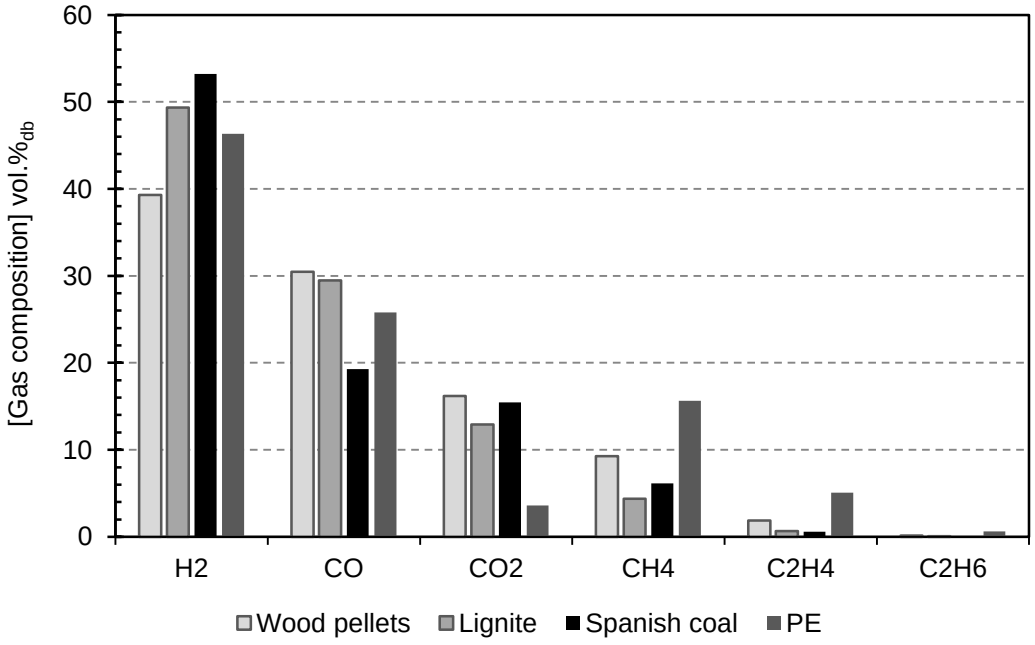

Figure 21: Main product gas components for gasification of pure fuels.

For coals compared to wood the lower content of volatile matter and higher value of fixed carbon are first indicators of the processes taking place in the gasification reactor for converting the solid fuel into product gas. The two global processes which form product gas are devolatilization

(pyrolysis) and char gasification. While for fuels with a high content of volatile matter, devolatilization dominates product gas formation, in the case of a low content of volatile matter in the fuel, char gasification is the main source of gaseous products. In the case of steam gasification the gas components H_2 and CO are formed by the char gasification reaction (Equation 4). Subsequent reactions, like the water-gas shift reaction (Equation 14), after the char gasification process can lead to minor amounts of CO_2. In the case of product gas made out of volatile matter, the formed gas shows characteristics of a gas made by pyrolysis which means that in addition to H_2 and CO, the gas components CO_2, CH_4 and higher hydrocarbons (C_2H_2, C_2H_4, …, C_xH_y, tar) can be released [18].

A second observation which influences the product gas composition significantly is the oxygen content in the fuel which mainly oxidizes H_2 to H_2O and CO to CO_2.

Basically the two coals (lignite and Spanish hard coal) yield significantly higher H_2 concentrations and lower values of methane and higher hydrocarbons than wood pellets. This can be ascribed to the lower content of volatile matter. However, for PE, which consists nearly completely out of volatile matter, respectable amounts of CH_4, C_2H_2 and even C_2H_4 were measured. This leads to the assumption that also a high tar content is formed which will be proven later. A special aspect for PE as a fuel is, beside the high value of volatile matter, the absence of any oxygen in the fuel. As a consequence of this, the CO_2 content is very low, only 3.6 vol.%$_{db}$ were detected. This low amount of CO_2 indicates the potential of homogeneous reactions (water-gas shift reaction) in the gas phase.

With a focus on the hydrogen production of the tested fuels, the following ranking can be made:

Spanish hard coal > Lignite > PE > Wood pellets

According to the different product gas composition the heating value of the gas changes significantly. The contribution of CH_4 and the higher hydrocarbons C_2H_2 and C_2H_4 is essential. This lifts the LHV (lower heating value) of the dry product gas from 11.0 MJ/Nm³$_{db}$ for lignite up to 18.6 MJ/Nm³$_{db}$ for PE. Based on the values of the LHV (Table 14) the performance of the tested fuels is outlined as:

PE > Wood pellets > Spanish coal > Lignite

Especially for any downstream utilization of the gas, more important than the main gas components are impurities like ammonia (NH_3), hydrogen sulfide (H_2S) and tar. The main focus of sulfur conversion is that of H_2S in which form most sulfur released in the product gas is present [98], although minor concentrations of COS can also be found. CS_2 is generally a product of secondary reactions of COS and H_2S, but only to a negligible extent as these reactions only occur at temperatures above 850 °C. As a result, CS_2 formation is only a matter of interest with respect to entrained flow gasification, during which process such high temperatures are observed, and not in fluidized bed gasification [99]. Entrained dust and char in the product gas usually do not cause problems like the components mentioned before as particle removal is well performed and cheap, compared to tar, H_2S and NH_3 removal. Entrained char lowers the carbon conversion of the system, but in industrial plants char can be recovered and used as a fuel in the combustion reactor.

The contents of NH_3 and H_2S in the product gas for the fuels tested are provided in Figure 22. As both impurities are formed from the nitrogen and sulfur content of the feedstock, they go along

with the fuel composition. In a previous investigation it has been found that nearly the total amount of nitrogen introduced by the solid fuel can be found as NH_3 in the product gas and up to 90 % of the sulfur present in the solid fuel is converted to H_2S in the product gas while the larger part of the rest is transported with the char to the combustion reactor where SO_2 is formed [100]. No amounts of those two impurities are present in the product gas during gasification of PE as the pure PE is completely free of the two components. The used wood pellets are also nearly free of sulfur, so the gas is also nearly free (21 ppm_v) of H_2S. As contents of nitrogen and sulfur are significantly higher in the used coals, their products can be found at vast quantities. However, the sulfur and nitrogen content is still low compared to other types of lignite commonly used.

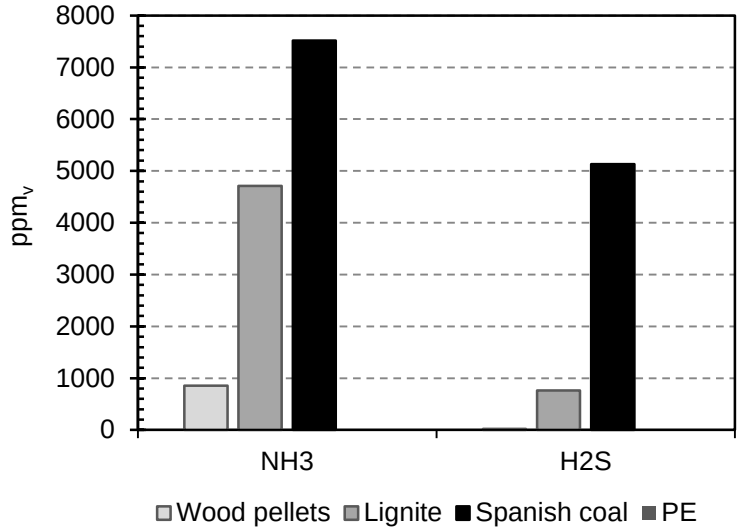

Figure 22: Detected concentrations of NH_3 and H_2S in the product gas for the used pure fuels.

The most interesting part concerning product gas quality in solid feedstock gasification research is the content of condensable components (tar). In Figure 23, the tar contents (GC/MS detectable and gravimetric detectable tars) are plotted together with the particulate matter found in the product gas. As explained before, tar is in general a product of feedstock devolatilization and not of char gasification. Consequently, fuels with a higher content of volatile matter cause higher tar contents if constant process conditions are maintained and no change in catalytic activity in the system takes place. Basically this fact goes along with the findings here. The highest tar load was caused by PE gasification. However, the result for the two coals here in terms of the tar content is somehow surprising on a first view as the Spanish hard coal produced a higher tar content (4.5 g/Nm^3_{db} and 2.4 g/Nm^3_{db} GC/MS and grav. tar, respectively) compared to the lignite (3.0 g/Nm^3_{db} and 0.8 g/Nm^3_{db} GC/MS and grav. tar, respectively) although its content of volatile matter is significantly lower (27.2 $wt.\%_{db}$ for Spanish coal and 51.8 $wt.\%_{db}$ for lignite). This improved tar removal potential of the lignite will be explained in section 5.6 as the ash of this feedstock is found to be catalytically active for tar reduction reactions.

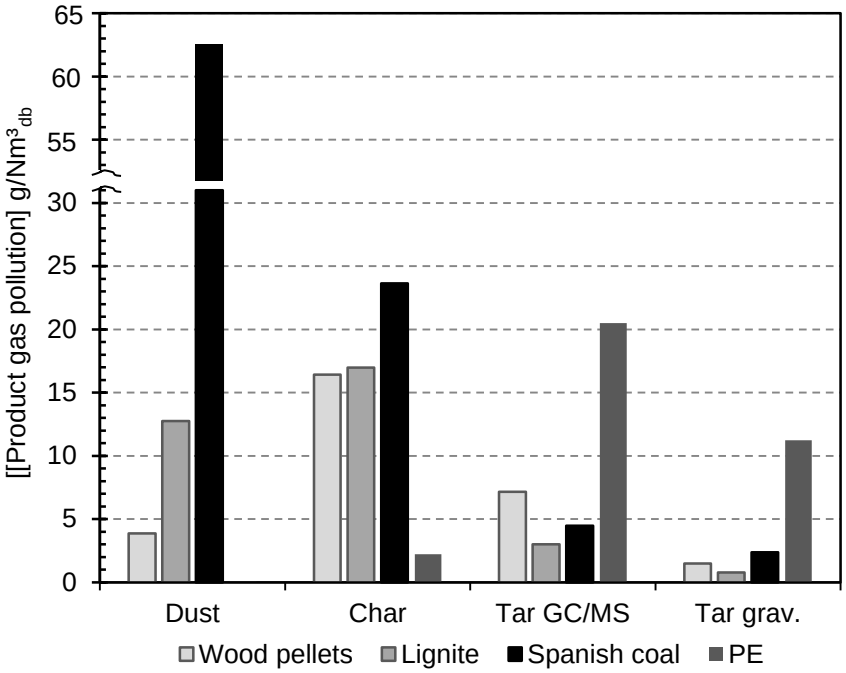

Figure 23: Particulate matter and tar content (GC/MS and gravimetric) detected for gasification of pure fuels.

Concerning the gas quality in terms of tar the following ranking for the fuels starting with the lowest GC/MS tar amount can be stated:

Lignite > Spanish hard coal > Wood pellets > PE

Entrained char is basically a reason of the fuel particle size, the fixed carbon content and the reactivity of the feedstock. The content of entrained char in the product gas stream was nearly equal for wood pellets gasification and lignite gasification which is an indicator that the reactivity of the lignite is at a comparably high level as this fuel shows a higher content of fixed carbon compared to wood pellets. In contrast to this, the Spanish coal shows significantly higher unconverted char values in the product gas. This may be caused by the high fixed carbon content and therefore a higher char content in the reactor. This aspect including the critical particle size of the fuel to be entrained to the gas stream is explained in detail in Paper V. On the other side, PE causes the lowest char amount in the product gas. The content of inorganic particulate matter (dust) is caused by the fuel ash. This statement is proven by gasification of PE, as this ash-free fuel does not cause any dust in the product gas. Consequently this means that the used bed material does not show any significant attrition. With the enormous ash load of the Spanish coal, the high dust content caused by this feedstock is a logical result.

The most relevant data of the tests are summarized in Table 14. An essential value here is the amount of product gas. Beside the total product gas amount, which includes unconverted water that is used for the calculation of the gas residence time in the reactor the dry product gas amount is essential as the product gas is cooled and cleaned in most of the cases prior to any utilization. Due to the high water conversion during lignite gasification, the dry product gas amount obtained from lignite tops the amount made by wood pellets slightly. The chemical power in the product gas is an indicator for the conversion performance which is the product of the gas heating value

multiplied by the product gas amount. This delivered chemical power by the product gas goes in line with the volatile matter in the fuel. Nearly the complete feedstock was converted in the case of PE gasification while only 47.3 kW are produced by the Spanish hard coal. These values do not include the energy demand of the combustion reactor which provides the heat for the gasification process by burning residual char and additional fuel for combustion (light heating oil here). As more or less all of the introduced amount of PE is converted in the gasification reactor to product gas, all of the heat for gasification has to be provided by additional fuel for combustion that makes up 48.9 kW (Paper IV). On the other side, during gasification of the comparably unreactive Spanish hard coal, only 2.3 kW of the heat for gasification were necessary by addition fuel (Paper V). This has to be included for the calculation of the cold gas efficiency of the process. By using Equation 29, the ranking of the cold gas efficiency leads to:

PE > Wood pellets > Lignite > Spanish hard coal

To complete the results of the gasification tests, more specific values which are not discussed above are listed. A complete description of these results can be found in Papers I, II, III, IV and V.

Table 14: Specific data for gasification of pure fuels (wood pellets, lignite, Spanish coal, PE).

Value	Unit	Wood pellets	Lignite	Spanish coal	PE
Total product gas amount	Nm^3/h	27.5	24.1	28.8	20.9
H_2O content in product gas	vol.-%	32.6	19.1	51.4	19.0
Dry product gas amount	Nm^3_{db}/h	18.1	19.3	14.5	17.0
Specific product gas yield	$Nm^3_{db}/kg_{fuel,daf}$	1.0	1.5	1.3	2.4
LHV	MJ/Nm^3_{db}	13.6	11.0	11.8	18.6
Chemical product gas power $_{excl.\ tar}$	kW	68.4	58.8	47.3	87.4
Cold gas efficiency, $\eta_{c,IP}$	%	69.0	67.4	59.8	72.4
Logarithmic deviation from CO-shift equilibrium, $p\delta_{eq,CO\text{-}shift}$	-	-0.45	0.03	-0.55	-0.50
Water conversion, $X_{H20,rel}$	$kg_{H2O}/kg_{fuel,daf}$	0.13	0.47	0.50	0.63
Water conversion, $X_{H20,rel}$	$kg_{H2O}/kg_{fuel,daf,N,S,Cl\ free}$	0.13	0.48	0.51	0.63
Stoichiometric steam demand	$kg_{H2O}/kg_{fuel,daf,N,S,Cl\ free}$	0.27	0.74	1.10	1.29
Stoichiometric steam demand	$mol_{H2O}/kg_{fuel,daf,N,S,Cl\ free}$	14.76	41.06	61.16	71.54
Ratio of water conversion to stoichiometric steam demand	kg_{H2O}/kg_{H2O}	0.50	0.65	0.47	0.49
Carbon conversion in the gasification reactor, X_C	%	66.85	65.47	41.28	95.44
Overall carbon conversion of the DFB system, $X_{C,DFB}$	%	96.62	95.90	96.04	99.38
Specific tar content, GC/MS	$g/kg_{fuel,daf}$	7.43	4.42	5.99	49.22
Specific tar content, grav.	$g/kg_{fuel,daf}$	1.54	1.15	3.18	27.00
Specific tar content, GC/MS	g/kg_{carbon}	14.75	6.46	7.49	57.24
Specific tar content, grav.	g/kg_{carbon}	3.06	1.68	3.98	31.40
Tar intensity per kWh of prod. gas, GC/MS	g/kWh_{syngas}	1.89	0.99	1.37	3.98
Tar intensity per kWh of prod. gas, grav.	g/kWh_{syngas}	0.39	0.26	0.73	2.18
Mean gas res. time freeboard gasification reactor, τ_F	s	3.77	4.62	4.06	5.22
Mean gas res. time combustion reactor, τ_C	s	0.86	0.86	0.83	0.77

5.3.2 Char gasification

For other gasification study, coal (Polish coal) and wood (wood pellets) were used. Char gasification performance was compared for both fuels and their chars separately which means that the operating conditions for the gasification process have been kept constant for each original feedstock and its char (Papers VI and VII). The main reason for this is that the reference test with Polish coal was done prior to the investigations of Paper II where the operating conditions were set. In order to compare the coal char gasification performance with its original feedstock (Polish coal), the operating conditions have been chosen to the conditions of the original feedstock. In terms of simplification the operating conditions for the char gasification tests are summarized in Table 15.

Table 15: Operating conditions for char gasification and gasification of the original feedstock.

Value	Unit	Coal gasification	Coal char gasification	Wood gasification	Wood char gasification
Gasification temp.	°C	870 ± 2		852 ± 2	
Temp. comb. reactor	°C	926	912	890	887
Fuel power	kW	78		90	
Fuel mass flow	kg/h	10.9	9.0	18.6	9.1
Mean particle size bed material, dp_{50}	µm	520		375	
Steam-to-carbon ratio, φ_{SC}	kg_{H2O}/kg_{carbon}	1.9	2.0	1.3	1.4
Steam-to-fuel ratio, φ_{SF}	$kg_{H2O}/kg_{fuel,daf}$	1.5	1.8	0.7	1.3

Figure 24 shows the main product gas components at the outlet of the gasification reactor for coal and coal char. There can be seen that for both fuels the H_2 content was relative high, but for char gasification this value increased up to 56.0 $vol.\%_{db}$ compared to 54.0 $vol.\%_{db}$ for coal gasification. This behavior can be explained as the char gasification reaction with H_2O results in H_2 and CO and the higher carbon content of the char highlights this reaction. This fact was strengthened by the forced production of CO for char gasification: Also here the CO content increased from 18.0 $vol.\%_{db}$ for coal gasification to 21.6 $vol.\%_{db}$ for char gasification. The content of CO_2 was nearly not affected at all. Methane showed a significant decrease for char gasification. Here the CH_4 content decreased from 5.8 $vol.\%_{db}$ down to 1.6 $vol.\%_{db}$. For the higher hydrocarbons C_2H_4 and C_2H_6 this effect was even more drastic as they vanished completely for char gasification. This showed that methane and the higher hydrocarbons are predominantly formed by devolatilization of the fuel while hydrogen and carbon monoxide is mainly a result of char gasification. This leads to the expectation of a significant decrease of tar in the product gas which will be shown in the following section. The water content in the product gas was between 46 and 49 vol.%, which was at a higher level than for standard operation with biomass due to the comparably high steam-to-carbon ratio (φ_{SC}).

As the tests were done, amongst others, to identify the origin of tar compounds, a focus is set on the tar content of the product gas. The gravimetric as well as the GC/MS detectable tars are also plotted in Figure 25. The major finding here was that for char gasification nearly all of the tar components disappeared. For coal gasification 3.8 g/Nm^3_{db} of gravimetric and 5.8 g/Nm^3_{db} of

GC/MS detectable tars were found, which are already lower values compared to gasification of wood (pellets or chips).

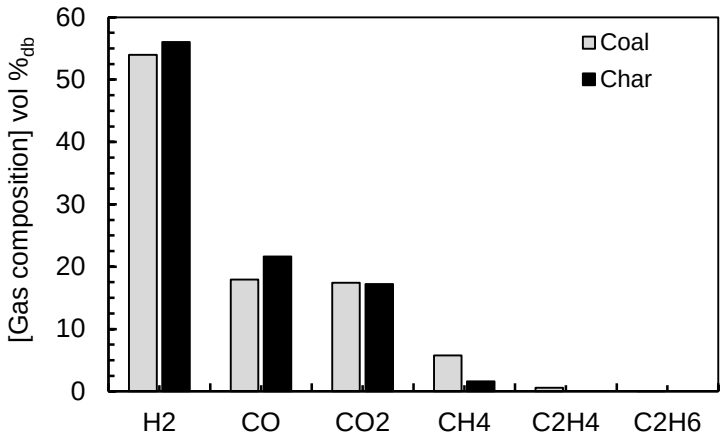

Figure 24: Main gas components for coal and coal char gasification.

For coal char gasification the GC/MS tar vanished, only 3 mg/Nm^3_{db} were found in the gas and the only component that was found was naphthalene. As for the applied gasification conditions, the gravimetrically detected tar is usually lower than the GC/MS detectable tar. Therefore the focus is here on the GC/MS tar. However, a little amount of gravimetrically detectable tar was measured. The reason for this is explained in detail in Paper VI.

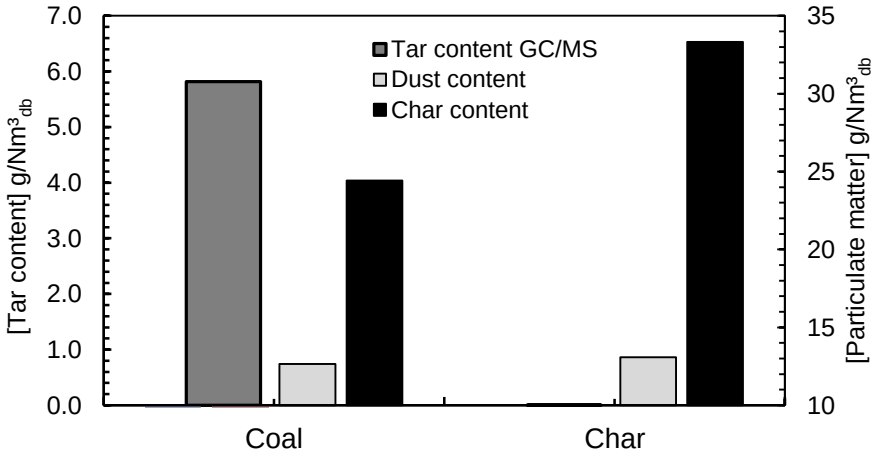

Figure 25: Particulate matter and tar content for coal and coal char gasification.

As explained before, the NH_3 and H_2S concentration is mainly depending on the nitrogen and sulfur load in the solid feedstock. A positive side effect of the pre-pyrolysis step is in this case that a part of the sulfur was released, so the H_2S concentration is reduced from 1756 ppm_v for coal gasification to 472 ppm_v for gasification of coal char.

Due to the promising results concerning the amount of tar for coal char it was decided to make a second test series with wood pellets. The idea behind this is that usually wood pellets or biomass in general, causes a much higher content of tar in the product gas as the devolatilization process dominates the char gasification process by the high content of volatile matter in the feedstock. By

the larger difference of the fuel composition in case of wood pellets and wood pellets char, compared to coal and coal char, the product gas composition is quite different (Figure 26).

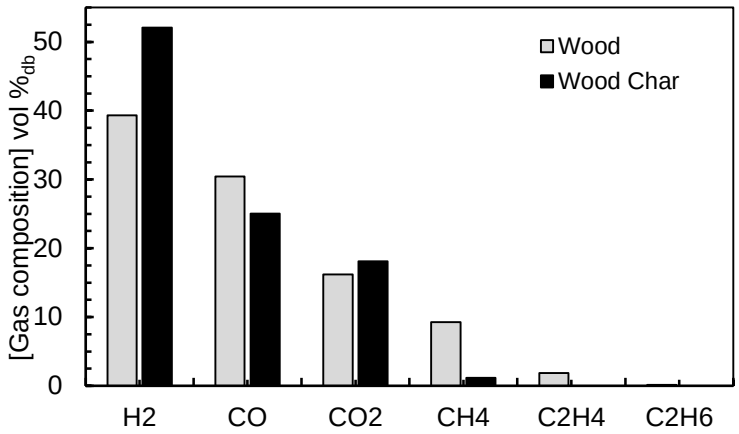

Figure 26: Main gas components for wood pellets and wood pellets char gasification.

For gasification of char the H_2 content increased massively while the CH_4 content was drastically reduced and the higher hydrocarbons vanished completely due to the absence of volatile matter in the fuel. The CH_4 content in this case is in the range for thermodynamic equilibrium (Paper V). As a consequence also here the GC/MS tar (Figure 27) vanished (only 10 mg/Nm^3_{db} of naphthalene were detected).

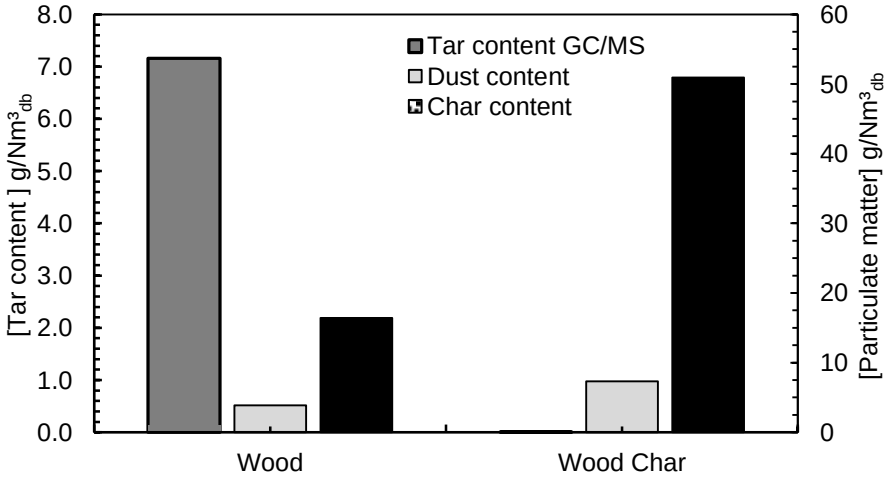

Figure 27: Particulate matter and tar content for wood pellets and wood pellets char gasification.

By comparison of the specific values of the tests in Table 16, there can be seen that the lower steam-to-carbon ratio φ_{SC} for wood pellets and wood pellets char gasification resulted in a lower content of unconverted water in the product gas. As a logical consequence, the amount of product gas was reduced by char gasification as the gasification reaction is much slower compared to pyrolysis/devolatilization (Table 6 and

Table 7 in chapter 3.3) which means that the cold gas efficiencies suffered during char gasification. An energetic comparison dealing with the penalty due to pre-pyrolysis of the feedstock can be found in Paper VI and Paper VII.

Table 16: Specific data for char gasification and their original fuels.

Value	Unit	Polish coal	Polish coal char	Wood pellets	Wood pellets char
Total product gas amount	Nm^3/h	25.82	25.01	27.52	21.31
H_2O content in product gas	vol.-%	49.63	45.96	32.62	34.56
Dry product gas amount	Nm^3_{db}/h	13.81	13.51	18.09	14.92
Specific product gas yield	$Nm^3_{db}/kg_{fuel,daf}$	1.51	1.58	1.04	1.45
LHV	MJ/Nm^3_{db}	10.97	9.61	13.62	9.40
Chemical product gas power $_{excl.\ tar}$	kW	42.07	36.06	68.40	38.98
Cold gas efficiency, η_c	%	59.12	50.08	68.97	48.30
Logarithmic deviation from CO-shift equilibrium, $p\delta_{eq,CO\text{-}shift}$	-	-0.20	-0.21	-0.45	0.00
Water conversion, $X_{H20,rel}$	$kg_{H2O}/kg_{fuel,daf}$	0.64	0.82	0.13	0.86
Water conversion, $X_{H20,rel}$	$kg_{H2O}/kg_{fuel,daf,N,S,Cl\ free}$	0.66	0.83	0.13	0.86
Stoichiometric steam demand	$kg_{H2O}/kg_{fuel,daf,N,S,Cl\ free}$	1.14	1.32	0.27	1.39
Stoichiometric steam demand	$mol_{H2O}/kg_{fuel,daf,N,S,Cl\ free}$	63.17	73.28	14.76	77.27
Ratio of water conversion to stoichiometric steam demand	kg_{H2O}/kg_{H2O}	0.58	0.63	0.50	0.62
Carbon conversion in the gasification reactor, X_C	%	45.40	41.00	66.85	39.10
Overall carbon conversion of the DFB system, $X_{C,DFB}$	%	95.53	94.20	96.62	92.34
Specific tar content, GC/MS	$g/kg_{fuel,daf}$	8.81	0.00	7.43	0.01
Specific tar content, grav.	$g/kg_{fuel,daf}$	5.72	0.65	1.54	0.45
Specific tar content, GC/MS	g/kg_{carbon}	10.66	0.00	14.75	0.02
Specific tar content, grav.	g/kg_{carbon}	6.92	0.72	3.06	0.46
Tar intensity per kWh of prod. gas, GC/MS	g/kWh_{syngas}	1.91	0.00	1.89	0.00
Tar intensity per kWh of prod. gas, grav.	g/kWh_{syngas}	1.24	0.15	0.39	0.12
Mean gas res. time freeboard gasification reactor, τ_F	s	4.87	5.37	3.77	5.72
Mean gas res. time combustion reactor, τ_C	s	0.78	0.70	0.86	0.61

5.3.3 Co-gasification

Co gasification was conducted with lignite as the main fuel in two test series with wood pellets and PE. The applied operating conditions were the defined by conditions used in Paper II. One important aspect that has to be mentioned here is the feeding position that was applied. Up to now only in-bed feeding of the fuel was applied. As only one in-bed feeding hopper was in operation, the second fuel was fed on top of the bed. This means that lignite was fed into the bed by hopper 1 while wood pellets (hopper 2) and PE (hopper 3) were both introduced into the reactor by on-bed feeding. This is important as the feeding position significantly influences the product gas composition and process performance. The product gas made by on-bed feeding shows in general more characteristics of a gas made by pyrolysis (higher tar content) [101]. This will be explained in more detail chapter 5.4.

Adding coal to fuels like wood pellets or plastics can be beneficial for the process especially for the reduction of the tar content by several mechanisms:

- The most important aspect is to increase the char content in the system by an increase of the fixed carbon content in the fuel mix. Char has been identified to be a natural catalyst for tar reduction in the gasification process. The higher content of fixed carbon in the lignite compared to wood pellets or PE causes a higher char load in the fluidized bed. Abu El-Rub et al. [19] found that char particles can act as a catalyst in the gasification reactor as they are capable of adsorbing higher hydrocarbon tars and promote their cracking and reforming.
- Fuel analysis shows that lignite has a much lower content of volatile components and a higher amount of fixed carbon. Therefore, lignite causes less gaseous products during devolatilization and more during gasification of carbon. As many tar components are caused by devolatilization of the solid fuel in the fluidized bed, it is therefore likely that lignite produces less condensable hydrocarbons (tars) in the product gas.
- A very interesting aspect is the catalytic effect of the fuel ash. It was found that certain ash components can act as a catalyst if they are present in the system in a sufficient amount. In chapter 5.6 the catalytic activity of the lignite ash will be discussed. The main components in the lignite ash were found to be calcium, magnesium, iron and sodium.

Co-gasification of lignite and wood pellets

In the case of co-gasification of lignite and wood pellets, the gas main composition is changing linearly with the lignite ratio. Consequently, the lower heating value (LHV) of the gas can be influenced by the lignite ratio continuously (Figure 28 and Figure 29).

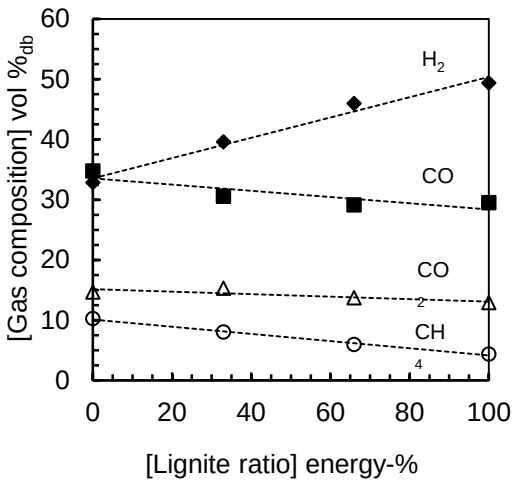

Figure 28: Main gas components in the product gas for co-gasification with wood pellets vs. lignite ratio.

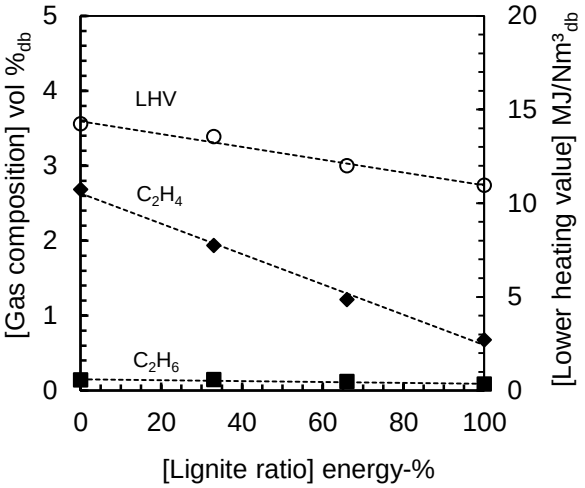

Figure 29: Ethane and ethylene in the product gas and LHV of the product gas for co-gasification with wood pellets vs. lignite ratio.

However, the tar content of the product gas is not linearly dependent on the lignite ratio, as shown in Figure 30. The data show that the tar contents decreased with higher lignite ratios. Taking a closer look at the trends in the tar content in Figure 30, it can be seen that the most rigorous abatement of gravimetric and GC/MS tars occurred with an increase in the lignite fraction from 0 to 33%. During this step, the GC/MS tars decreased by about 59.1% (down to 6.9 g/Nm³$_{db}$ at a lignite fraction of 33%) and the gravimetric tars went down even more, by about 74.5% (down to 2.5 g/Nm³$_{db}$ for a lignite ratio of 33%), so even a low amount of lignite in the fuel mix can significantly improve the gas quality with regard to tar levels.

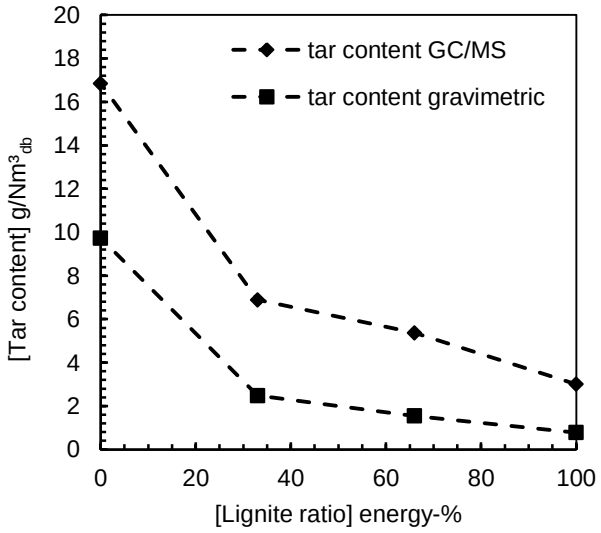

Figure 30: Gravimetric and GC/MS tar content in the product gas for co-gasification of lignite with wood pellets.

More details about co-gasification of lignite and wood pellets can be found in Paper III.

Co-gasification of lignite and PE

The H_2 content varied for the tests between 40.4 and 49.4 vol.%$_{db}$ where the highest value was reached for 100 % lignite and the lowest for 33 % lignite in the feedstock. Gasification of pure PE yielded a H_2 content of 46.3 vol.%$_{db}$. This non-linear behavior, especially for 33 % lignite, indicates that the components and structure of the two fuels, with completely different nature and origin, can interact with one another and influence the behavior in the gasification reactor. This was also observed for the CO content in the product gas, where the lowest value (20.3 vol.%$_{db}$) was found for 33 % lignite and the highest (29.5 vol.%$_{db}$) for pure lignite gasification. The main products of char gasification, H_2 and CO, were produced by gasification of pure lignite. Nevertheless, pure PE produced a CO content of 25.8 vol.%$_{db}$, which was not the lowest value for the four operating points. The presence of CO_2 in the product gas, from gasification using pure steam as the gasification agent, is mainly due to the oxygen content of the feedstock. Compared to gasification of wood pellets, which have a much higher content of oxygen and therefore yield about 17 vol.%$_{db}$ of CO_2 in the product gas, CO_2 levels for the fuels used here were lower. The contents of CH_4, C_2H_4 and C_2H_6 are traditionally higher when gasifying plastics [102]. This was also observed here as the methane content reached 15.6 vol.%$_{db}$ for PE compared to 4.4 vol.%$_{db}$ for lignite. As C_2H_4 is a monomer of polyethylene, which decomposes in the gasification reactor to its origin, significant amounts of this gas component were present in the gas when PE was added to the feedstock mix.

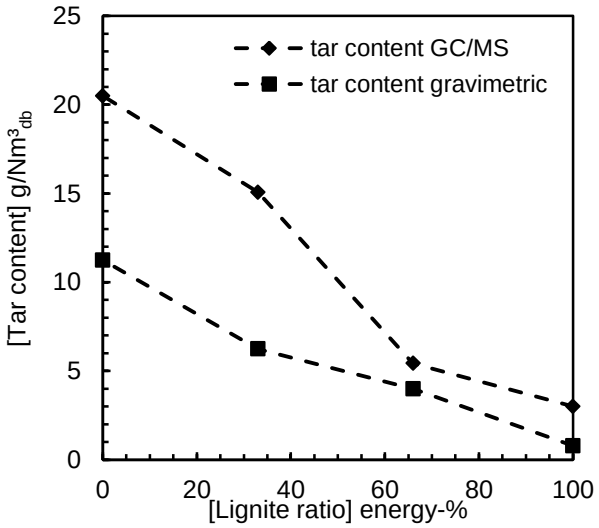

Figure 31: Gravimetric and GC/MS tar content in the product gas for co-gasification of lignite with PE.

The tar content (Figure 31) decreased also here with higher lignite ratios, consistent with the results of co-gasification with wood pellets. In the case of gravimetrically-detectable tars, the tar content in the product gas decreased from 11.2 g/Nm$^3_{db}$ for gasification of PE to 0.8 g/Nm$^3_{db}$ for gasification of pure lignite, giving a reduction of 92.9%. The situation was similar for the GC/MS detectable tars where a reduction of 85.3% was reached, from 20.5 to 3.0 g/Nm$^3_{db}$. The most dramatic decrease in gravimetrically- and GC/MS-detectable tar levels happened using a lignite ratio of 66%, where 73.6% of the GC/MS tars produced from pure PE vanished and reached values that were lower than those from biomass gasification at comparable process conditions. More details about including a comprehensive summary of the specific values as well as the GC/MS tar compositions can be found in Paper IV.

5.4 Influence of the fuel feeding position

To identify the influence of the location where the solid fuel is introduced into the gasification reactor, a comparative study of wood pellets gasification with variation of the feeding position was carried out. It has to be distinguished between fuel feeding into the bubbling bed (hopper 1) and onto the bubbling bed (hopper 2 and 3). The findings of these investigations are published in Paper I.

In the case of autothermal gasification with oxygen and steam in a bubbling fluidized bed it has already been found that the location of fuel feeding influences the gas composition since the gas obtained if the feedstock is introduced at the top of the reactor has a pyrolytic nature compared to the case where the feedstock is fed into the middle of the bubbling bed [101]. For dual fluidized bed gasification with steam there is no knowledge available and a direct transfer of the findings cannot be made as due to the circulating bed material the energy balance might be different.

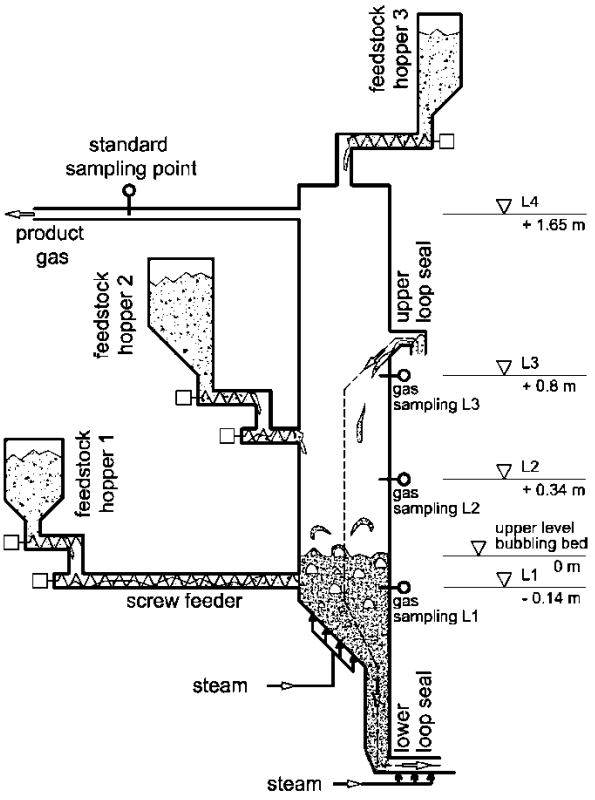

Figure 32: On-bed (hopper 2) vs. in-bed (hopper 1) feeding of wood pellets in the gasification reactor.

To distinguish between the two cases of fuel feeding the main gas composition and tar load of the product gas but also the overall energy balance of the dual fluidized bed system is essential. Those aspects will be discussed here.

The main gas composition, measured for both tests, is shown in Figure 33. As mentioned before, a fuel feeding position above a bubbling bed produces a gas that shows more characteristics of a pyrolysis gas, namely a lower H_2 content and higher contents of higher hydrocarbons and tar [101]. This behavior can also be seen here. Compared to the standard case, which is in-bed fuel feeding,

with fuel feeding on the bed the product gas consists of significantly less H_2 (-6.5 vol.%$_{db}$) while CO, CH_4 and the higher hydrocarbons were formed at a higher extent. The expectation of a higher tar content by on-bed feeding is proven with the measurement presented here (Figure 34). The mean GC/MS tar content measured for on-bed feeding was 2.4 times higher than for in-bed feeding. For the gravimetic detectable tar components the situation is much worse as this tar content was 6.5 times higher for on-bed feeding. This maladjustment of the increasing two tar contents (GC/MS tar and grav. tar) shows the shift of the tar composition towards larger components with high molecular weight as they are usually found in pyrolysis or low temperature gasification.

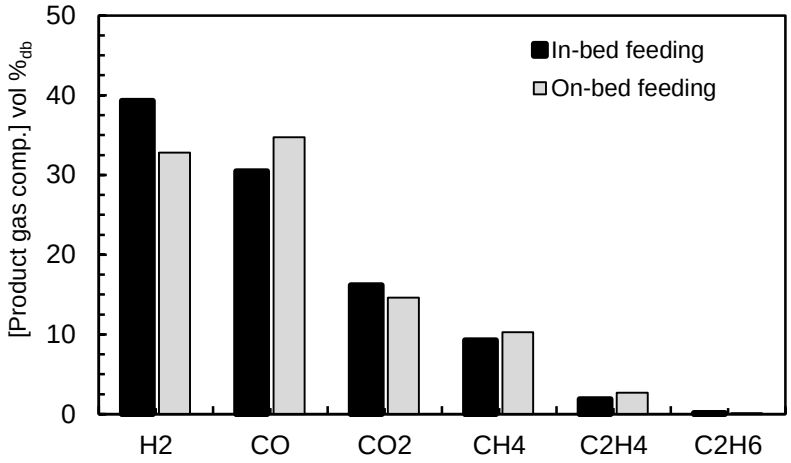

Figure 33: Main gas components for in-bed- and on-bed feeding (wood pellets gasification).

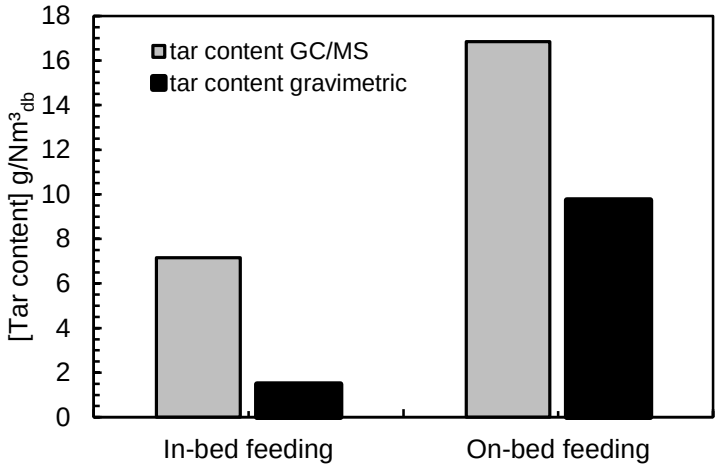

Figure 34: GC/MS and gravimetric tar content for in-bed- and on-bed feeding (wood pellets gasification).

In Paper I the GC/MS tar composition is classified according to ECN [103], Milne et al. [104] and Wolfesberger et al. [105]. From these data it can be seen that the relative contribution of naphthalene, as the most dominant GC-MS tar component, to the GC-MS tar decreased for on-bed feeding compared to in-bed feeding. Further components whose shares decrease are indene and phenols. In contrast to this, the share of components like anthracene, fluoranthene and benzo[g,h,i]perylene increased for in-bed feeding. On the other hand there were also substances

found in the tar with on-bed feeding of the feedstock that were not present with in bed-feeding. These are listed in Table 17.

Table 17: GC/MS tar components that were found only for on-bed fuel feeding.

Component	Unit	Amount
Benzo[a]pyrene	mg/Nm³	99.80
Dibenz[a,h]anthracene	mg/Nm³	99.46
Carbazole	mg/Nm³	27.38
4-Methylphenol	mg/Nm³	23.68
Isoquinoline	mg/Nm³	13.83
1-Benzothiophene	mg/Nm³	11.10
Indole	mg/Nm³	1.90

On the way that the feedstock dropped on the bed and not being fed in the lower section, the fuel particle is devolatilizing on the bed surface or the splash-zone where no or only little contact of the product gas with the hot bed material particles can take place. On the other side, in the case of in-bed feeding the product gas has to pass the bubbling bed. By the very intense gas-solid contact with the hot bed material, tar reducing reactions like steam reforming of hydrocarbons and tar cracking reactions can take place. This is only possible to a very little extent during on-bed feeding.

A second effect of the different feeding position is the residence time of a fuel particle in the gasification reactor. As the bed material is continuously circulating between gasification and combustion reactor, it carries some char particles to the combustion reactor. When the feedstock is introduced on top of the bubbling bed the residence time of the particle is higher till it moves to the combustion reactor via the lower loop seal. The effect of this is a higher gas yield obtained in the gasification reactor. Quantification of this effect is made in Table 7 of Paper I, where specific data of the two tests is listed. As a result of the increased residence time of the fuel/char particles in the gasification part of the system, the heat demand for gasification is higher and less char for combustion is available. This leads to a higher demand of additional fuel for combustion in the case of on-bed feeding. The additional fuel demand increased about 51 %, in total numbers from 24 to 37 kW. Nevertheless, the higher product gas amount leads to a higher cold gas efficiency of the process with the penalty of a lower gas quality (Table 18). Table 18 further summarizes the most relevant specific data of the tests. Those values are discussed in detail in Paper I.

Table 18: Specific data for wood pellets gasification comparing in-bed and on-bed feeding of the solid feedstock.

Value	Unit	In-bed feeding	On-bed feeding
Total product gas amount	Nm^3/h	27.52	30.68
H_2O content in product gas	vol.-%	32.62	35.76
Dry product gas amount	Nm^3_{db}/h	18.09	19.88
Specific product gas yield	$Nm^3_{db}/kg_{fuel,daf}$	1.04	1.15
LHV	MJ/Nm^3_{db}	13.62	14.23
Chemical product gas power $_{excl.\ tar}$	kW	68.40	78.60
Cold gas efficiency, η_c	%	68.97	70.60
Logarithmic deviation from CO-shift equilibrium, $p\delta_{eq,CO\text{-}shift}$	-	-0.45	-0.49
Water conversion, $X_{H20,rel}$	$kg_{H2O}/kg_{fuel,daf}$	0.13	0.14
Water conversion, $X_{H20,rel}$	$kg_{H2O}/kg_{fuel,daf,N,S,Cl\ free}$	0.13	0.14
Stoichiometric steam demand	$kg_{H2O}/kg_{fuel,daf,N,S,Cl\ free}$	0.27	
Stoichiometric steam demand	$mol_{H2O}/kg_{fuel,daf,N,S,Cl\ free}$	14.76	
Ratio of water conversion to stoichiometric steam demand	kg_{H2O}/kg_{H2O}	0.50	0.52
Carbon conversion in the gasification reactor, X_C	%	66.85	82.31
Overall carbon conversion of the DFB system, $X_{C,DFB}$	%	96.62	97.19
Specific tar content, GC/MS	$g/kg_{fuel,daf}$	7.43	19.34
Specific tar content, grav.	$g/kg_{fuel,daf}$	1.54	11.18
Specific tar content, GC/MS	g/kg_{carbon}	14.75	38.39
Specific tar content, grav.	g/kg_{carbon}	3.06	22.19
Tar intensity per kWh of prod. gas, GC/MS	g/kWh_{syngas}	1.89	4.26
Tar intensity per kWh of prod. gas, grav.	g/kWh_{syngas}	0.39	2.46
Mean gas res. time freeboard gasification reactor, τ_F	s	3.77	4.15
Mean gas res. time combustion reactor, τ_C	s	0.86	0.85

5.5 Influence of the fuel particle size

The investigation on the effect of fuel particle size was carried out in line with the tests done with Spanish coal. This coal is somehow a low grade coal as the ash content is very high and the particle size distribution of the coal is very wide which means that a high fraction of small particles (coal dust) was present together with particles that mark the upper limit (10 mm) to be handled in the DFB pilot plant. Therefore, one test has been accomplished with the coal as delivered, including fines, and a second test where a large part of the fine fraction has been removed by sieving. The two tests are only different in the feedstock particle size range, the operating conditions have been kept equal to the values defined in Paper II.

Table 19: Coal particle size distribution.

Value	Unit	Coal with fines (as delivered)	Coal without fines(sieved)
d_{p10}	µm	280	1400
d_{p50}	µm	2600	4990
d_{p90}	µm	7700	7860

The characteristic values (d_{p10}, d_{p50}, d_{p90}) of the particle size distribution of the used coal can be found in Table 19. An initial impression of the behavior of coal gasification using the dual fluidized bed system can be achieved by highlighting the temperatures in the gasifier at the different operating points, as well as the fluidization conditions in the system. An overview of the fluidization regime is presented in Table 20.

Table 20: Fluidization conditions in the DFB system.

Value	Unit	Coal with fines (as delivered)	Coal without fines(sieved)
Minimum fluidization velocity, U_{mf}	m/s	0.07	
Terminal velocity, U_t	m/s	3.36	
Superficial velocity gasification reactor, U_g	m/s	0.40	0.41
Fluidization number gasif. reactor, U_g/U_{mf}	-	5.51	5.64
Transport number gasif. reactor, U_g/U_t	-	0.12	0.12
Superficial velocity combust. reactor, U_c	m/s	9.42	9.23
Fluidization number combust. reactor, U_c/U_{mf}	-	130.79	128.19
Transport number combust. reactor, U_c/U_t	-	2.80	2.74

The velocities U_{mf}, U_t and their ratios to the actual superficial velocity in the gasification and combustion reactors can be used to characterize the fluidized bed system. The process conditions presented in Table 20 and the fuel particle size distribution listed in Table 4 illustrate the problem caused by the presence of fine particles in a fluidized bed reactor. Gasification of fuel particles should take place in the bubbling olivine bed, but in order to maintain the fluidization regime for a bubbling bed a certain fluidization velocity is required. In the case presented here, coal gasification was accompanied by a resulting superficial velocity in the gasifier U_g of about 0.4 m/s.

At this fluidization velocity the terminal velocity U_t of the olivine particles is far from resulting in their elutriation into the product gas. For the fuel particles, however, the situation is different, as the density of coal is lower and the particle size widely distributed, especially that of the fuel used as delivered; some of these particles are entrained into the product gas flow. The critical particle size for coal in the applied gasification atmosphere is about 160 μm, so coal particles that are smaller than this size are elutriated immediately after feeding into the gasifier. For the coal size distribution for the coal including fines, about 6.8 wt.% of the fuel was smaller than 160 μm. In the case of sieved coal, where most of the fine fraction was removed prior to introduction into the system, only 2.0 wt.% of the initial mass were smaller than 160 μm..

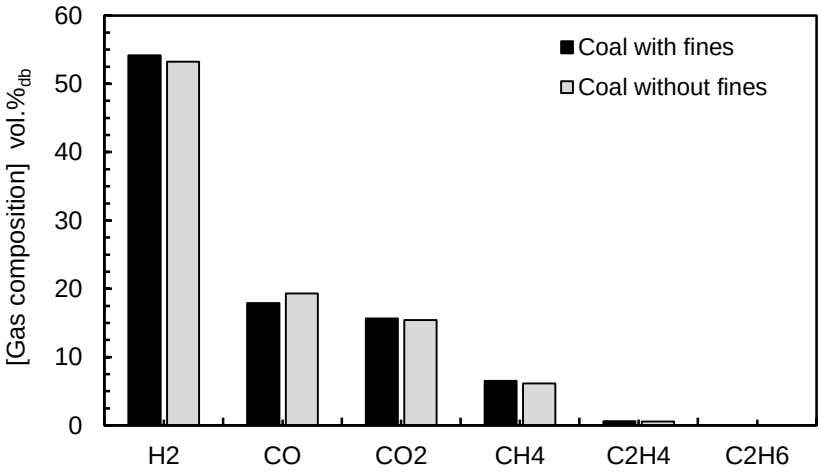

Figure 35: Influence of the fuel particle size on the main gas components in the product gas.

The influence of the particle size on the main permanent product gas components can nearly be neglected (Figure 35). However, a slight increase of CH_4 and the higher hydrocarbons can be observed. Huge differences were found in the load of particulate matter (Figure 36). Since, as mentioned previously, coal particles smaller than 160 μm were entrained to the product gas straight after fuel feeding, the concentration of particulate matter was significantly higher for the not sieved coal compared to the sieved coal. Considering the high fuel ash content found during initial fuel analysis, it is not surprising that such an amount of inorganic dust was also present in entrained coal particles. The amount of inorganic particulate matter (dust) was more than twice (nearly three times) that of char (organic particulate matter) due to the fact that levels of the latter were reduced in the freeboard as a result of partial gasification and carbon consuming reactions, such as the water gas reactions or the Boudouard reaction. The effect of solid carbon reduction in the freeboard of a bubbling fluidized bed gasifier has been described for wood gasification by Miccio et al. [106]. In this section only considerations about the organic particulate matter are made while inorganics will be part of chapter 5.6.

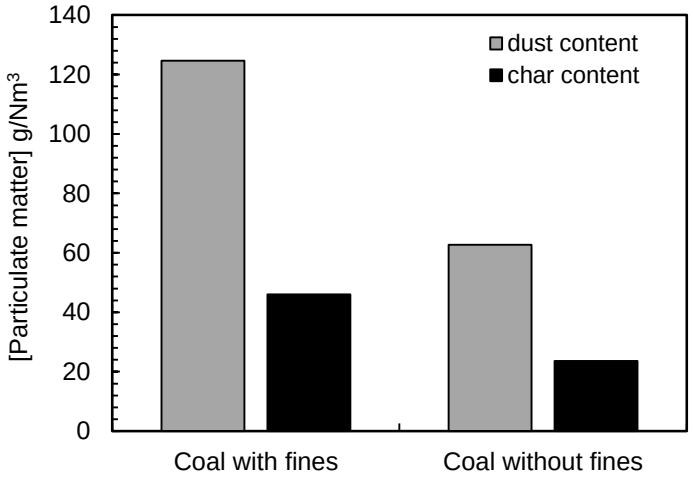

Figure 36: Influence of the fuel particle size on the load of particulate matter in the product gas.

The detected amount of tar in Figure 37 shows that fine fuel particles cause a large increase of the tar content. This finding matches the results of other investigations examining biomass. In their analysis of the steam gasification of a mixture of sawdust and pellets, Wilk and Hofbauer [107] found about twice as much GS/MS and gravimetric tar compared to the gasification of 100 % pellets. The authors argued that the main reason for this difference was that about 9 % of the mixed fuel mainly saw dust was transported immediately out of the fluidized bed with the fluidization steam. As a result, pyrolysis and gasification took place in the freeboard section of the gasifier, where the interaction of the pyrolysis products with the hot and catalytically-active bed material was absent. This process ultimately led to a significantly reduction in tar decomposition.

Another common interpretation of the higher tar content of fine particles is that they provide less resistance for the devolatilizing gases; in larger particles the pyrolysis gas has to pass a layer of char, and thus secondary catalytic tar cracking reactions can take place [18]. The relative contribution of each tar compound to GC/MS tar can be found in Paper V. As the origin of the feedstock used in both scenarios was the same, the actual composition of the GC/MS tar did not differ much when small fuel particles were entrained in the freeboard. Nevertheless, a tendency towards typical tar classes produced by devolatilization can be imagined for the case including fines, as evidenced by the lower contribution of naphthalene, a tar component which is mostly a product of secondary and tertiary tar reactions.

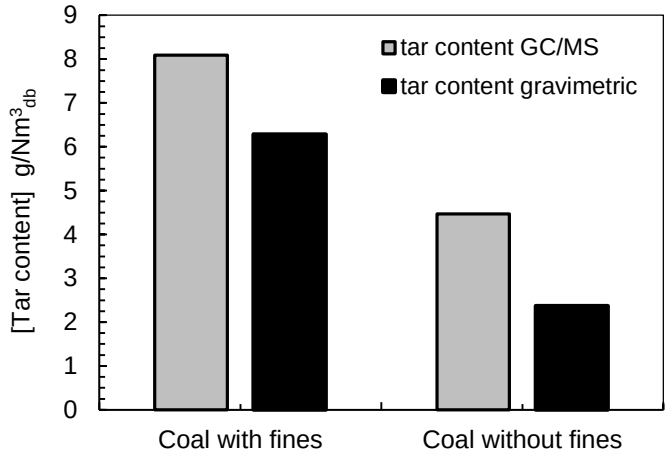

Figure 37: Influence of the fuel particle size on the tar content.

The higher amount of entrained fuel in the product gas also leads to drawbacks in the performance of the system (Table 8 in paper V). Significantly higher conversion rates of carbon in the gasification reactor (X_C) and in the DFB system ($X_{C,DFB}$) as well as a higher water conversion can be reached if the content of fuel dust is limited before feeding. Furthermore, by the higher residence time of larger particles the chemical energy delivered by the product gas stream is higher. By the loss of carbon particles, carbon for the combustion reactor is lost and the enhanced char reactions in the freeboard consume additional energy which has to be compensated with a slightly higher amount of additional fuel for the combustion reactor. By summing up these facts, the cold gas efficiency increased if less fine fuel particles are present in the reactor.

5.6 Impact of fuel ash

Considerations about the influence of inorganic matter (fuel ash) have been made for coals only as the used coals (lignite and Spanish coal) contain sufficient amounts of ash that are able to cause an influence on the gasification process. The XRF analyses of these two coals are listed in Table 21.

Table 21: XRF analyses of the coal ashes (values in wt.%).

Component	Lignite	Spanish coal
Na_2O	4.51	0.38
MgO	12.22	1.11
Al_2O_3	1.58	21.39
SiO_2	0.83	55.62
P_2O_5	0.30	0.10
SO_3	32.39	1.16
K_2O	0.90	3.09
CaO	36.11	3.40
TiO_2	0.26	1.33
V_2O_5	0.00	0.15
Cr_2O_3	0.02	0.16
MnO	0.13	0.16
Fe_2O_3	10.01	10.98
NiO	0.02	0.12
CuO	0.02	0.03
ZnO	0.01	0.15
Rb_2O	0.00	0.05
SrO	0.26	0.04
PbO	0.00	0.13
Cl	0.44	0.15

For the consideration of the influence of the fuel ash of lignite, the tests accomplished for Paper II, and for Spanish coal, the results of Paper V, are used. The two fuels are discussed here separately as from the lignite ash the process benefits while from the ash of the Spanish coal the process suffers.

5.6.1 Catalytic effect on tar reduction during lignite gasification

Mentioned already in chapter 5.3, lignite produced less tar although its content of volatile matter is higher. This can be caused by the catalytic activity of the fuel ash. As an ash mass flow of 0.58 kg/h was introduced by the lignite into the gasifier at the applied fuel mass flow rate to maintain a fuel power of 90 kW_{th}, the amount of ash present can be sufficient to contribute for some reactions in the system.

The results in Table 21 show the main ash components as calcium, sulfur, magnesium, iron and sodium. The high content of Fe_2O_3 is promising in this case due to the reason that a high content of Fe_2O_3 in combination with calcium works very well as catalyst for tar-reducing reactions. Several research groups [108][109] identified iron(III) as the active part regarding tar reduction. The latter researchers found that dolomite with a higher content of Fe_2O_3 performed better for tar conversion, which is an indicator for the catalytic activity. For steam reforming reactions, alkali metals are also catalytically active. It has been found that potassium carbonate is the most active

species followed by sodium carbonate [110]. The potassium content of the ash can be neglected here compared to other fuels [111], but the sodium present in the ash is able to contribute significantly to the catalytic activity.

5.6.2 Behavior of Spanish coal with high ash content in the gasification reactor

The high ash content of the Spanish coal makes it necessary to consider the effect of this ash on the system. The applied (wet) fuel feeding rate of 16.2 kg/h corresponds to 4.86 kg/h of ash being introduced into the gasifier for both gasification tests accomplished (chapter 5.5, paper V). According to the measurements of dust concentration in the product gas (Figure 36), the product gas stream and the total ash in the product gas and flue gas streams, the balance of the ash is closed.

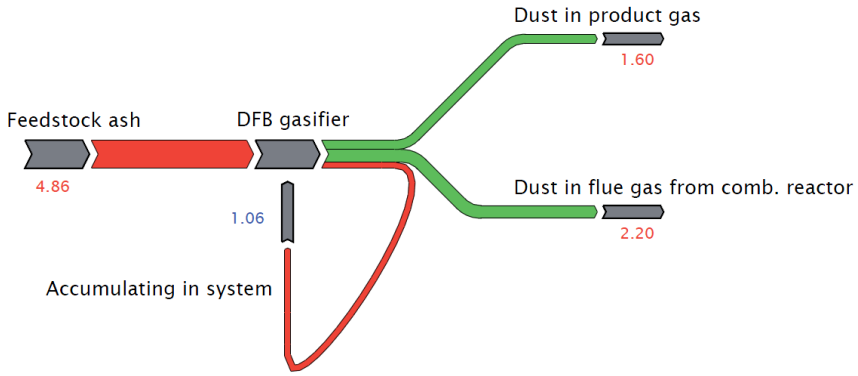

Figure 38: Ash balance of the gasification reactor in the case of gasification including fines in the feedstock.

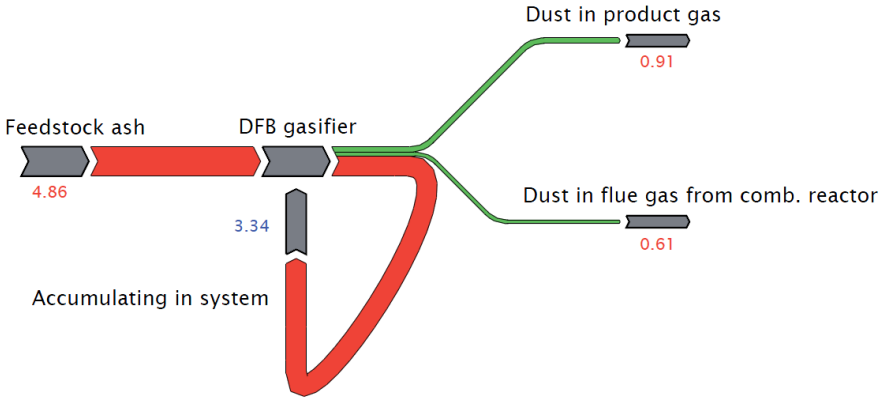

Figure 39: Ash balance of the gasification reactor in the case of gasification without fines in the feedstock (sieved).

Figure 38 and Figure 39 show the mass flows in kg/h for inorganic matter entering and leaving the gasification reactor. The most important fact to consider here is that the entrained particles also include a large amount of inorganic matter. Since larger coal particles also likely contain larger (sand/gravel) ash particles, it is not surprising that in the case of gasification of the coal including fines a total of 3.80 kg/h of ash left the DFB system via the product and flue gas streams, whereas

for sieved coal only 1.52 kg/h of ash was observed. In addition, as the mean ash particle size increased after fuel sieving, the terminal velocity U_t of most of the ash particles was increased above the superficial gas velocity U_g in the gasification reactor. Only the fraction that was small enough in size was able to escape the system. Hence, for gasification of the coal as it was delivered only 1.25 kg/h of ash accumulated in the system, while for sieved coal 3.34 kg/h were not able to leave the fluidized bed as no bottom ash removal device is installed at the pilot plant. However, the operation of the DFB pilot plant was not imperiled due to the accumulating ash, as the system was in operation for less than eight hours with coal as a feedstock. Nevertheless, a slight pressure increase in the bubbling bed was recorded for gasification of the coarse fraction, demonstrating the increase of inorganic matter in the system. For operations on an industrial scale, an ash removal system should therefore be installed to remove such ash from the bed. Therefore the compositions of the fuel ash and the ash collected from the gas streams exiting the reactor were detected via XRF analysis. Table 21 reveals that the main compounds contained in the fuel ash were silicon, aluminum and iron, with minor amounts of calcium, potassium, phosphorus, titanium and magnesium. Although fuel ash can play a significant role in increasing catalytic activity, no enhancement was observed in the present study in terms of tar reduction. This suggests that the large quantities of silicon and aluminum measured here were not catalytically active. In contrast, the minor components potassium, magnesium and calcium are known to be active catalysts, although the extent of this activity depends on their compounds. For the current study, it is probable that most of these alkali metals were present as silicates and thus not quite so active. The mass flow rates of the measured elements into and out of the reactor as part of fuel and particles in gas, respectively, are summarized in Table 22. The higher output of magnesium compared to its input likely reflects attrition of bed material.

A very interesting issue observed here was that after the gasification test and the release of the bed material out of the reactor, a few agglomerates of the fuel ash were found. It did not cause problems due to the comparably short operation time. This should be avoided by checking the ash melting behavior of the fuel ash before gasification in the fluidized bed system. This was also done here and the results showed an ash deformation temperature of 1230°C and an ash melting temperature of 1390 °C, which is sufficiently high enough to be suitable for gasification in the DFB system. However, in Table 22 the balance of the inorganic elements provides some information about this. There is listed that significantly less potassium is released via the gas streams compared to the input stream by solid fuel which leads to accumulation of potassium. With the very high amount of silica in the ash, which is also accumulating in the system, compounds like potassium silicates might be formed. As an example this compound ($K_2O_5Si_2$) has a melting point of 905 °C which leads to the assumption that the sintering temperature is below the operating temperature of the system that was applied.

Table 22: Mass flow rates of ash components for sieved coal.

Component	Unit	Input (feedstock ash)	Output (sieved coal gasification)
SiO_2		2703.0	789.0
Al_2O_3		1039.6	335.4
Fe_2O_3		533.5	203.2
K_2O		150.0	44.5
CaO		165.4	34.5
MgO		54.0	60.0
TiO_2	g/h	64.6	17.1
V_2O_5		7.4	2.1
Cr_2O_3		7.7	2.6
MnO		7.7	2.0
NiO		5.9	3.4
ZnO		7.1	2.8
Others		114.1	23.4
Sum	**kg/h**	**4.86**	**1.52**

5.7 Influence of gasification temperature

The influence of the temperature of the bubbling bed in the gasification reactor on the product gas composition and tar content and the process performance for co-gasification of wood pellets and Polish coal will be shortly summarized in this section. Co-gasification tests with a coal ratio of 20 % in terms of energy were carried out with a variation of the gasification temperature from 750 °C to 870 °C. The detailed results of this test series can be found in Paper VIII.

The applied operating conditions differed slightly from the conditions defined in Paper II as the tests here were investigated prior to those in Paper II. The operating conditions chosen here were:

- Input fuel power: 100 kW
- Mean particle size bed material, d_{sv}: 510 μm
- Steam-to-fuel ratio, φ_{SF}: 0.8 $kg_{H2O}/kg_{fuel,dry}$

Figure 4 (in Paper VIII) shows the main syngas components and Figure 5 (in Paper VIII) displays the higher hydrocarbons as well as the lower heating value. The main effect of an increase in the gasification temperature on the product gas composition can be well explained by an increase in the H_2 and CO contents and a decrease of CO_2, CH_4 and the higher hydrocarbons in the gas. This is primary caused by the enhanced energy consuming char gasification reaction whose production increased and therefore lowered the concentration of the typical products made by devolatilization by reduction and dilution with H_2 and CO.

Another positive effect of a higher gasification temperature is a lower tar content. Especially the gravimetric tar (larger tar compounds) showed a massive decrease in their amount towards higher gasification temperatures. This can be explained with tar cracking and tar reforming in the reactor of the condensable products made by devolatilization. These reactions require high temperatures to be sufficiently efficient. The effect of this tar cracking reactions is that the tar compounds become smaller. Phenolic compounds vanished completely at 870 °C. Furans and the group of aromatic compounds showed a massive abatement at higher temperatures. Only polyaromatic hydrocarbons (PAH) increased slightly as former tar compounds are broken down and recombine to PAHs.

The carbon and water conversion are positively influenced by higher temperatures in the gasification section which leads to a higher conversion efficiency from solid fuel to product gas. On the other side more additional fuel for the combustion reactor has to be used as less char is available for combustion at higher temperatures (higher carbon conversion in the gasification reactor) and the increased heat demand achieving advanced conversion of fuel. The net effect of this on the process efficiency (overall process efficiency in Paper VIII is the cold gas efficiency with included heat losses of the pilot plant) is a more or less constant trend.

5.8 Approach for indirect indication of the tar content

With the exception of direct firing of product gas in a boiler for heat generation, all downstream utilization of product gas require a tar free [112] gas. In industrial gasification plants the operating conditions are selected in the way to achieve the highest process efficiencies while the tar content has to be as low as possible. With the explained results of the gasification tests in this studies in chapters 5.3-5.7 it is obvious that high process efficiency often goes along with a penalty in the gas quality concerning the tar content. So it is in many cases nontrivial to achieve this, especially in continuous operation. The problem is that the established methods for tar measurement use discontinuous tar sampling where the results of the actual tar content in the gas is available after a comparably long time [113-115]. For active control of the tar content in the gas an online measurement of the tar in the product gas has to be used. There are methods available [116], with the drawback of high investment and operating costs.

Online measurement of the main permanent gas components (H_2, CO, CO_2, CH_4, C_2H_4, C_2H_6) is state of the art, so an easy way of estimating the tar value for online plant optimization would be to find out if there is any correlation between the tar values and the values of permanent gas components. The question is which gas component is the most suitable.

During the accomplished work for this thesis, quite a lot of tests have been done, so a huge amount of tar values and gas measurement is available with a wide range of values: GC/MS tar values from nearly 0.0 g/Nm^3_{db} for char gasification mark the lowest content while the highest GC/MS tar content was reached for gasification of pure PE with 21 g/Nm^3_{db}. As any process influences are avoided in the following consideration, only the results of in-bed feeding tests are used which means that the highest value is caused by the test of wood pellets gasification with in-bed feeding.

In Figures 43-46 the GC/MS tar contents are plotted in dependence of the concentration of the main gas components. As a large part of H_2 and CO is formed by char gasification while tar is (like CH_4, C_2H_4 and C_2H_6) formed by devolatilization of volatile fuel components (see chapter 5.3.2), there cannot be made a proper correlation between H_2 or CO and the GC/MS tar content (Figures 43 and 44). Also CO_2 is influenced by too many factors (fuel O_2 content, water-gas shift reaction, etc.), so this correlation is not considered here further. For CH_4, C_2H_4 and C_2H_6 the situation is becoming more clear, a constant trend for increasing tar values with higher concentration of the applied gas component is visible, especially for the first two gas components. CH_4 and C_2H_4 both show good trends. The best correlation can be made with C_2H_4 as the linear correlation hits both, the x- as well as the y-axis at zero, so there is no offset present.

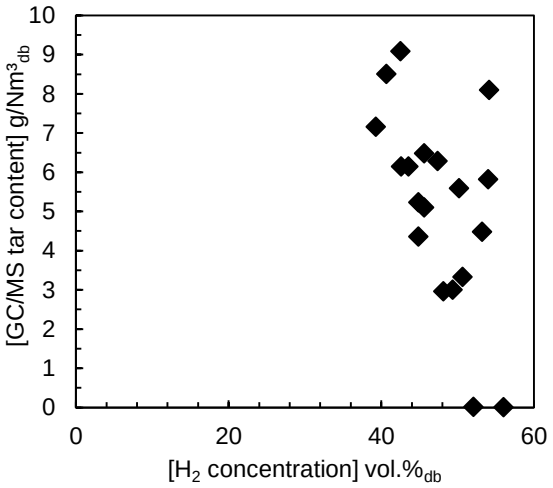

Figure 40: Measured GC/MS tar content vs. H_2 concentration.

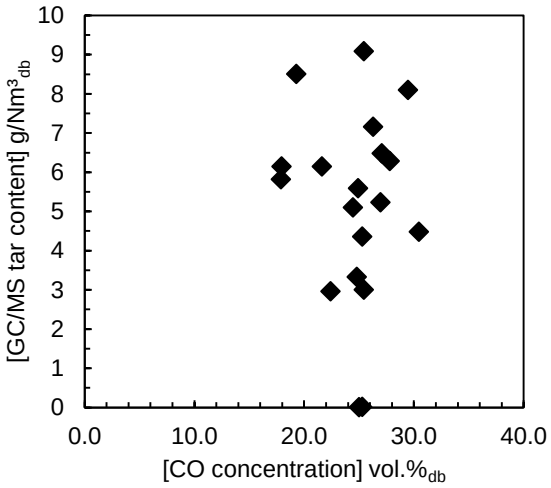

Figure 41: Measured GC/MS tar content vs. CO concentration.

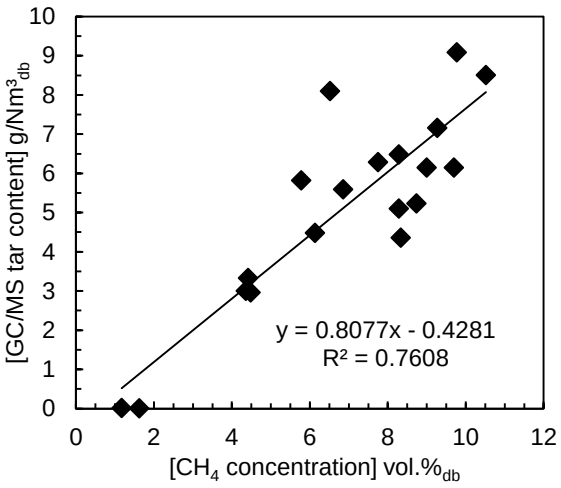

Figure 42: Measured GC/MS tar content vs. CH_4 concentration.

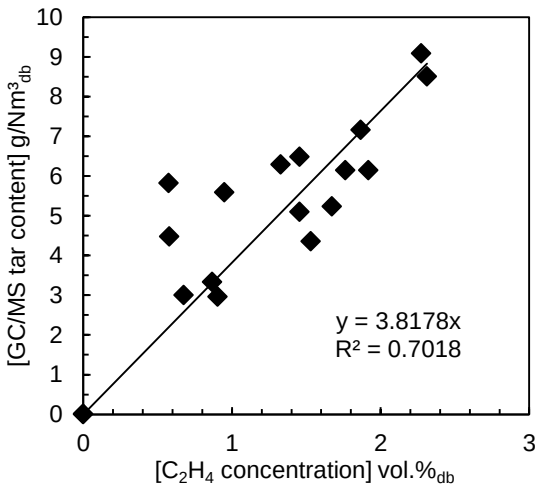

Figure 43: Measured GC/MS tar content vs. C_2H_4 concentration.

For an estimation of the GC/MS tar content the ethylene (C_2H_4) content can be used as an effective component for the GC/MS tar content. If the ethylene content is not measured also the methane (CH_4) content can be used.

The observed correlations are:

- For ethylene: $GC-MS\ tar\ content\ \left[g/Nm^3_{db}\right] = 3.82\ \cdot C_2H_4[vol.\%_{db}]$
- For methane: $GC-MS\ tar\ content\ \left[g/Nm^3_{db}\right] = 0.81\ \cdot CH_4[vol.\%_{db}] - 0.43$

Here only the GC/MS tar was considered. However, unlike as for pyrolysis, where the gravimetric tar content is higher than the GC/MS tar content [8], in the case of gasification the GC/MS tar content always exceeds the gravimetric tar. Therefore, it makes sense to use the GC/MS tar here, the gravimetric tar will be lower anyway.

6. Conclusions

Dual fluidized bed gasification is a fuel-flexible technology capable of the conversion of carbonaceous feedstock into high quality product gas. Originally designed for wood chips, it has turned out that fuel flexibility is a key issue for economic breakthrough. With this work, the suitability of the dual fluidized bed gasification system for a wide spectrum of solid fuels was proven. Unlike wood, with a content of volatile matter of around 80 wt.%, the fuel range was extended by gasification of different kinds of coals towards lower amounts of volatiles in the fuels with char gasification that marks the lowest possible content of volatile matter in the fuel. On the other end of the range for volatile matter, PE as a reference for a fuel consisting completely out of volatile matter was gasified successfully in the DFB system.

For the process itself the amount of fixed carbon in the fuel changes the product gas formation step in the gasification reactor as the product gas formation is dominated by devolatilization for fuels with a high content of volatile matter whereas for fuels with a low content of volatile matter the gas is primary formed by char gasification. The fuel tested with the highest amount of volatile matter in this study was PE, so the whole range of volatile matter in the fuels (4-100%) was covered with the tests. As a result of the changed shares of volatile matter and fixed carbon, the product gas composition changed towards a higher heating value (higher CH_4 content and higher hydrocarbons and lower H_2 content) while the gas quality in terms of condensable compounds (tars) suffered. A tar-free product gas was reached with the utilization of coal char or wood pellets char which shows that the volatile matter in the fuel is a crucial factor for the formation of condensable products in the product gas.

During the fuel tests it turned out that not only the organic components in the feedstock are responsible for changes in the product gas composition and product gas quality, also inorganic matter (ash) can be catalytically active. For the ash of the used lignite a high catalytic activity that enhances tar reducing reactions was found while for the ash of the Spanish bituminous coal no significant activity was found. These investigations offer the possibility to use the positive effect of the lignite for fuels that usually form higher tar amounts (wood, plastics) by co-gasification of lignite with wood pellets or PE. With these co-gasification tests it was found that already at low shares of lignite in the fuel the tar load was reduced massively. This strengthens the fact that primary co-gasification has positive effects on the system and opens an additional degree of freedom for influencing the product gas composition by simple adjustment of the fuel mixture.

With optimization of operating conditions the performance of the system in terms of product gas quality and product gas amount can also be influenced effectively as the tests showed. The location where the solid feedstock is introduced in the system is an essential fact (in-bed vs. on-bed feeding). While in-bed feeding causes much less tar in the product gas, the amount of product gas is significant lower compared to on-bed feeding.

The gasification temperature is an essential value as higher gasification temperatures provide advantages concerning gas quality and fuel conversion with the penalty of losses in the process efficiency.

The fluidization conditions are also very important for the system performance. As it was shown in, the variation of the bed material particle size and the amount of steam for gasification showed that the product gas quality was not affected for the used feedstock, but a noticeable influence on the performance for both measures (particle size and steam-to-carbon ratio) was found. Furthermore, the reduction of the bed material particle size offers the possibility to operate the gasification reactor with a lower amount of steam for fluidization, maintaining a good fluidization regime in the gasification reactor.

In terms of fuel conversion performance and especially product gas quality the size is very important as small fuel particles might be entrained immediately into the gas stream and cause a high loss of unconverted carbon. A second drawback of too small fuel particles is the increased production of tar by the missing interaction of the formed condensable products with the char surface and the lower residence time in the bubbling bed.

To summarize the measures for limitation of the tar content in the product gas by the methods obtained in this work the following aspects can be listed:

- Limitation of the content of volatile matter in the fuel by pre-pyrolysis of the feedstock or adding coal by direct co-gasification to the feedstock;
- Introduction of the solid fuel by in-bed fuel feeding into the gasification reactor;
- Removal of fine fuel particles before utilization in the fluidized bed gasification system;
- Favor of fuels with a catalytic active ash in terms of tar reforming and tar cracking;
- High gasification temperature;

On the other hand side the measures for enhancing conversion performance (of solid fuel in the gasification section of the DFB system) are:

- Utilization of high volatile fuels;
- Introduction of the solid fuel by on-bed fuel feeding into the gasification reactor;
- High gasification temperature;

In summary, in its current configuration the system is limited with regard to large fractions of fine material in the feedstock and the residence time of the formed product gas with condensable products in contact with the hot bed material to effectfully reduce tars. However, a new design has been proposed by the working group "Gasification and Gas Cleaning" at Vienna University of Technology [117] which will be able to convert fine material by using a separator for fine particles at the gasification reactor outlet which will be recycled to the system. Furthermore, with this new system the bed material holdup in the freeboard of the gasification reactor will be increased by structural measures and the contact time of the formed product gas with the hot and catalytically active bed material will be increased to significantly lower the tar load of the product gas.

The fuel flexibility of the dual fluidized bed gasification system has been proven with the large number of tests with different kinds of fuels in this work. The production of a high quality product gas from a wide range of fuels in the same plant will be a key aspect for competitive plants in the market for energy and synthetic fuels.

7. Notation

7.1 Abbreviations

ACFBG	Atmospheric circulating fluidized bed gasifier
ATP	Adenosine triphosphate
BTX	Benzene, toluene, xylene
CHP	Combined heat and power plant
DFB	Dual fluidized bed
E & E	Electrics and electronics
ECUST	East China University of Science and Technology
EPS	Expanded polystyrene
GE	General Electrics
GTI	Gas Technology Institute
HDPE	High-density polyethylene
HTW	High-temperature Winkler
GC/MS	Gas chromatography mass spectrometry
IGCC	Integrated Gasification Combined Cycle
IPA	Isopropanol
KBR	Kellog, Brown and Root
LHV	Lower heating value
MHI	Mitsubishi Heavy Industries
OECD	Organisation for Economic Co-operation and Development
PCFBG	Pressurized circulating fluidized bed gasifier
PE	Polyethylene
PET	Polyethylene terephthalate
PG	Product gas
PP	Polypropylene
PS	Polystyrene
PU(R)	Polyurethane
PVC	Polyvinyl chloride
VUT	Vienna University of Technology
XRF	X-ray fluorescence

7.2 Symbols

A	Pre-exponential factor	1/s
Ar	Archimedes number	-
C_D	Drag coefficient	-
d_P	General particle diameter	µm
d_{P10}	Particle size with mass fraction < 10 %	µm
d_{P50}	Mean particle size	µm

d_{P90}	Particle size with mass fraction > 90 %	µm
d_s	Diameter of a sphere with the same surface as the particle	µm
d_v	Diameter of a sphere with the same volume as the particle	µm
d_{sv}	Mean sauter diameter of the particle	µm
E, EA	Activation energy	kJ/mol
g	Apparent gravity	m/s^2
$\Delta H_{R,850}$	Heat of reaction at 850°C	kJ/mol
k	Reaction rate constant	1/s
k_G, k_L, k_C	Reaction rate constants for pyrolysis to gas (k_G), liquids (k_L) and char (k_C)	1/s
K1, K2	Empirical constants for calculation of U_{mf}	-
K_p	Equilibrium constant	-
$K_{p,CO-shift}$	Equilibrium constant of CO-shift	-
LHV_{PG}	Lower heating value of the product gas (dry)	MJ/Nm^3_{db}
$\dot{m}_{air}$	Mass flux of air	kg/h
$\dot{m}_{air,stoich.}$	Stoichiometrically required amount of air for the reaction	kg/h
$\dot{m}_{C_{FG}}$	Carbon flux in the flue gas stream originating from solid feedstock (neglecting additional fuel for combustion)	kg/h
$\dot{m}_{C_{PG}}$	Carbon flux in the product gas stream	kg/h
$\dot{m}_{fuel}$	Mass flux of solid fuel into the gasification reactor	kg/h
$\dot{m}_{H_2O,actual}$	Actual mass flux of steam in the gasification reactor	kg/h
$\dot{m}_{H_2O,stoich.}$	Stoichiometrically required amount of steam for the reaction	kg/h
$\dot{m}_{H_2O,con.}$	Amount of water that is converted to product gas	kg/h
$\dot{m}_{steam}$	Mass flux of steam in the gasification reactor	kg/h
$p\delta_{eq,CO-shift}$	Logarithmic deviation from CO-shift equilibrium	-
$P_{fuel,C}$	Input fuel power of fuel for the combustion reactor (light heating oil)	kW
$P_{fuel,G}$	Input fuel power of solid fuel into the gasification reactor	kW
p_i	Actual measured gas phase partial pressure of the species i	Pa
$\dot{Q}_{IP}$	Heat loss from an industrial-sized plant with the same fuel power as the pilot plant	kW
$\dot{Q}_{PP}$	Heat loss from the pilot plant	kW
R	Universal gas constant	J/(mol K)
Re	Reynolds number	-
T	Temperature	°C or. K
U_{mf}	Minimum fluidization velocity for a single particle	m/s
U_t	Terminal velocity for a single particle	m/s
U_{se}	Superficial velocity where significant entrainment of solids occurs	m/s
U_g	Superficial velocity gasification reactor	m/s
U_c	Superficial velocity combustion reactor	m/s

$\dot{V}_{PG}$	Volumetric flow rate of product gas (dry)	Nm^3_{db}/h
w_{ash}	Ash mass fraction in the fuel	-
w_C	Carbon mass fraction in the fuel	-
w_{H_2O}	Water mass fraction in the fuel	-
$X_{C,G}$	Carbon conversion in the gasification reactor	%
$X_{C,DFB}$	Carbon conversion in the complete DFB system	%
X_{H_2O}	Water conversion in the gasifier, related to total amount of introduced water	%
$X_{H_2O,rel}$	Water conversion in the gasifier, related to the dry and ash free fuel input	$kg_{H2O}/kg_{fuel,daf}$
x	Molarity of carbon in the fuel (dry, ash, N, Cl and S free basis)	$mol/kg_{C,H,O}$
y	Molarity of hydrogen in the fuel (dry, ash, N, Cl and S free basis)	$mol/kg_{C,H,O}$
z	Molarity of oxygen in the fuel (dry, ash, N, Cl and S free basis)	$mol/kg_{C,H,O}$

7.3 Greek letters

δ	Deviation	-
ε_S	Solid particle volume fraction	-
ε_f	Void particle volume fraction	-
ϕ	Sphericity	-
ϕ_{H_2O}	Stoichiometric H_2O demand	$mol_{H_2O}/kg_{daf,N,S,Cl\ free}$ or $kg_{H_2O}/kg_{daf,N,S,Cl\ free}$
$\eta_{C,IP}$	Cold gas efficiency calculated for an industrial plant with the same fuel power as the used pilot plant	-
$\eta_{C,PP}$	Cold gas efficiency of the pilot plant	-
$\varphi_{SF,wt}$	Steam-to-fuel ratio	$kg_{H2O}/kg_{fuel,daf}$, –
$\varphi_{SC,wt}$	Steam-to-carbon ratio	kg_{H2O}/kg_C , –
$\varphi_{SC,mol}$	Molar steam-to-carbon ratio	mol_{H2O}/mol_C , –
λ_{H_2O}	Stoichiometric H_2O ratio	mol/mol, kg/kg
λ	Air ratio	-
μ	Absolute/dynamic viscosity	$kg/(m\ s)$
ρ_g	Gas density	kg/m^3
ρ_p	Density of a solid particle	kg/m^3
τ_F	Product gas residence time in the freeboard of the gasification reactor	s
τ_C	Gas residence time in the combustion reactor	s
ν_i	Stoichiometric coefficient of the species i	-

ω	Speed of a reaction	1/s

7.4 Super- and Subscripts

c	Carbon, cold gas (efficiency), combustion reactor
daf	Dry and ash free basis
db	Dry basis
g	Gasification reactor
mf	Minimum fluidization
PG	Product gas
sv	Surface volume

8. References

[1] International Energy Agency (IEA), World Energy Outlook 2012, Paris, France, **2012**.

[2] BP, Statistical Review of World Energy 2012, London, UK, **2012**. Available at: bp.com/statisticalreview

[3] S.M. Al-Salem, P. Lettieri, J. Baeyens. Recycling and Recovery Routes of Plastic Solid Waste (PSW): A Review. Waste Management, 29, 2625-2643, **2009**.

[4] USEPA. Municipial Solid Waste in the United States: 2007 Facts and Figures. Executive Summary. Office of solid waste management and emergency response (5306P), EPA530-R-08010, November **2008**. Available at: http://www.epa.gov

[5] M.L. Mastellone. Thermal Treatments of Plastic Wastes by Means of Fluidized Bed Reactors. Ph.D. Thesis. Department of Chemical Engineering, Second University of Naples, Italy, **1999**.

[6] A.V. Bridgwater. The technical and economic feasibility of biomass gasification for power generation. Fuel, 74, 631-653, **1995**.

[7] D.A. Bell, B.F. Towler, M. Fan. Coal Gasification and its Applications. 1st ed. Oxford, UK: William Andrew, Elsevier, **2011**.

[8] S. Kern, M. Halwachs, G. Kampichler, C. Pfeifer, T. Pröll, H. Hofbauer. Rotary kiln pyrolysis of straw and fermentation residues in a 3 MW pilot plant - Influence of pyrolysis temperature on pyrolysis product performance. Journal of Analytical and Applied Pyrolysis, 97, 1-10, **2012**.

[9] U. Arena, L. Zaccariello, M.L. Mastellone. Tar Removal During Fluidized Bed Gasification of Plastic Waste. Waste Management, 29, 783-791, **2009**.

[10] L. Wang, C.L. Weller, D.D. Jones, M.A. Hanna. Contemporary issues in thermal gasification of biomass and its application to electricity and fuel production. Biomass and Bioenergy, 32, 573-581, **2008**.

[11] A. Brems, J. Bayens, R. Dewil. Recycling and Recovery of Post-Consumer Plastic Solid Waste in a European Context. Thermal Science, 16, 669-685, 2012.

[12] M. Kaltschmitt, H. Hartmann, H. Hofbauer (Hrsg.). Energie aus Biomasse. Grundlagen, Techniken und Verfahren. 2. Auflage, Springer, Berlin u.a., **2009**, ISBN 978-3-540-85095-3.

[13] J. Zhang, Y. Wang, L. Dong, S. Gao, G. Xu. Decoupling Gasification: Approach Principle and Technology justification. Energy & Fuels, 24, 6223-6232, **2010**.

[14] R. Rosal, F.V. Diez, H. Sastre. Catalytic hydrogenation of multiring aromatic hydrocarbons in a coal tar fraction. Industrial & engineering chemistry research, 31 (4), 1007-1012, **1992**.

[15] J. Corella, A. Orio, J.M. Toledo. Biomass Gasification with Air in a Fluidized Bed: Exhaustive Tar Elimination with Commercial Steam Reforming Catalysts. Energy & Fuels, 13 (3), 702-709, **1999**.

[16] T. Namioka, A. Saito, Y. Inoue, Y. Park, T. Min, S. Roh, K. Yoshikawa. Hydrogen-rich gas production from waste plastics by pyrolysis and low-temperature steam reforming over a ruthenium catalyst. Applied Energy, 88 (6), 2019-2026, **2011**.

[17] D. Świerczyński, S. Libs, C. Courson, A. Kiennemann. Steam reforming of tar from a biomass gasification process over Ni/olivine catalyst using toluene as a model compound. Applied Catalysis B: Environmental, 74 (3-4), 211-222, **2007**.

[18] P. Basu. Biomass gasification and pyrolysis: practical design and theory. Elsevier, Academic Press: Kidlington, Oxford, UK, **2010**.

[19] Z. Abu El-Rub, E.A. Bramer, G. Brem. Review of Catalysts for Tar Elimination in Biomass Gasification Processes. Industrial & engineering chemistry research, 43, 6911-6919, **2004**.

[20] D. Sutton, B. Kelleher, J.R.H. Ross. Review of literature on catalysts for biomass gasification. Fuel Processing Technology, 73, 155-173, 2001.

[21] S. Koppatz. Outlining active bed materials for dual fluidised bed biomass gasification - In-bed catalysts and oxygen/carbonate looping behavior. PhD Thesis, Vienna University of Technology, **2012**.

[22] A.A.C.M Beenackers. Biomass gasification in moving beds, a review of European technologies. Renewable Energy, 16, 1180-1186, **1999**.

[23] Z.A. Zainal, A. Rifau, G.A. Quadir, K.N. Seetharamu. Experimental Investigation of a Downdraft Biomass Gasifier. Biomass & Bioenergy, 23, 283-289, **2002**.

[24] H. Hofabuer. Gasification – Technology Overview. In: A.V. Bridgwater, H. Hofbauer, S. van Loo, editors. Thermal Biomass Conversion. Newbury, Berks, UK: CPL Press, 13-16, **2009**.

[25] A.V. Bridgwater. Renewable fuels and chemicals by thermal processing of biomass. Chemical Engineering Journal, 91, 87-102, **2003**.

[26] A.M Squires. Clean fuels from coal gasification. Science, 184, 340-346, 1974.

[27] A.V. Bridgwater. The technical and economic feasibility of biomass gasification for power generation. Fuel, 74, 631-653, **1995**.

[28] M. Gabra, E. Petterson, R. Backman, B. Kjellstrom. Evaluation of cyclone gasifier performance for gasification of sugar cane residue - Part 1: gasification of bagasse. Biomass & Bioenergy, 21, 371-380, **2001**.

[29] W.F. Castle. Air separation and liquefaction: recent developments and prospects for the beginning of the new millennium. International Journal of Refrigeration, 25, 158-172, **2002**.

[30] S. Rapagna, N. Jand, A. Kiennemann, P.U. Foscolo. Steam-gasification of biomass in a fluidised-bed of olivine particles. Biomass & Bioenergy, 19, 187-197, **2000**.

[31] G. Schuster, G. Löffler, K. Weigl, H. Hofbauer. Biomass steam gasification - an extensive parametric modeling study. Bioresource Technology, 77, 71-79, **2001**.

[32] A. Molina, F. Mondragón. Reactivity of coal gasification with steam and CO_2. Fuel, 77, 1831-1839, **1998**.

[33] J. Zhang, Y. Wang, L. Dong, S. Gao, G. Xu. Decoupling Gasification: Approach principle and Technology Justification. Energy & Fuels, 24, 6223-6232, **2010**.

[34] P. Bielansky, A. Weinert, C. Schönberger, A. Reichhold. Gasoline and gaseous hydrocarbons from fatty acids via catalytic cracking. Biomass Conversion and Biorefinery, 2, 55-61, **2012**.

[35] S. Koppatz, C. Pfeifer, H. Hofbauer. H_2 rich product gas by steam gasification of biomass with in situ CO_2 absorption in a dual fluidized bed system of 8 MW fuel input. Fuel Processing Technology, 90, 7-8, 914-921, **2009**.

[36] P. Kolbitsch, T. Pröll, J. Bolhar-Nordenkampf, H. Hofbauer. Design of a Chemical Looping Combustor using a Dual Circulating Fluidized Bed (DCFB) Reactor System. Chemical Engineering & Technology, 32, 398-403, **2009**.

[37] T. Pröll, J. Bolhar-Nordenkampf, P. Kolbitsch, H. Hofbauer. Syngas and a separate nitrogen/argon stream via chemical looping reforming - A 140 kW pilot plant study. Fuel, 89, 1249-1256, **2010**.

[38] H. Hofbauer, R. Rauch, G. Loeffler, S. Kaiser, E. Fercher, H. Tremmel. Six years experience with the FICFB-gasification process. In: W. Palz, J. Spitzer, K. Maniatis, K. Kwant, P. Helm, A. Grassi, editors. 12th European Biomass Conference, ETA Florence, Italy, 982-985, **2002**.

[39] H. Hofbauer, R. Rauch, K. Bosch, R. Koch, C. Aichernig. Biomass CHP plant Güssing - A success story. In: A.V. Bridgewater , editor. Pyrolysis and Gasification of Biomass and Waste. Newbury, Berks, UK: CPL Press, 527-536, **2003**.

[40] F. Kirnbauer, J. Kotik, H. Hofbauer. Investigations on inorganic matter in DFB biomass steam-gasification plants in Güssing/Austria and Oberwart/Austria. In: Proceedings of the 19th European Biomass Conference and Exhibition, Berlin, Germany, 849-853, **2011**.

[41] T. Klotz. A regional energy-supply-showcase - the 15 MW fuel-power biomass gasification plant Villach. In: International Seminar on Gasification, Gothenburg, Sweden, **2010**.

[42] I. Gunnarsson. The GoBiGas project – efficient transfer of biomass to biofuels. In: International Seminar on Gasification, Gothenburg, Sweden, **2010**.

[43] J.C. van Dyk, K.J. Keyser, M. Coertzen. Syngas production from South African coal sources using Sasol-Lurgi gasifiers. International Journal of Coal Geology, 65, 243-253, **2006**.

[44] A.M Squires. Clean fuels from coal gasification. Science, 184, 340-346, **1974**.

[45] National Energy technology Laboratory. Gasification in Detail – Types of Gasifiers – Entrained Flow Gasifiers, **2013**. Available at: http://www.netl.doe.gov

[46] L. Zheng, E. Furinsky. Comparison of Shell, Texaco, BGL and KRW gasifiers as part of IGCC plant computer simulations. Energy Conversion and Management, 46, 1767-1779, **2005**.

[47] M. Gazzani, G. Manzolini, E. Macchi, A.F. Ghoniem. Reduced order modeling of the Shell–Prenflo entrained flow gasifier. Fuel, 104, 822–837, **2013**.

[48] R.W. Breault. Gasification Processes Old and New: A Basic Review of the Major Technologies. Energies, 3, 216-240, **2010**.

[49] H. Morehead. Siemens Gasification and IGCC Update. In: PowerGEN International, Orlando, Florida, USA, December 3, **2008**.

[50] C. Higman, M. van der Burgt. Gasification. Burlington, MA, USA: Elsevier Science, pp. 107, **2003**.

[51] National Energy technology Laboratory. Gasification Database, **2010**. Available at: http://www.netl.doe.gov

[52] American Society for Testing and Materials, Annual Book of ASTM Standards 2006, Volume 5 Part 6, Gaseous Fuels; Coal and Coke, **2006**.

[53] NEWAG NIOGAS, Verbundkraft. Der sanfte Weg, Kraftwerk Dürnrohr, Die neue Generation der Wärmekraftwerke. Wien-Berlin , A.F. Koska, **1987**.

[54] The Compelling Facts about Plastics 2009: An Analysis of Plastics Production, Demand and Recovery for 2008 in Europe; Plastics Europe, Association of Plastics Manufacturers: Brussels, Belgium, **2009**.

[55] S. Rapagná, H. Provendier, C. Petit, A. Kiennemann, P.U. Foscolo. Development of catalysts suitable for hydrogen or syn-gas production from biomass gasification. Biomass & Bioenergy, 22, 377-388, **2002**.

[56] P. Hasler, T. Nussbaumer. Gas cleaning for IC engine applications from fixed bed biomass gasification. Biomass & Bioenergy, 16, 385-395, **1999**.

[57] S. Kern. Niedertemperatur Drehrohrpyrolyse als Vorschaltprozess für die Co-Verbrennung von unkonventionellen Brennstoffen in thermischen Anlagen. Master Thesis, Institute of Chemical Engineering, Vienna University of Technology, **2010**.

[58] H. Hofbauer. Thermische Biomassenutzung I und II. Lecture notes, Vienna University of Technology, 2007.

[59] X.G. Zhu, S.P Long, D.R. Ort. What is the maximum efficiency with which photosynthesis can convert solar energy into biomass? Current Opinion in Biotechnology, 19, 153-159, **2008**.

[60] J.V. Kumar, B.C. Pratt. Compositional analysis of some renewable biofuels. American Laboratory, 28, 15–20, **1996**.

[61] A. Demirbas. Yields of oil products from thermochemical biomass conversion processes. Energy Conversion and Management, 39, 685-690, **1998**.

[62] D. van Krevelen. Coal: Typology-Physics-Chemistry-Constitution. Elsevier Science Publishers: Amsterdam, The Netherlands, **1993**.

[63] E. Dorrestijn, L.J.J. Laarhoven, I.W.C.E. Arends, P. Mulder. The occurrence and reactivity of phenoxyl linkages in lignin and low rank coal. Journal of Analytical and Applied Pyrolysis, 54, 153-192, **2000**.

[64] J.C. Crelling, D.H. Sauter, D. Leininger, B. Bonn, R. Reimert, W. Gatzka. Ullmann's Encyclopedia of Industrial Chemistry, 5th Ed., Vol. A7, VCH Verlagsgesellschaft: Weinheim, Germany, p. 153, **1986**.

[65] M. Krzesińskaa, U. Szelugaa, S. Czajkowskaa, J. Muszyńskia, J. Zachariasza, S. Pusza, B. Kwiecińskab, A. Koszorekc, B. Pilawaa. The thermal decomposition studies of three Polish bituminous coking coals and their blends. International Journal of Coal Geology, 77, 350-355, **2009**.

[66] T. Faravelli, G. Bozzano, C. Scassa, M. Perego, S. Fabini, E. Ranzi, M. Dente. Gas product distribution from polyethylene pyrolysis. Journal of Analytical and Applied Pyrolysis, 52, 87-103, **1999**.

[67] HSC. HSC Chemistry 5.1. Pori, Finland: Outokumpu Research Oy; **2002**.

[68] P.O. Morf. Secondary reactions of tar during thermochemical biomass conversion. PhD thesis, ETH Zrich, **2001**.

[69] Y. Haseli, J.A. van Oijen, L.P.H. de Goey. Numerical study of the conversion time of single pyrolyzing biomass particles at high heating conditions. Chemical Engineering Journal, 169, 299-312, **2011**.

[70] C. Di Blasi, C. Branca. Kinetics of primary product formation from wood pyrolysis, Industrial and Engineering Chemistry Research, 40, 5547–5556, **2001**.

[71] W. Klose, M. Wölki. On the intrinsic reaction rate of biomass char gasification with carbon dioxide and steam. Fuel, 84, 885-892, **2005**.

[72] S. Kern, C. Pfeifer, H. Hofbauer. Reactivity tests of the water-gas shift reaction on fresh and used fluidized bed materials from industrial DFB biomass gasifiers. Biomass & Bioenergy, in press, **2013**. doi: 10.1016/j.biombioe.2013.02.001.

[73] N. Laosiripojana, S. Assabumrungrat. Catalytic dry reforming of methane over high surface area ceria. Applied Catalysis B: Environmental, 60, 107-116, **2005**.

[74] F. Kirnbauer, V. Wilk, H. Kitzler, S. Kern, H. Hofbauer. The positive effects of bed material coating on tar reduction in a dual fluidized bed gasifier. Fuel, 95, 553–562, **2012**.

[75] M. Stidl. Prozesssimulation von spezifischen Anwendungsfällen der Zweibett-Wirbelschicht-Dampfvergasungs-Technologie für die Papier- und Zellstoffindustrie. PhD Thesis, Vienna University of Technology, p. 112, **2012**.

[76] J. Kotik. Über den Einsatz von Kraft-Wärme-Kopplungsanlagen auf Basis der Wirbelschicht-Dampfvergasung fester Biomasse am Beispiel des Biomassekraftwerks Oberwart. PhD Thesis, Vienna University of Technology, **2010**.

[77] D. Kunii, O. Levenspiel. Fluidization Engineering, 2nd ed. Stoneham, MA, USA: Butterworth-Heinemann, Reed Publishing, **1991**.

[78] W.C. Yang. Handbook of Fluidization and Fluid-Particle Systems. Chemical Industries Series. Marcel Dekker, **2003**.

[79] L.S. Fan and C. Zhu. Principles of Gas-Solid Flows. Cambridge Series in Chemical Engineering. Cambridge University Press, **2005**.

[80] J.R. Grace, A.A. Avidan, T.M. Knowlton. Circulating fluidized beds. Blackie Academic & Professional, **1997**.

[81] D. Geldart. Types of gas fluidization. Powder Technology, 7, 285-292, **1973**.

[82] D. Geldart, A.R. Abrahamsen. Homogeneous fluidization of fine powders using various gases and pressures. Powder Technology, 19, 133-136, **1978**.

[83] C.Y. Wen, Y.H. Yu. A generalized method for predicting the minimum fluidization velocity. AIChE Journal, 12, 610-612, **1966**.

[84] J.F. Richardson. Fluidization. J.F. Davidson, D. Harrison (Eds.), Academic Press: New York, USA, **1971**.

[85] S.C. Saxena, G.J. Vogel. Segregation and fluidization characteristics of a dolomite bed with a range of particle sizes and shapes. Chemical Engineering Journal, 14, 59-63, **1977**.

[86] S.P. Babu, B Shah, A Talwalkar. Fluidization correlations for coal gasification materials-minimum fluidization velocity and fluidized bed expansion ratio. AIChE Symposium Series, p. 176, **1978**.

[87] J.R. Grace, G. Hetsroni. Handbook of multiphase systems. G. Hetsroni (Editor), Hemisphere: Washington D.C., USA, **1982**.

[88] D.C. Chitester, R.M. Kornosky, L.S. Fan, J.P. Danko. Characteristics of fluidization at high pressure. Chemical Engineering Science, 39, 253-261, **1984**.

[89] Neft, J.P.A.; Knoef, H.A.M.; Zielke, U.; Sjöström, K.; Hasler, P.; Simell, P.A. Guideline for Sampling and Analysis of Tar and Particles in Biomass Producer Gases (Tar Protocol), ERK6-CT1999-20002 Version 3.1, ECN; **1999**.

[90] S. Koppatz, C. Pfeifer, H. Hofbauer. Comparison of the Performance Behaviour of Silica Sand and Olivine in a Dual Fluidised Bed Reactor System for Steam Gasification of Biomass at Pilot Plant Scale. Chemical Engineering Journal, 175, 468-483, **2011**.

[91] R. Rauch, C. Pfeifer, K. Bosch, H. Hofbauer, D. Świerczyński, C. Courson, A. Kinnemann. Comparison of Different Olivines for Biomass Steam Gasification. . In: A.V. Bridgewater, D.G.B. Coocock, editors. Science in Thermal and Chemical Biomass Conversion. Vol. 1, CPL Press: UK, 799-809, **2006**.

[92] F. Kirnbauer, H. Hofbauer. Investigations on bed material changes in a dual fluidized bed steam gasification plant in Güssing, Austria. Energy & Fuels, 25 3793-3798, **2011**.

[93] E. Perz. A computer method for thermal power cycle calculation. Journal of Engineering for Gas Turbines and Power, 113(2), 184-189, **1991**.

[94] S. Kern. Report on assessment of the integrated fluidised bed process. FECUNDUS Project, Deliverable 6.2, **2013**.

[95] T. Pröll, H. Hofbauer. Development and Application of a Simulation Tool for Biomass Gasification Based Processes, International Journal of Chemical Reactor Engineering, 6(89), **2008**.

[96] SimTech Homepage, IPSEpro system description, **2009**. Available at: http://www.simtechnology.com/IPSEpro/english/IPSEpro.php

[97] T. Pröll, R. Rauch, C. Aichernig, H. Hofbauer. Fluidized bed steam gasification of solid biomass - analysis and optimization of plant operation using process simulation. In 18th International Conference on Fluidized Bed Combustion, Toronto, Canada, May 22-25, **2005**.

[98] A.G. Collot. Matching gasification technologies to coal properties. International Journal of Coal Geology, 65 (3-4), 191-212, **2006**.

[99] W.H. Calkins. Investigation of organic sulfur-containing structures in coal by flash pyrolysis experiments. Energy & Fuels, 1(1), 59-64, **1987**.

[100] S. Kern, C. Pfeifer, H. Hofbauer. Dual fluidized-bed steam gasification of solid feedstock : Matching syngas requirements with fuel mixtures. The South African Journal of Chemical Engineers (SAJChE), 17 (1), 13-24, **2012**.

[101] A. Gómez-Barea, P. Ollero, B. Leckner. Optimization of char and tar conversion in fluidized bed biomass gasifiers. Fuel, 103, 42-52, **2013**.

[102] V. Wilk, S. Kern, H. Kitzler, S. Koppatz, J.C. Schmid, H. Hofbauer. Gasification of Plastic Residues in a Dual Fluidized Bed Gasifier - Characteristics and Performance Compared to Biomass. In: Proceedings of the International Conference on Polygeneration Strategies (ICPS11), Vienna, Austria, 55-65, **2011**.

[103] ECN. Tar Classification System. **2009**. Available at: http://www.thersites.nl.

[104] T.A. Milne, N. Abatzoglou, R.J. Evans. Biomass Gasifier 'Tars': Their Nature, Formation, and Conversion. National Renewable Energy Lab, Golden, CO, USA, **1998**.

[105] U. Wolfesberger, S. Koppatz, C. Pfeifer, H. Hofbauer. Effect of iron supported olivine on the distribution of tar compounds derived by steam gasification of biomass. In: Proceedings of the International Conference on Polygeneration Strategies (ICPS11), Vienna, Austria, 69-76, **2011**.

[106] F. Miccio, O. Moersch, H. Spliethoff, K. R. G. Hein. Generation and conversion of carbonaceous fine particles during bubbling fluidised bed gasification of a biomass fuel. Fuel, 78, 1473-1481, **1999**.

[107] V. Wilk, H. Hofbauer. Influence of physical properties of the feedstock on gasification in a dual fluidized bed steam gasifier. In: Proc. of the 21st International Conference on Fluidized Bed Combustion (FBC), Naples, Italy, 797-804, **2012**.

[108] D. Świerczyński, C. Courson, L. Bedel, A. Kiennemann, J. Guille. Characterization of Ni−Fe/MgO/Olivine Catalyst for Fluidized Bed Steam Gasification of Biomass. Chemistry of Materials, 18(17), 4025-4032, **2006**.

[109] A. Orio, J. Corella, I. Narváez, Performance of Different Dolomites on Hot Raw Gas Cleaning from Biomass Gasification with Air. Industrial and Engineering Chemistry Research, 36, 3800-3808, **1997**.

[110] L.K. Mudge, E.G. Baker, D.H. Mitchell, M.D. Brown. Catalytic steam gasification of biomass for methanol and methane production. Journal of Solar and Energy Engineering, 107, 88-92, **1985**.

[111] H. Kitzler, C. Pfeifer, H. Hofbauer. Gasification of different kinds of non-woody biomass in a 100 kW dual fluidized bed gasifier. In: Proc. of the 21st International Conference on Fluidized Bed Combustion (FBC), Naples, Italy, 760-766, **2012**.

[112] P. Hasler, T. Nussbaumer. Gas cleaning for IC engine applications from fixed bed biomass gasification. Biomass & Bioenergy, 16(6), 385-395, **1999**.

[113] P. Hasler, T. Nussbaumer. Sampling and analysis of particles and tars from biomass gasifiers. Biomass & Bioenergy, 18(1), 61-66, **2000**.

[114] N. Abatzogloua, N. Barkerb, P. Haslerc, H. Knoef. The development of a draft protocol for the sampling and analysis of particulate and organic contaminants in the gas from small biomass gasifiers. Biomass & Bioenergy, 18(1), 5-17, **2000**.

[115] H.A.M. Knoef, H.J. Koele. Survey of tar measurement protocols. Biomass & Bioenergy, 18(1), 55-59, **2000**.

[116] O. Moersch, H. Spliethoff, K.R.G. Hein. Tar quantification with a new online analyzing method. Biomass & Bioenergy, 18(1), 79-86, **2000**.

[117] C. Pfeifer, J.C. Schmid, T. Pröll, H. Hofbauer. Next Generation Biomass Gasifier. In: Proceedings of the 19th European Biomass Conference, Berlin, Germany, 1456-1462, **2011**.